

Effects of Limestone Powder, Olive Waste Ash and Sea Sand Powder on Properties of Self Compacting Concrete

Raheleh Cheraghizadeh

Submitted to the
Institute of Graduate Studies and Research
in partial fulfillment of the requirements for the degree of

Doctor of Philosophy
in
Civil Engineering

Eastern Mediterranean University
March 2019
Gazimağusa, North Cyprus

Approval of the Institute of Graduate Studies and Research

Assoc. Prof. Dr. Ali Hakan Ulusoy
Acting Director

I certify that this thesis satisfies all the requirements as a thesis for the degree of Doctor of Philosophy in Civil Engineering.

Assoc. Prof. Dr. Serhan Şensoy
Chair, Department of Civil Engineering

We certify that we have read this thesis and that in our opinion it is fully adequate in scope and quality as a thesis for the degree of Doctor of Philosophy in Civil Engineering.

Asst. Prof. Dr. Tülin Akçaoğlu
Supervisor

Examining Committee

1. Prof. Dr. Şakir Erdoğan

2. Prof. Dr. Şemsi Yazıcı

3. Assoc. Prof. Dr. Mürüde Çelikağ

4. Assoc. Prof. Dr. Khaled Marar

5. Asst. Prof. Dr. Tülin Akçaoğlu

ABSTRACT

Utilization of standardized local and waste resources is of great importance to the economic development in the world. Besides, application of waste material results in more eco-friendly concrete at the same time. In this study, the effects of two different new fillers, named as sea sand powder (SS), as a local available material and olive waste bottom ash, (OW) as a waste material of different proportions incorporated with two different quantities of superplasticizer (SP), on physical and mechanical properties of SCC were aimed to be investigated and compared to those of limestone powder (LS) as a common filler. For these aims rheology of fresh concrete, compressive and tensile strengths, initial defects, fracture energy and volume changes during hydration were measured.

Results showed that there is no considerable difference in hardened properties of SCC by using SS instead of LS; however, differences in volumetric shrinkage and rheological properties, especially for bleeding and segregation, were more pronounced. On the other hand, OW mixes show different outcomes. OW gives more viscosity to SCC mixes and eliminates segregation and bleeding of the mixes containing this filler. Nevertheless, reduced compressive strength and fracture energy and increased volumetric shrinkage and porosity in these mixes were noticeable compared to LS mixes; however, when 5% OW was used, the results found to be more tolerable.

Keywords: Self-consolidated concrete, Olive waste ash, Sea sand powder, Limestone powder, Compressive strengths, Fracture energy

ÖZ

Standardlaşmış yerel ve atık malzeme kaynaklarının kullanılması; dünyanın ekonomik gelişimi açısından büyük önem taşır. Atık malzemelerin beton üretiminde kullanılması, aynı zamanda doğa dostu beton üretmek anlamındadır. Bu çalışmanın amacı, iki farklı miktardaki süper akışkanlaştırıcı (SA) ile birleştirilen farklı oranlardaki zeytin atık külü (ZK) ve deniz kum tozu (DK) olarak adlandırılan iki farklı yeni dolgu maddesinin; KYB'nun fiziksel ve mekanik özellikler ve davranışlar üzerindeki etkilerini araştırmaktır. Bu araştırmada ayrıca; iki farklı dolgu malzemesi ile üretilmiş olan KYB özellik ve davranışlarının, etkileri iyi bilinen kireçtaşı tozu (KT) dolgu maddesi ile üretilmiş KYB özelliklerinin karşılaştırılması amaçlanmıştır. Bu amaçlar için taze betonun reolojisi, basınç ve çekme dayanımı, ilk kusurlar, kırılma enerjisi ve hidrasyon sırasındaki hacim değişiklikleri ölçüldü.

Sonuçların değerlendirilmesi neticesinde; kireçtaşı tozu yerine deniz kumu tozu kullanılmasının önemli bir fark yaratmadığını, ancak betonda oluşan kanama ve ayrışma miktarlarının kontrol edilmesi gerektiği anlaşılmıştır. Zeytin atık külü kullanılmış olan betonlarda, farklı sonuçlar elde edilmiştir. Bu betonlarda; viskozite miktarının arttığı, dolayısıyla bu dolguyu içeren karışımlarda kaydedilen ayrışma ve kanamanın daha az olduğu gözlemlenmiştir. Bununla birlikte, düşük basınç dayanımı ve kırılma enerjisi ve bu karışımlardaki hacimsel büzülme ve gözeneklilik artışları, kireçtaşı tozu karışımlarına kıyasla daha belirgindi.

Anahtar Kelimeler: Kendiliğinden yerleşen beton, Zeytin atık külü, Deniz kumu tozu, Kireçtaşı tozu, Basınç dayanımı, Kırılma enerjisi

ACKNOWLEDGEMENT

First and foremost, I would like to thank my supervisor Asst. Prof. Dr. Tülin Akçaoğlu. It has been an honor to be her first Ph.D. student. I appreciate all her contributions of time, ideas, and supports to make my Ph.D. experience productive and stimulating.

I gratefully acknowledge the funding sources of Civil Engineering Department of Eastern Mediterranean University; that made my Ph.D. work possible. Special thanks go to Materials of Construction Laboratory staff and especially Mr. Ogun Kilic for their kind help during the experimental work.

I would like to thank Romina who is not just my sister but my best friend. She helped and motivated me during my study. Also, thanks go to my friend Nima, who helped me too much during editing this thesis.

Lastly, I would like to thank my family for their loving and patience encouragement. And most of all for my loving, supportive, encouraging, and patient husband Mohammad whose faithful support during the final stages of this Ph.D. is so appreciated. I would like to single out my lovely son Radin for his understanding and patience during this study.

In closing, thanks go to Dayan, my younger son, who was born just two days after finishing the laboratory experiments. He was with me in the civil engineering department during thesis writing when he was just 10 days old.

To my family

TABLE OF CONTENTS

ABSTRACT	iii
ÖZ	iv
ACKNOWLEDGEMENT	v
DEDICATION	vi
LIST OF TABLES	xii
LIST OF FIGURES	xiii
LIST OF ABBREVIATIONS	xvi
1 INTRODUCTION.....	1
1.1 Introduction.....	1
1.2 Scope of the Research	1
1.2.1 Olive Waste.....	2
1.2.2 Sea Sand.....	3
1.3 Research Objectives	4
1.4 Research Methodology.....	4
1.5 Outline of the Thesis	4
1.6 Thesis Output	5
2 A CRITICAL REVIEW: FRESH AND HARDENED PROPERTIES OF SCC	6
2.1 Introduction.....	6
2.2 Development of SCC	6
2.3 Advantages Versus Limitations of SCC	7
2.4 Functional Requirements for SCC	10
2.4.1 Filling Ability.....	10
2.4.2 Passing Ability	11

2.4.3 Segregation Resistance	12
2.5 Methods of SCC Achievements	12
2.6 Filler for SCC	14
2.6.1 Mineral Fillers	15
2.6.1.1 Limestone Powder	15
2.6.2 Pozzolanic Filler	17
2.6.3 Hydraulic Filler	18
2.6.4 Other Filler	19
2.6.5 Green and Waste Material Utilization in Constructions	19
2.6.5.1 Olive Waste Ash	20
2.6.5.2 Sea-sand Powder, Problems and Limitations	21
2.7 Mixing Proportions of SCC	22
2.8 Material Quantities for SCC	23
2.9 Test Methods for SCC	24
2.9.1 Slump Flow	24
2.9.2 V-funnel	26
2.9.3 L-box	27
2.10 Critical Review on Hardened Behavior of SCC	28
2.10.1 Strength Characteristics of SCC	28
2.10.2 Fracture Properties of SCC	32
2.10.2.1 Evaluation of Fracture Energy of Concrete	34
2.10.2.2 RILEM Methods for Fracture Energy Calculation of Concrete	35
2.10.2.3 Work of Fracture Method by RILEM	36
2.10.2.4 Fracture Energy of SCC	38
2.10.2.5 Fracture Process Zone Length of SCC	38

2.10.3 Shrinkage in Concrete, Definitions and Types	39
2.10.3.1 Drying Shrinkage	41
2.10.3.2 Autogenous Shrinkage	41
2.10.3.3 Plastic Shrinkage.....	42
2.10.3.4 Carbonation Shrinkage.....	42
2.10.3.5 Shrinkage in SCC.....	43
2.10.4 Presence of Porosity in VC and SCC.....	44
2.10.4.1 Detection of Porosity by X-Ray CT.....	46
3 MATERIALS AND METHODS.....	48
3.1 Introduction.....	48
3.2 Materials Used for SCC Mixes	48
3.2.1 Powder Materials Used for Aggregate Replacement.....	50
3.2.1.1 Limestone Powder (LS)	50
3.2.1.2 Sea Sand Powder (SS).....	50
3.2.1.3 Olive Waste Ash (OW)	51
3.3 SCC Mix Materials and Proportions	52
3.4 Experimental Procedure	53
3.4.1 Mixing Procedure.....	53
3.4.2 Fresh SCC Tests.....	53
3.4.2.1 Slump Flow Test	54
3.4.2.2 V-Funnel Test	54
3.4.2.3 L-Box Test	54
3.4.3 Hardened SCC Evaluation	54
3.4.3.1 Compressive Strength Measurements.....	54
3.4.3.2 Splitting Tensile Strength Test.....	55

3.4.3.3 Porosity Analysis of SCC by X-Ray CT and ImageJ Computer Program.....	55
3.4.3.3.1 X-Ray Computed Tomography for Internal Inspection.....	56
3.4.3.3.2 Concrete Assessment by X-Ray CT.....	57
3.4.3.3.3 Different X-Ray CT Methods for Specimen Evaluation.....	57
3.4.3.3.4 Rapid X-Ray CT on Concrete, Quality and Advantages.....	58
3.4.3.4 Computer programs for porosity evaluation of X-Ray CT images....	58
3.4.3.5 Fracture Energy Calculation of SCC.....	60
3.4.3.6 Shrinkage Measurement in Concrete by Demec Gauge.....	62
4 RESULTS AND DISCUSSIONS.....	64
4.1 Effect of Filler Type and Amounts on Fresh Performance of SCC.....	64
4.2 Behavior of SCC with Different Filler Types and Amounts under Compressive Strength.....	70
4.3 Effect of OW, SS and LS Replacement to Aggregate on Splitting Tensile Strength of SCC.....	72
4.4 Porosity Analysis of SCC with Different Filler Types and Amounts by X-Ray CT.....	73
4.5 Experimental Results on Fracture Energy of SCC with Different Filler Types and Quantities.....	77
4.6 Effect of Filler Types and Quantities on Volumetric Shrinkage of SCC.....	84
4.6.1 Correlation of 28 days Compressive Strength and 30 Days Volumetric Shrinkage of SCC.....	87
5 CONCLUSION AND RECOMMENDATIONS FOR FURTHER RESEARCH..	88
5.1 Conclusion.....	88
5.2 Recommendations for Future Studies.....	90

REFERENCES.....	91
APPENDICES	112
Appendix A: Three Point Bending Load-Deformation Curves of Limestone Powder (LS) mixes (Figure A.1 to A. 4).....	113
Appendix B: Three Point Bending Load-Deformation Curves of Sea Sand Powder (SS) mixes (Figure B. 1 to B. 4).....	115
Appendix C: Three Point Bending Load-Deformation Curves of Olive Waste Ash (OW) mixes (Figure C. 1 to C. 6)	117

LIST OF TABLES

Table 1: Filler classification (EFNARC, 2005)	15
Table 2: Regular ranges for components of SCC	24
Table 3: Consistency classes of SCC	25
Table 4: Viscosity classes of SCC according to slump flow test.....	25
Table 5: Viscosity classes of SCC according to V-funnel test.....	26
Table 6: Passing ability classes of SCC according to L-box test.....	28
Table 7: Chemical and physical properties of cement and fillers used.....	48
Table 8: Manufacturer's Stated Values for Glenium 27	50
Table 9: Mix proportions and properties of SCC.....	52
Table 10: Result of SCC classification according to BS EN 206-9 (2010).....	65
Table 11: Compressive strength results of Control and SCC mixes after 7, 28 and 91 days of casting.....	71
Table 12: 30 days volumetric shrinkage of SCC specimens produced with LS, SS and OW	86

LIST OF FIGURES

Figure 1: Filling ability of SCC (www.concreteconstruction.net).....	8
Figure 2: Good surface finish by using SCC without any repairs, Perham tower	9
Figure 3: Functional necessities of SC.....	10
Figure 4: Schematic of blockage, coarser aggregates can bridge or arch at small openings that could be resulted in blockage of the rest of the concrete (After: RILEM TC 174 SCC, 2000).....	11
Figure 5: The schematic illustration of composition differences of SCC and VC from Okamura and Ouchi (2003).....	23
Figure 6: Slump flow test.....	26
Figure 7: Schematic of V-funnel test equipment	27
Figure 8: L-Box test equipment (EFNARC 2005).....	28
Figure 9: Splitting tensile strength test on cylindrical specimen	31
Figure 10: Typical load-deflection response for quasi-brittle materials under tension or flexural loading (Karihaloo 1995)	34
Figure 11: Notched Beam details – Three Point Bending Test.....	36
Figure 12: The gradation of the coarse aggregate and the reference curves.....	49
Figure 13: The gradation of the fine aggregate and the reference curves.....	49
Figure 14: Olive waste cylinders for energy source of chimneys.....	51
Figure 15: Mixing process of SCC	53
Figure 16: Placement of cylindrical specimen in aligning jig for splitting tensile strength.....	55
Figure 17: Schematic representation of the X-RAY CT image locations along X-direction	56

Figure 18: Tomography images of a concrete cylinder (left) and air voids (center) and the image processing of the aggregates (right).....	59
Figure 19: Front view of a beam with applied notch	60
Figure 20: Prismatic beam prepared for fracture energy test with 40 mm notch.....	60
Figure 21: Notched beam under TBT test.....	61
Figure 22: Demec positions on the cubes and Demec Gauge instrument.....	63
Figure 23: SS specimen with pins in three directions for volume change measurement	63
Figure 24: Effect of filler type and quantities on slump flow of SCC	65
Figure 25: Bleeding and segregation in slump-flow test of SS10SP2	66
Figure 26: Effect of filler type (LS, SS, and OW) and quantities on segregation of SCC produced with 1.5% and 2% SP	68
Figure 27: Effect of filler type and quantities on V-Funnel test of SCC	69
Figure 28: Effect of filler type and quantities on L-Box test of SCC	70
Figure 29: Effect of filler type and quantities on 7, 28 and 91 days fc.....	72
Figure 30: Effect of filler type and quantities on 28 days split tensile strength	73
Figure 31: X-Ray CT images of a) SS10SP1.5, b) SS10SP2, c) SS15SP1.5 and d) SS15SP2 from center sections	73
Figure 32: X-Ray CT images of OW5SP2 in six different directions of specimen...	74
Figure 33: Effect of filler types and quantities on porosity of SCC	75
Figure 34: Total pore areas versus slump flow of SCC	75
Figure 35: Average pore areas versus maximum pore areas of SCC.....	76
Figure 36: Correlation between pore areas along casting direction and 91 days fc for OW specimens	76

Figure 37: Load-deformation curves of a) LS15SP2, b) SS15SP2 and c) OW15SP2 notched beams	78
Figure 38: Effect of filler type and quantities on fracture energy of SCC.....	79
Figure 39: Correlation of 91 days f_c and G_f for (a) LS, (b) SS and (c) OW mixes....	80
Figure 40: Effect of filler type and quantities on f_i	81
Figure 41: Characteristic length of SCC mixes in TBT.....	82
Figure 42: Correlation of f_c and G_f for a) LS mixes, b) SS mixes and c) OW mixes	83
Figure 43: Effect of filler type and quantities on volumetric shrinkage of SCC produced with 1.5% SP	84
Figure 44: Effect of filler type and quantities on volumetric shrinkage of SCC produced with 2% SP.....	85
Figure 45: Effect of filler type and quantities on 30 days volumetric shrinkage of SCC specimens	86
Figure 46: 30 days volumetric shrinkage of SCC versus 28 days f_c	87

LIST OF ABBREVIATIONS

CO ₂	Carbon dioxide
Corr.	Correlation
FAO	Food and agricultural organization
E	Modulus of elasticity
f _c	Compressive strength
f _{sp1}	Splitting tensile strength
f _t	Flexural tensile strength in three-point bending test
G _f	Fracture energy
GGBS	Ground granulated blast furnace slag
LS	Limestone powder
OW	Olive waste bottom ash
SCC	Self-consolidated concrete
SiO ₂	Silicon dioxide
SP	Super plasticizer
SS	Sea- sand powder
TBT	Three-point bending test
VC	Normal vibrated concrete

Chapter 1

INTRODUCTION

1.1 Introduction

This chapter presents the research scope, highlights the objectives as well as methodology of the research, summaries the thesis structure and presents the outputs of the research.

1.2 Scope of the Research

In order to well operation of the world, it is necessary for concrete to be adapted to the economic and technical developments around the world. According to the population growth statistics (around 82 million people per year), increasing population invariably increase the concrete demand every year. On the other hand, SCC has been introduced in recent decades as one of the greatest novelties with several advantages in the concrete technology with high flowability. This type of concrete can be poured into places and fills the formworks while encapsulating the reinforcement with no mechanical compaction. Moreover, it possesses the ability to flow without segregation or excessive bleeding via narrow spaces (ACI237R-07 2007). SCC is more common nowadays due to its valuable advantages. In comparison to normal vibrated concrete (VC), different proportions of materials are required for SCC to decrease settlement, collapse and segregation.

To reach adequate cohesion and stability, different mixing proportions of powder or viscosity modifiers are needed. Generally, silica fume, fly ash or LS are used as

fillers but these materials are not available in all regions in the world such as non-industrial countries with limited resources. In these areas, the cost of SCC increases and makes it uneconomical. Therefore, replacing locally available materials with lower cost is important.

This study is aimed at introducing two new filler materials; OW, a waste material, and SS, a widely available material in the world and in Cyprus, for SCC production. Therefore, fresh and hardened concrete properties of SCC produced by these new materials were evaluated and compared to those of SCC made by LS as a common filler.

This study is conducted in Northern Cyprus which is an island in Mediterranean Sea. This country has limited sources and industries. Certainly, limestone is available in this country; however, the cement factory in this island produces cement by use of imported clinker and slag from other countries and local limestone from limited mines in Cyprus. Most of the construction companies import silica fume and limestone from Turkey and the shipping imposes more expenses to the projects. Regarding the small dimensions of this island and related exhaustible sources, utilization of endless materials seems to be very significant. In sections 1.2.1 and 1.2.2, aims of choosing these two materials among different waste and locally available materials are described.

1.2.1 Olive Waste

Regarding the enforcing of more difficult environmental rules, utilization of bottom ash in concrete is a valuable achievement, even for ashes with lower pozzolanic activities. The grinding cost can compete with the higher costs of ash disposal; therefore, SCC could be an attractive nomination for consumption of high amount of

bottom ash, not just in the role of cement developer, but similarly as a powdered material with low reactivity. Moreover, bottom ash could be more worth full and proper material for utilization in SCC by grinding to smaller particles.

According to FAO (2014) reports, olive production increases every year and exceeded twenty million tons in the world. In the Mediterranean countries, olive-oil production is one of the foremost agricultural industries that produces considerable amount of residual biomass. By recycling this olive waste, environmental impacts and economic costs will be decreased (Rajamma et al. 2009). However major replacement of olive waste ash in place of other fillers looks more feasible in the countries with olive agriculture and filler production limitations. Previously olive waste ash has been used in soil stabilization (Nalbantoglu and Tawfiq 2006) and fire-resistant concrete (Al- Akhras et al. 2009). Moreover, some properties of SCC made by olive waste fly ash (Cuencaa et al. 2013) have been studied but still questions exist about mechanical properties of olive waste bottom ash (OW).

1.2.2 Sea Sand

It is well-known that coastal areas are rich in sea-sand and this material is widely used in concrete construction due to ease of mining and transportation, lower costs and mature technology. Moreover, many codes indicate that despite existence of chloride ions in sea sand, it is possible to use it in reinforced or precast reinforced concrete structures (ACI 2001, Ministry of construction of the PR China 2006, Architectural Institute of Japan 1993). Therefore, in this thesis, the fresh behavior and some hardened properties of SCC containing treated sea sand have been studied to evaluate the feasibility of SS utilization in this type of concrete.

1.3 Research Objectives

In recent decades, a rapid increment in production of waste and by-product materials has been identified especially due to the tremendous rate of growth in population, development of industries and technologies as well as the growth of consumerism. While natural resources are decreasing globally, wastes produced by the industries are increasing considerably.

The main purpose of this research is to introduce practical resources to produce eco-friendly materials with low cost. Particularly in this thesis the feasibility of new filler materials (OW and SS) for utilization in SCC is evaluated by different tests on rheology and mechanical properties of concrete.

1.4 Research Methodology

In this study, effects of OW and SS of different proportions on fresh properties of SCC were investigated by means of the methods introduced by EFNARC (2005). Moreover, compressive and tensile strengths, volume variations during hydration and porosity have been evaluated. Alongside, three-point bending tests (TBT) were conducted on beams with center notches for all mixes. For better evaluation of introduced fillers, similar mixes with limestone powder (LS) were prepared. LS is known as the most prevalent additive used in SCC.

1.5 Outline of the Thesis

Chapter 1 describes the scope, objectives and the methodology of the research. Also, this chapter specifies the thesis structure and expresses outputs of the research.

Chapter 2 reviews the SCC properties, materials using for SCC production, filler materials for SCC and their related influences on concrete and proportioning of

materials for SCC. Also, this chapter describes standard tests applied for evaluation of SCC.

Chapter 3 reviews the experimental work. Materials, mix design, experimental procedure for testing the quality of SCC mixes in fresh state and testing of hardened properties of SCC are included in this chapter.

Chapter 4 presents the outcomes of experiments on fresh and hardened characteristics of SCC mixes containing different percentages of filler incorporated two dosages of SP.

Chapter 5 covers the conclusions of this study. Alongside recommendations are given for further studies in this chapter.

1.6 Thesis Output

Two publications have been published in a Journal and a conference proceeding from the results of this thesis. Further article has been sent to “Advances in concrete construction” and waiting for consideration by the journal. For easy referencing, articles are listed below:

1. Cheraghalizadeh, R., Akcaoglu, T., Utilization of olive-waste ash and sea-sand powder in self-compacting concrete. Iranian Journal of Science and Technology: Transactions of Civil Engineering.
2. Cheraghalizadeh, R., Akcaoglu, T., Effects of Sea Sand Powder on Viscosity and Compressive Strength of Self-Consolidated Concrete, International Conference on Civil Engineering, Architecture and Urban Management in Iran, Tehran University, December 2018.

Chapter 2

A CRITICAL REVIEW: FRESH AND HARDENED PROPERTIES OF SCC

2.1 Introduction

SCC is defined as a high workable concrete which is compacting itself just by means of its own weight. It can also attain remarkable deformability during its fresh state while filling all corners even through narrow areas and the shapes with complex geometries. The mass made by SCC is expected to be more uniform as well as void-free. In this type of concrete, vibration is not required while segregation or bleeding does not occur (BS EN 206-9, 2010; Desnerck et al., 2014).

2.2 Development of SCC

SCC development occurred in two different phases. The early development initiated through the 1980's decade from Japan while approximately 10 years later this technology spread to Europe. The first prototype of SCC started to be produced in Japan in 1988, however the publications which focused on the principles required for SCC were published during years of 1989 to 1991 (Goodier, 2003). Afterward, concentrated studies in several places have been done in Japan, mainly in research organizations of big construction companies. Therefore, utilization of SCC has been started in several real-world applications. Later, the positive profits in utilization of SCC in Japan construction industry have attracted the other countries especially from Europe to consider SCC as a new generation of concrete. In European countries,

Sweden was the first country that started to develop SCC and later, the technology extended to the other Scandinavian countries. (Goodier, 2003)

SCC has received extensive acceptance to use in several structural applications. Nowadays, specifications and guidelines have been recommended by different organizations for this type of concrete with the aims of material and their requirements, mix proportioning and methods of necessary tests for production and assessment (EFNARC 2005; BS EN 206-9 2010). Meanwhile, beside developments of specifications and guidelines, many regions of the world started to use SCC and many wonderful constructions with this concrete have been built. (Pamnani 2014; Deeb 2013 and Badry 2015).

2.3 Advantages Versus Limitations of SCC

SCC offers several advantages compared to VC as listed below: (Okamura and Ouchi 2003):

- With SCC, vibration can be eliminated as SCC can flow around and through obstacles under self-weight. This ability is very helpful especially in congested reinforcement (Figure 1);



Figure 1: Filling ability of SCC (www.concreteconstruction.net)

- SCC allows to place the large quantity of reinforcement to small sections, mostly in high-rise structures;
- SCC improves working environment and safety due to fewer requirements to workers in case of transportation and concrete placement;
- Due to the absence of vibration, the noise pollution can be reduced, and the construction environment can be improved;
- The time of construction and the cost of labor can be reduced by SCC;
- The permeability can be decreased and therefore, in SCC, the compressive and tensile strength as well as the durability is more expected to be improved.
- Structures made by using SCC show more improved surface finish and visual appearance with the surfaces generally void-free is desired. (Naik et al., 2004). Figure 2 shows the improved surface of SCC in Perham tower in Minnesota.



Figure 2: Good surface finish by using SCC without any repairs, Perham tower

On the other hand, the probable limits of SCC utilization in comparison with VC are the cost of materials which can be greater than VC. Nevertheless, less construction time, improved productivity and enhanced condition of working may reduce the effect of this higher cost. Moreover, in several situations, the final prices can be lower. Hence, during casting of extremely congested reinforcements, SCC could be more productive and effective and also shows superior benefits compared to other concrete.

The inescapable variations in the quality and properties of raw materials could be the next important difficulty in SCC industry compared to VC. Furthermore, the mixing proportions should be controlled well-timed; otherwise, it could not be easy to be insured about the SCC quality (Ji et al. 2008). As a final limitation, it should be mention that according to the characteristics of SCC and its high fluidity, handling and similarly transportation of fresh SCC turn into susceptible activities.

2.4 Functional Requirements for SCC

Concrete needs to have enough filling ability, adequate passing ability incorporating with segregation resistance with the purpose of being classified as SCC (Figure 3). All these features must remain during whole construction processes (such as mixing, handling, transportation, placement and casting of concrete).

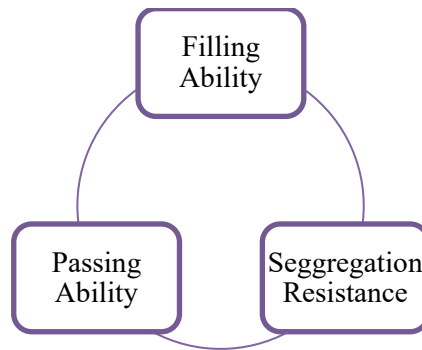


Figure 3: Functional necessities of SC

2.4.1 Filling Ability

This ability is defined as the SCC aptitude to flow by means of its self-weight and absolutely fill formwork. To attain filling ability, frictions among solid particles of SCC (coarse aggregate and fine aggregate) have to be decreased. It can be reached by adding extra quantities of water or SP. The former can reduce the friction between particles and improves the filling ability; nevertheless, this addition may leads to segregation as well as its resulting decrease in durability and strength on the other hand. The latter, dissimilar to water addition, reduces the particles friction by dispersion of cement particles resulted in maintained deformability as well as homogeneity of the mix in SCC.

To achieve superior filling ability of SCC, it is necessary to design an adequate paste in order to cover surface areas of the aggregate. This technique will be resulted in

minimizing the quantity of aggregate friction. Without the participation of the paste coat, excessive friction among aggregate would be caused and results in exceedingly limited workability.

2.4.2 Passing Ability

This ability is defined as the aptitude of SCC to pass through congested reinforced constructions or thin places by way of maintaining proper suspension of coarse aggregate in the paste in lack of blocking. It is possible to refer the passing to several parameters. Increased paste content associated with limited size and reduced amount of coarse aggregate, can efficiently improve the passing ability while the possibility of blockage can be reduced. The latter can be related to interactions between aggregate and between the reinforcement and aggregate. Wherever concrete approaches to a narrow space, unlike flowing velocities of mortar and coarse aggregate eventuate to a topically greater amount of coarse aggregate. (Noguchi et al. 1999) As a result, some of coarse aggregate can pass via narrow openings and of the remained concrete could be blocked, such as presented in Figure 4.

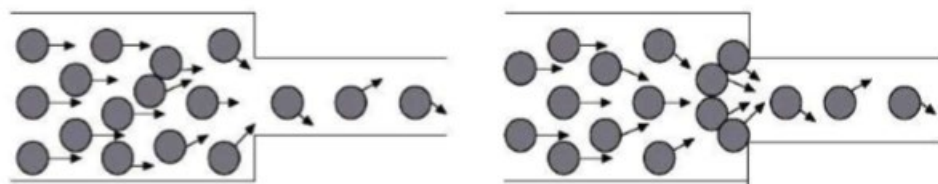


Figure 4: Schematic of blockage, coarser aggregates can bridge or arch at small openings that could be resulted in blockage of the rest of the concrete (After: RILEM TC 174 SCC, 2000)

Likewise, Okamura and Ouchi (2003) found that viscosity of the concrete paste is found to have relationship with the passing ability of SCC: very viscous paste avoids localized rises in inner stress by the attitude of coarse aggregate and consequently

SCC's passing ability will be enhanced. In order to evaluate SCC's passing ability, two more prevalent tests, named L-box and J-ring, are introduced.

2.4.3 Segregation Resistance

Stability or segregation resistance is defined as the ability of concrete to retain coarse aggregate uniformly distributed throughout flow beside rest time, till concrete has been set. An improvement in the stability of concrete is possible by creating appropriate viscosity by increment of the powder content or/and by means of viscosity modifying agents. Restricting the size and as well, decreasing the amount of coarse aggregate can reduce the risk of segregation.

All above three fundamental requirements are to a degree interrelated and interconnected. An alteration in any properties will result in changes in one or maybe both of other requirements. Both unsatisfactory segregation and filling ability give rise to insufficient passing ability. Segregation resistance improves as filling ability improves. As a result, SCC introduces as an interchange between above parameters (Pamnani, 2014).

2.5 Methods of SCC Achievements

During last two decades, comprehensive researches have been allocated to achieve self-compactibility in concrete. Generally, three different techniques have been introduced for SCC production:

- SCC with powder basis
- SCC with viscosity modifying agent basis
- The combination type SCC

Powder basis SCC can be achieved through using greater quantities of filler and cementitious material along with SP and low water powder ratios (Khayat, 1999). Increment of the powder content can be resulted in improved viscosity as well as enhanced stability concrete in fresh state. The flow efficiency is principally affected by SP. Nonetheless, the balance among stability and flow is very significant for the performance of fresh concrete.

In viscosity modifying agent type SCC, by adding viscosity modifying agents, the stability of the SCC mix improves by inhibiting segregation in concrete in absence of increasing powder amount (Khayat, 1998; EFNARC, 2005). Relevant to the utilization of powder in SCC, adding viscosity modifying agents increases the SCC robustness. Nevertheless, from economical point of view, most viscosity modifying agent type of SCC are very expensive and generally more expensive in comparison with powder type SCCs by utilization of, e.g. LS.

The last key approach to SCC is related to both other methods. For the last type, the viscosity modifying agent dosage is designed to be lower compared to the value in the SCC produced with only viscosity modifying agent and the powder amount is lower than the value in the SCC produced by just powder. Adding viscosity modifying agents reduce the powder content needed, and contrariwise. The viscosity is provided by the viscosity modifying agents in cooperation with the powder (EFNARC, 2005).

In this thesis, according to the cost and availability limitation of viscosity modifying agents, the powder type SCC was focused, produced and studied.

2.6 Filler for SCC

According to section 2.5, SCC is usually produced by utilization of high volume of paste, using viscosity modifying agents or limitation of aggregate content and/or size (Khayat 1999). Regarding to this approach, by using just cement incorporated with chemical admixture, the cost of SCC will be increased and meanwhile lead to higher temperature of hydration and resultant drying shrinkage. To prevent from these problems, it is required to utilize powder materials. These powder materials utilizations not just reduce the cost of raw materials for SCC but likewise improve the density of particle packing, stability, self-compactibility and besides the durability of SCC. Powder material introduces a material which its particles are finer than 125 μm (EFNARC 2005). These materials consist of fillers e.g. LS and cement replacement materials.

It is very important to determine the type and quantity of fillers while designing SCC. This quantity has important effect not just on self-compacting aptitudes (segregation, fluidity, etc.), but similarly on the mechanical property of the mixture. (Granata 2015) Pozzolanic/hydraulic and similarly inert fillers are generally consumed in SCC in order to increase and preserve the segregation resistance as well as the cohesion. Several industrial by-product materials such as fly ash, blast furnace slag (GGBS), silica fume and stone dust are usually utilized in the role of filler for SCC. (Uysal, Yilmaz et al. 2012) It is found that, filler types and contents have important effect on fresh properties of concrete (Elyamani et al. 2014). In Table 1 filler classifications by EFNARC (2005) according to the reactive capacity of fillers with water is tabulated.

Table 1: Filler classification (EFNARC, 2005)

Type I	Inert/ semi-inert fillers	Mineral fillers (dolomite, LS, etc.), Pigments
Type II	Pozzolanic fillers	Fly ash, Silica fume
	Hydraulic fillers	GGBS

2.6.1 Mineral Fillers

Mineral fillers define as finely graded materials which are added to the concrete mixture for attaining particular characteristics of mortar and concrete. Mineral admixtures may also be supposed as inert filler with low or without reactivity) (ACPA 2013). The cost of mineral fillers is generally less expensive in comparison to the Portland cement. This issue provides the economically advantageous alternative to SCC mixes and reduces environmental pollution in order to using by-products and especially waste materials (Uysal and Yimaz 2011).

For mineral fillers, the shape and distribution of particle size and the water absorption capacity of their particles can be effective, especially on water content and sensitivity and therefore appropriateness of using in the production of SCC. Mineral fillers with the bases of Calcium Carbonate are extensively used and able to give outstanding rheological properties beside good finish. The most beneficial portion of filler is that smaller size than 125 μ m and as a general rule more than 70% of filler should pass through 0.063mm sieve.

2.6.1.1 Limestone Powder

Limestone is a sedimentary rock which is principally made of calcium carbonate (Zhu and Bartos 2003). LS is the resultant fine material by grinding limestone rocks. It has been used as locally existing filler for mortar uses, blocks, cement and concrete

in different countries worldwide. LS particle size distribution and fineness vary by source and is dependent on the methods of grinding. Many studies in the literature show the advantages of using LS in SCC, for instance, superior workability while using lower amount of cement, better resistance to segregation and lower matrix porosity as well as pores distribution. From rheology viewpoint, LS utilization presented the reduced yield stress and also lower viscosity to SCC. Finely LS can augment the hydration speed that consequently increases early age compressive strength; nevertheless, for this issue fillers should be in general greatly finer compared to the Portland cement. LS increases the paste density, which is principally significant for improvement of compressive strength.

It is found that water and SP requirements are reduced with the addition of LS in concrete because this filler has superior particle size distribution (Nehdi et.al. 1998). Furthermore, Ghezal and Khayat (2002) reported that improved static stability as well as a decreased bleeding, can take place by adding this filler. They also concluded from their study, the viscosity beside yield stress can be reduced while LS is increasing. In another study, Yahia et. al. (2005) found a critical quantity of LS to add to concrete with the aim of increasing considerably viscosity of the concrete. They concluded in their study that the critical quantity can be associated by existing spaces in the concrete mix, and after surpassing this quantity; the distribution of particle size will not be improved and results in increased inter-particle friction.

The concrete compressive strength can be improved by enhanced workability achieved by LS utilization. This improved workability permits a decreased water quantity which can be resulted in increment in strength of concrete (Ghezal & Khayat 2002).

De Schutter (2011) studied the effect of SCC from different aspects. He has reported that LS can be effective in SCC in four ways. The first way is via physical views where the LS plays a role as nucleation places for hydration products, particularly in the phase of C3S. This action leads to faster cement hydration (The Weerd et al, 2010). The second way is about acting of LS as filler among coarser particles of cement which can improve packing density that leads to superior mechanical also transport behaviour of SCC (De Schutter et al, 2011). The next is due to the mostly inactive character of LS in concrete hydration. LS deliver a dilution influence which permits the major quantity of water to be consumed for hydration. Lastly, LS has a good potential to modify slightly the hydration phase of SCC.

2.6.2 Pozzolanic Filler

Pozzolan are whether siliceous or sometimes siliceous-aluminous materials containing no or slightly cementitious magnitude by itself; however, in a finely size, while water exists surrounding and at normal temperature, it can react with calcium hydroxide and produce mixture presenting cementitious characteristics (Mehta, 1987).

The general meaning of pozzolans lead to several materials vary extensively concerning sources, compositions and behaviour. Not only artificial but natural materials present pozzolanic activity. They are used in place of supplementary cementitious materials. Artificial pozzolan may be manufactured, e.g. through thermal activation of kaolin clays to achieve metakaolin. It may be also achieved by way of by-products or waste via high-temperature procedure like fly ash through electricity fabrication using coal. Silica fume, a by-product through melting silicon, highly reactive metakaolin, fly ash and organic residues which are burned with high

silica (SiO₂) content (for instance rice husk ash and bagasse ash) are the common pozzolans nowadays.

Figueiras et al. (2011) reported that the effect of materials with pozzolanic activities including silica fume, fly ash and metakaolin have been previously studied in development of high- performance concrete and improved workability governing with enhanced durability and strength has been achieved.

Fly ash is known to be effective while added to SCC and the mix cohesion found to be improved while the sensitivity of mix to variations of water quantities decreased. Nevertheless, great amounts of used fly ash can create cohesive mix that the resultant mixture can be highly resistant to flow.

In case of silica fume, it is found by researchers that the great level of fineness and almost spherical form of this pozzolanic material result in well cohesion and also enhanced resistance of segregation. Nevertheless, the effect of silica fume on reduction or eliminating the bleeding is reported and this property of silica fume can raise some difficulties; especially in concrete surface which can be quickly crusted. This issue can be concluded into cold joints as well as defects on surface whenever any breaks are available in delivery of concrete and similarly to troubles in finishing the surface (Elyamany et al. 2014).

2.6.3 Hydraulic Filler

GGBS is an example of this type of filler and it is a waste output from manufacturing iron. It contains reactive fine particles with a low hydration temperature. GGBS exists in cements type II or III already; however as well it exists in many countries as addition. A high quantity of GGBS can reduce robustness with the aim of

consistence control problems. It happens due to the lower speed of setting which may results in increased chance of segregation. In some countries, GGBS is available as a type I addition.

2.6.4 Other Filler

Air cooled slag, ground glass and other fillers with fine particles also have been used in SCC; however, short term and long-term effects of these materials on concrete properties must be carefully evaluated.

2.6.5 Green and Waste Material Utilization in Constructions

Green building materials are known generally as environmentally responsible (Spiegel and Meadows, 1999) or environmentally friendly (Kubba, 2010) materials, however a universally known definition of green building materials does not exist yet.

The idea of green building technology has motivated the researchers doing more to protect the environment (Wahyuni, 2014). In developing countries, applications of waste materials in place of ordinary building materials have come to be the widely held method dominating environmental problems (Chindaprasirt et al., 2008; Ismail and Enas, 2008). Reducing and recycling waste material are extremely significant issues in new decades since they assist supporting natural resources while reducing the need for worthless landfills spaces (Ling and Poon, 2011). Rice husk ash, sea shell, palm oil fuel ash, bagasse etc. are found to have good behavior for using as building materials and have been studied by many researchers.

Generally, the outcomes of many researches show that the addition of agricultural or construction waste for utilization in green concrete causes encouraging strength compared to the normal concrete (Abdul Samad et al., 2017).

2.6.5.1 Olive Waste Ash

Since the new developments in concrete production go towards green concrete, it becomes significant to study the possibility and effects of utilization of green waste materials as a component in SCC. SCC has disadvantages such as high cement content requirements and necessity to use chemical admixtures. Both requirements can increase the cost of materials. A technique for reducing the cost of SCC is to use pozzolanic/hydraulic or also waste materials. (Ranjbar et al. 2013) Moreover, by applying this method, the engineering behavior of SCC can be improved.

Olive waste residues are produced and accumulated every year in the countries with olive trees and this issue makes a significant environmental problem (Al-Akhras and Abdulwahid 2010). For example, one hectare of olive trees produces around three tons of pruning residues each year (AAE, 2008), which almost burnt or left on the ground (de Andalucia, 2009). OW as a residual biomass can be ground in a powder form and being used as an addition or replacement either to cement and/or aggregates. Therefore, in SCC production, the usage of OW could be advantageous but always there are significant worries about the behavior of this type of concrete which can be different from VC. In a study by Cruz-Yusta et al. (2011), it is remarked that, by replacing olive waste fly ash with the maximum rate of 10% of cement content the mechanical behaviour of mortar did not diminished. However, Alkhender et al. (2016) found that utilization of different percentages of olive waste in hardened blended cement paste somewhat decreased 3, 7 as well as 28 day's compressive strength. In another research by Al-Akhras et al. (2009) it is reported

that replacing different amounts of OW instead of cement in VC reduced the compressive strength however the performance of concrete exposed to elevated temperatures improved. In other research Cuenca et al. (2013) utilized olive waste fly ash instead of filler in SCC and concluded that, the produced SCC had good quality in fresh and hardened state.

2.6.5.2 Sea-sand Powder, Problems and Limitations

Sea sand is in widely use in concrete construction due to ease of mining and transportation and lower expenditures (Huiguanga et al, 2011). Sea-sand often consists of SiO₂ (silicon dioxide) in forms of crystal shapes and some other salt compounds depends on the situations but the greatest regular component of sand is SiO₂. The main worry of sea-sand utilization in concrete industry is about the durability of concrete since the sea-sand contains high quantities of salts. The United States codes and similarly Chinese and Japanese regulations specify that sea sand can be utilized for reinforced and as well precast reinforced concrete structures; nevertheless, the chloride ions content must be controlled (ACI, 2001, Ministry of Construction of the PRC China, 2006 and Japanese Architectural Standard Specification, 1993).

Most studies confirm that the chloride ion content is governable by treatment like washing sea sand with fresh water, using anti-corrosion admixtures or corrosion-resistant reinforcements. Mahalakshmi et al. (2017) found that by washing process, the rate of chloride content in sea sand can be eliminated. Consequently, purified sea sand presented sufficient compressive and tensile strength after 28 days. In another research by Karthikeyan and Nagarajan (2017), the chloride rate of treated sea sand found to be below the acceptable level of 0.075 % weight of sand. The outcomes of another research by Subashini et al. (2016) showed that concrete made by treated

sea-sand which had been washed by sufficient water presented superior strength than that of raw sea-sand and river sand and also the corrosion found to be controllable.

According to Cui et al. study (2011) on utilization of sea sand by rate of 50%-100% of fine aggregate in concrete, the possibility of applying sea sand in massive mixing quantities have been found without any harmful effect on durability as well as strength of produced concrete. In another research, the durability of concrete containing sea sand, desalinated sea sand and ordinary river sand compared to the combination of river sand and sea sand considered (Huiguang et al. 2011). The results indicated that the sea-sand concrete showed better resistance to chloride penetration compared to the ordinary river sand.

According to the literature review, it seems that SS utilization in concrete is feasible from chloride ions point of view in SCC but the influence of SS on both fresh properties and mechanical behaviour of SCC should be investigated by different experiments.

2.7 Mixing Proportions of SCC

SCC contains almost similar components like VC, e.g. cement, aggregate, water and if needed, chemical or mineral admixtures with different proportions. On the other hand, the decrease in coarse aggregate, the use of SP and powder and the decreased water powder ratio can be listed as the important differences which lead the mixture to be valid as self- compactible. The differences among composition quantities of SCC versus VC can be seen in Figure 5.

Two main dissimilarities are available in proportioning of SCC compared to VC. Former, in VC, the proportioning starts by determination of water/cementitious

materials ratio in order to fulfill strength requirements while finishes by designation the aggregate quantities. SCC, instead, is typically proportioned starting with the requirements for fresh property. Due to SCC, great cementitious and powder materials, that usually warranting higher strength compared to the required values, its design regularly do not focus on strength criterion (Ghazi and Al Jadiri 2010). Next, the behavior of SCC both in fresh as well as hardened state is not easy to forecast such as properties of VC. Moreover, additional tests are required before manufacturing SCC. Thus, it is necessary to determine the components of SCC attentively.

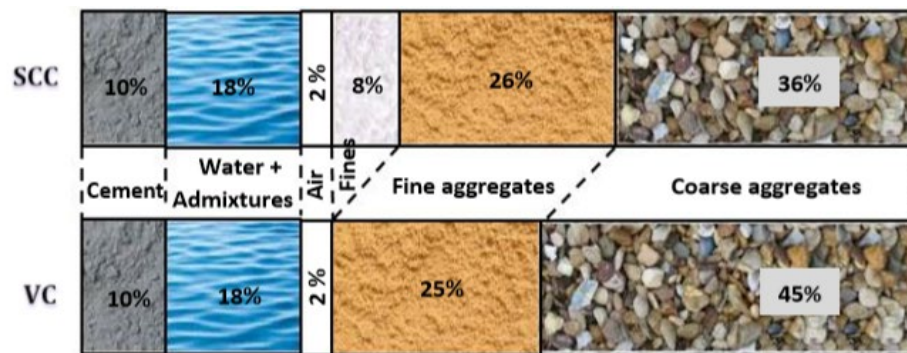


Figure 5: The schematic illustration of composition differences of SCC and VC from Okamura and Ouchi (2003)

2.8 Material Quantities for SCC

Usual proportions of components suggested for SCC production are presented in Table 2 (EFNARC 2005); however, the designed values will be dependent to the desired strength and many other performance necessities.

In a study by Domone (2006), 56 case studies constructed by SCC were focused and reported that SCC manufacturing is possible by using a wide-ranging constituent. In his study, it is discovered that the quantity ranges of used coarse aggregate were 28-

38% of the volume of concrete, the amount of fine aggregate varied between 38% and 54% of the volume of mortar, water to powder ratio ranges (by weight) were 0.26- 0.48, the volume of paste varied between 30%and 42% of volume of concrete and the powder amount varied from 445 kg/m³ to 605 kg/m³.

Table 2: Regular ranges for components of SCC

Material	Ordinary ranges kg/m ³	Ordinary ranges liters/m ³
Powder materials (cementitious materials + filler)	380–600	-
Water	150–210	150–210
Coarse aggregate	750–1000	270–360
Fine aggregate	Typically, 48–55% of total aggregate	
Water powder ratio (by volume)	0.85–1.10	

2.9 Test Methods for SCC

SCC has exclusive properties and it is impractical to use the testing methods which are used in case of VC to observe properly the fresh behaviour of the made SCC. There are several testing methods describing different behavior of SCC in fresh state; however, the more common tests applied are the tests which are summarized below.

2.9.1 Slump Flow

It is widespread to use the slump flow test for evaluation of the deformability of SCC in the lack of any obstacles (Figure 6). It is known as an effortless and common test (BS EN 12350-8 2010) and it may be performed both on sites as well as in laboratories. Three different aspects can be evaluated by this test; listing as filling ability, segregation resistance and viscosity. In SCC, filling ability can be calculated by measurement of the horizontal flow diameter. It is known that where the slump

flow diameter is greater, the aptitude of the mix to fill the formwork by the effect of self-weight is superior. The average of two perpendicular diameters as d_1 and d_2 should be reported. Then SF can be introduced out of Eq (1).

$$SF = \frac{d_1+d_2}{2} \quad (1)$$

According to Table 3, three different consistency classes are available for SCC mixes introduced by BS EN 206-9 (2010).

Table 3: Consistency classes of SCC

Slump-flow (mm)	Class
550-650	SF1
660-750	SF2
760-850	SF3

The mix viscosity can be determined through measuring the required time for SCC to touch 500mm flow named as T_{500} . Extended values of T_{500} , expresses the greater viscosity of SCC. Two viscosity different classes named as VS1 and VS2 are introduced by EFNARC (Table 4) related to whether T_{500} is smaller than 2 seconds or equal or greater than 2 seconds respectively (BS EN 206-9, 2010).

Table 4: Viscosity classes of SCC according to slump flow test

T_{500} (sec)	Class
≤ 2	VS1
> 2	VS2

Furthermore, the slump flow provides some information about segregation resistance of the mixture via visual inspection when concrete stops flowing. Segregation can be observed by the existence of paste or uneven distribution of coarse aggregate within the mixture.

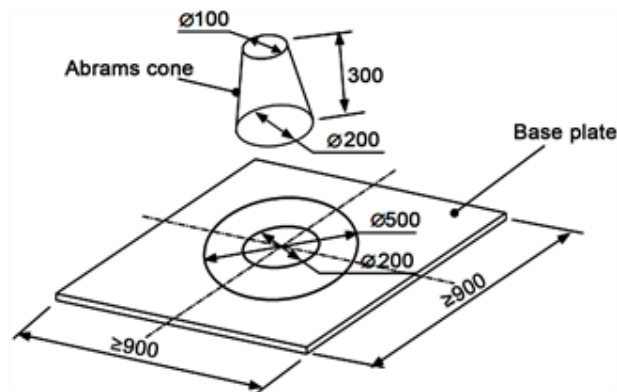


Figure 6: Slump flow test

2.9.2 V-funnel

The V-funnel test apparatus is presented in Figure 7. This test is usually applied for evaluation of filling ability as well as the viscosity of SCC (BS EN 12350-9 2010; EFNARC 2005) and is executed by evaluating the needed time for the mix to pass via the funnel by effect of its self-weight. Regarding to BS EN 206-9 (2010) classification, two classes are available for viscosity of SCC named as VF₁ and VF₂ (Table 5) depends on whether VF₁ < 8s or VF₂ 8- 25s. In SCC, segregation resistance can also be assessed through evaluating the homogeneity of SCC flow during the V-funnel.

Table 5: Viscosity classes of SCC according to V-funnel test

V-Funnel (sec)	Class
≤ 8	VF1
9 to 25	VF2

In a study by Roussel et al. (2009) it is found that the paste with low viscosity could be more exposed to blocking in close spaced areas especially with congested reinforcements. This occurrence is interrelated to the instability of mixture as well as increment of local volume fractions of coarse aggregate near obstacles due to the non-stable material.

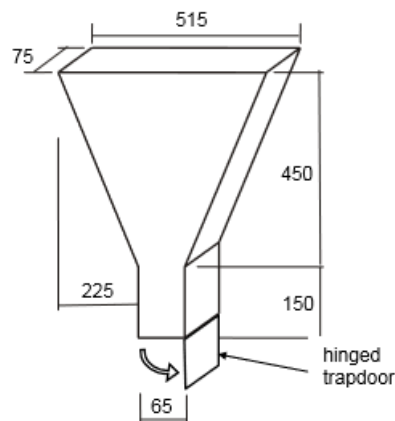


Figure 7: Schematic of V-funnel test equipment

2.9.3 L-box

This test is designed to evaluate passing ability as well as filling ability of SCC mixtures. The L-box apparatus is shown in Figure 8. The heights of SCC at both ends of horizontal unit of L-box named as H_1 and H_2 once SCC stops flowing are recorded. The ratio of H_2/H_1 characterizes filling ability of the mix which should be typically between 0.80 and 1.00. The passing ability of SCC may be also observed via checking the areas nearby rebars. The passing ability can be determined by Eq (2):

$$PA = H_2/H_1 \quad (2)$$

According to Table 6, there are two different SCC classification named as PA1 and PA2 (BS EN 206-9 2010).

Table 6: Passing ability classes of SCC according to L-box test

Class	Passing ability
PA1	$\geq 0,80$ with 2 rebars
PA2	$\geq 0,80$ with 3 rebars

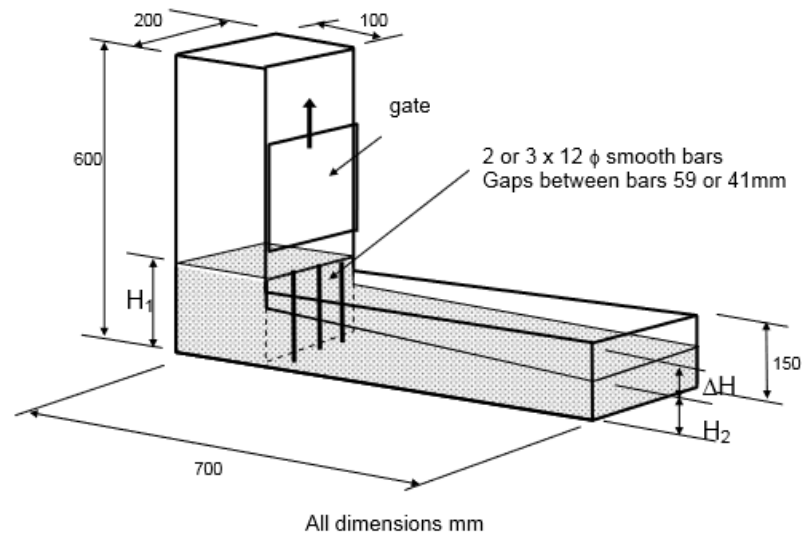


Figure 8: L-Box test equipment (EFNARC 2005)

2.10 Critical Review on Hardened Behavior of SCC

The difference concerning hardened properties of SCC and those of VC can be attributed to mainly three reasons; a different mixture magnitude, altered microstructure and lack of vibration. This part represents a review on hardened properties of SCC particularly on compressive and tensile strength, shrinkage and fracture energy.

2.10.1 Strength Characteristics of SCC

Compressive strength is a momentous property of concrete in hardened state which controls further properties. It also provides an indication of concrete quality (Neville, 1995). Many of concrete properties might be interrelated to its compressive strength

which is an exclusive engineering property of concrete regularly specified (EFNARC, 2005).

It is clear that variation in composition of concrete leads to different properties of hardened state. Different researchers studied the SCC's compressive strength with different properties. Grauers et al. (1997) found that the rate of gaining compressive strengths in SCC with age is principally similar to those of VC using equal amount of cement as well as same water/ cement ratio. It is reported by Klug and Holschemacher (2003) that in SCC the microstructure is improved by reason of the greater packing density available in the paste. Besides w/c ratio, several studies (Desnerck et al. 2014; Parra 2011; Domone 2007; Hoffmann and Leemann 2005; Persson 2001) reported that in SCC compressive strength is affected by many other aspects; for instance, cement type and cement replacement materials, materials with pozzolanic activity, size, shape and type of aggregate and type and quantities of admixtures.

As a general rule, SCC is expected to present greater compressive strength compared to VC with the same water/cement ratio. This transcendence is the outcome of better microstructure and improved homogeneity of SCC. In SCC, the enhanced microstructure is interconnected with the interfacial transition zone since it is more uniform and denser compared to VC.

As an example, the results of a research by Bradu et al. (2016), showed that SCC produced by same amount of cement and water/ cement ratio, presented greater compressive strength compared to VC. They concluded that, this is because of

packing effect of filler which reduces porosities and resulted in a denser microstructure and a more uniform stress distribution via compression.

It is reported by other researchers that presence of mineral admixtures increases the compressive strength of produced concrete. Nevertheless, GGBS and fly ash are those mineral admixtures postpone the growth of compressive strength to later ages regarding to their slower pozzolanic reactivity and/or smaller surface area. In a research by Satish et al. (2017) SCC specimens produced with different fractions of silica fume and fly ash with equal water/ binder ratio and the strengths of SCC mixes containing silica fume were reported to be greater compared to mixes with fly ash..

Sahmaran et al. (2007) found that utilization of high amount of fly ash reduces the SCC strength but improving its workability. However, Mohamed (2011) found that if higher fly ash content is replaced in place of cement, higher strength can be expected for concrete and the peak value happens by replacing 30% of cement by fly ash.

In case of waste materials, different outcomes are available in the literature review. Ahmadi et al. (2007) studied the properties of SCC produced by rice husk and stated that by replacing maximum 20% of cement with rice husk ash the quality of SCC after sixty days improved. Bagasse ash likewise has been used in concrete in many countries. It is reported that this material has the aptitude to improve properties of cement paste and concrete as well as compressive strength (Balaji & Miravali, 2015). Mortar and concrete test results of a research by Moretti et al. (2018) revealed that sugar bagasse ash was feasible to use in SCC as filler and it showed good fresh behaviour and strength levels were satisfactory for many present civil engineering uses.

The tensile strength in concrete is extremely lower compared to the compressive strength, as a result of the ease of crack diffusion under tensile loadings (Neville, 1971). Nevertheless, it is a significant property; meanwhile concrete usually cracks mostly as a result of tensile stresses regarding to loading, or by reason of environmental changes.

It is usual to evaluate the tensile strength in concrete by applying split tensile test on cylinders, where a cylinder shaped concrete specimen is located on its side and the load is applied by diametrical compression, in order to apply transversal tension (Figure 9). Basically, applied load on the concrete cylinder creates tensile stresses on the plane of load and comparatively high compressive stresses in the nearby area instantly. When the concrete cylinder is compressed by faceplates, the major tensile stresses starts to develop and at their limit, reach the fracture value, f_{spl} as Eq (3):

$$f_{spl} = \frac{2P}{\pi DL} \quad (3)$$

In this equation P is the fracture compressive force applied along the specimen generatrix, D refers to the specimen diameter and L is the length of the specimen.

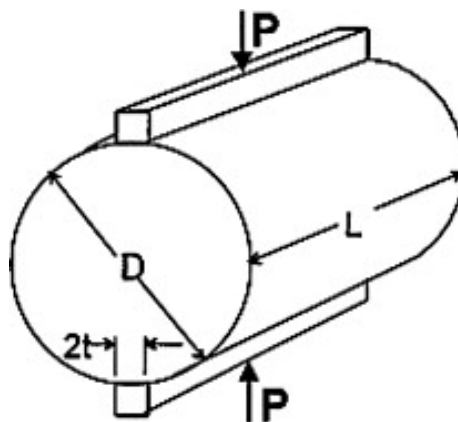


Figure 9: Splitting tensile strength test on cylindrical specimen

Regularly, the splitting tensile strength to compressive strength ratio varies between 0.06 and 0.20 (Avram et al., 1981).

SCC may be produced with any values of compressive strength. EFNARC (2005) states that for any concrete with similar strength class and same maturity, the tensile strength is as same as the values of VC because the paste volume has not important effects on tensile strength. Many studies are available on direct and, indirect tensile strength of VC and SCC with different ingredients.

In a study, the effect of different fly ash amounts on hardened properties of SCC was studied (Jalal et al. 2013). It was reported that increment of fly ash yields a decrement in 7 and 28 days flexural strength; however, after 90 days, the flexural strength was found to be improved whereas rheological properties were developed. In another study by Sandhya and Reshma (2013), the tensile strength of concrete is found to be decreased with increasing percentages of bottom ash however the strength increased with increasing curing time. In another study by Dehn et al. (2000) greater splitting tensile strengths for SCC have been stated compared to VC. Correspondingly, the bond performance was better for SCC than that of VC.

2.10.2 Fracture Properties of SCC

Regarding to the fact that higher amount of fine material, higher paste volume and also lower content of coarse aggregate used in SCC, to consider its principal parameters, its fracture behavior turns into an important subject for researchers which needs to be borne in mind.

Fracture energy is explained as the energy needed to produce a unit area of fracture surface. Several experimental results are available on the fracture energy of various

materials while most of these results were achieved by using the three-point bending test (TBT). This method is extensively used, since it is easy to perform it and it does not require too many equipment. Several researchers have investigated TBT theoretically and have developed the methods in practices. Petersson (1981) firstly utilized TBT in determination of the fracture energy in concrete. Later, most researchers have found that there is a size effect by applying TBT for determination of the fracture energy of materials. Fracture energy is a material parameter and it must be a constant value and similarly it must not be dependent to the dimensions of the specimen. For concrete materials, the dimensions of structural elements are usually larger; therefore the size effect can be more important. Nevertheless in this study, due to the comparison type of the fracture energy evaluation, the materials, size of the specimens, notches and the other geometries kept constant and TBT applied to SCC mixes to find the fracture energy ratios compared to LS mixes.

It is well-known that in concrete, properties of the interfacial transition zone and mix compositions are considerably influencing the fracture behavior of concrete (Akçaoğlu et al. 2004).

Concrete structure may be disposed to defects for instance distributed pockets of air voids some shrinkage cracks even sometimes before applying loads and likewise lenses of bleeding water. These defects develop steadily when external load applies; coalesce with previous or newly created tiny cracks till great fracture is formed and the failure of the structure occurs. After load applied, a great concentrated stress will be available nearby these cracks which is greater compared to the stresses at the other places of the structure. These formed cracks spread through service and could create critical problems in structures (Karihaloo, 1995).

2.10.2.1 Evaluation of Fracture Energy of Concrete

Several methods have been suggested for determination of fracture energy using size-dependent technique indicated by RILEM recommendation (RILEM 1985), boundary effect method suggested by Hu and Wittmann (1992) and the simplified version (SBE) proposed by Abdalla and Karihaloo (2003). The Wedge Splitting Test was also used for fracture energy determination. The methods are based on two different fracture mechanics:

- **Linear-elastic fracture mechanics** is only valid for elastic homogeneous brittle materials like glass (Karihaloo, 1995). Concrete is known as quasi-brittle material and a significant non-linearity occurs in three different regions. The first region is before maximum stress is touched (AB in Figure 10) because of the strain-hardening response of the material. The second part (BC in Figure 10) is the softening part after the achievement of the maximal load because of the randomly shaped micro-cracks. The last part is the tail of tension softening part (CD in Figure 10) produced by the aggregates interlock and another frictional effects.

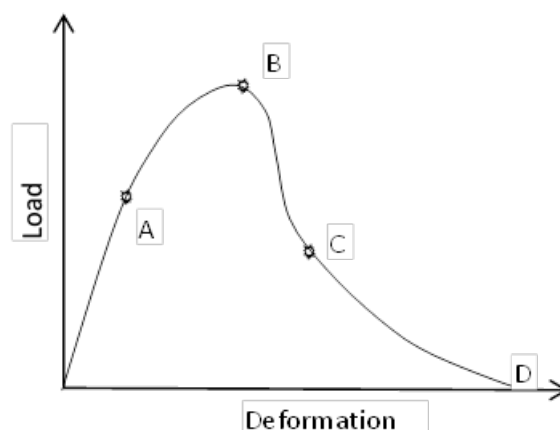


Figure 10: Typical load-deflection response for quasi-brittle materials under tension or flexural loading (Karihaloo 1995)

Thus, linear-elastic fracture mechanic cannot be applied to concrete in order to the presence of the inelastic toughening mechanism due to fracture process zone appearance surrounding a crack after crack propagation:

- **Nonlinear fracture mechanic** is capable fracture theory which to explain the material softening procedure and happens in the fracture process region (Karihaloo, 1995). The fictitious crack model is the initial non-linear theory related to the fracture mechanics of quasi-brittle materials such as concrete and introduced by Hillerborg et al. (1976). Later, another non-linear theory for fracture, named as the crack band model introduced (Bažant 1984). The application of these models requires the knowledge of two key factors: the fracture energy, G_F and the tension softening diagram of the concrete. Both factors create the foundation for evaluating the load carrying capacity of cracked concrete elements (Karihaloo 1995; Bazant and Planas 1997).

2.10.2.2 RILEM Methods for Fracture Energy Calculation of Concrete

Regarding to RILEM -50FMC (1985), in concrete, the specific fracture energy could be calculated by use of work-of-fracture method which requires TBT on notched beams of altered dimensions and notch to depth ratios. This technique, which was initially established for ceramic materials, is known as the earliest technique of evaluating fracture properties of concrete which is recommended as a standard. The foundation of using this method for concrete material was initially developed by Hillerborg and his co-workers by utilization of "fictitious crack" theory. This technique can be applied to the specimens with different geometries. Furthermore, it is suggested to use a beam with a central notch in TBT.

2.10.2.3 Work of Fracture Method by RILEM

The schematic requirements of TBT according to RILEM guideline for calculation of fracture energy of concrete and cementitious materials on notched beams is shown in Figure 11.

The fracture energy (G_f), according to RILEM definition, is the average energy which is obtained by the total work of fracture value over the cross-section area of primarily un-cracked ligament regarding to the load-displacement curve. Therefore, for a concrete beam schematically presented in Figure 11 with initial notch/depth of a , the fracture energy (G_f) could be calculated by Eq (4):

$$G_f = \frac{1}{(w-a)B} \int P d \delta \quad (4)$$

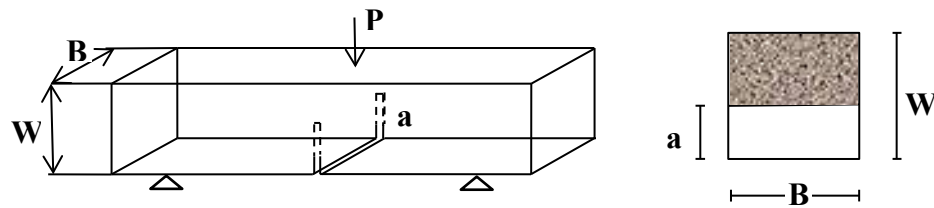


Figure 11: Notched Beam details – Three Point Bending Test

Where W is the depth of the beam and B is the thickness of the beam and $\int P d \delta$ is the area under load- deformation curve. TBT consists of the steps below:

1. The depth of the beam should be designed almost six times higher than the size of the aggregate.
2. The vertical load-deflection of the specimen should be continuously measured and plotted alongside with the applied load (P).

3. TBT should be performed in a way to create stable crack progression. During closed-loop testing the strain control must be selected. In absence of closed-loop system it is suggested to use stiff testing machine.

Hillerborg (1983-85) investigated the effect of beam dimensions on fracture energy of concrete according to RILEM TC50-FMC. In his study, this technique has been verified by twelve laboratories in diverse countries. The outcomes of his study showed that specimen size has an influence on the value of G_f . As an average, the value seems to be increased by nearly 20 % while the depth increased by a factor of 2 and by nearly 30 % once the depth increased by a factor of 3. It has been concluded from this study that the doubts in the evaluation of G_f and evaluation of the compressive strength are of about the equal importance for the calculated strength of an element. Accordingly, from this point of view the suggested G_f test seemed to be as suitable as the ordinary cylinder or cube tests for compressive strength.

Jueshi and Hui (1997) applied TBT on mortar with dissimilar sizes and reported that TBT test is a practicable procedure for determination of the fracture energy. Furthermore, they concluded that the fracture energy of large specimens would be more affected by size. To some extent, smaller beam would present a reduced amount of errors.

Therefore, in this study, in order that LS is an accepted and used filler material in concrete and test results of fracture energies of concrete are available in the literature review for this material, the TBT was applied on unique size of specimens and the results of all mixes compared.

2.10.2.4 Fracture Energy of SCC

The concern about fracture energy of SCC is principally due to the lower content of coarse aggregate used compared to VC of the similar grade. SCC is expected to have reduced capacity of energy absorption as well as reduced ductility. Beygi et al. (2013) found the decrement in fracture energy when water/cement ratio increases in SCC. Furthermore, low values of G_f for high strength SCC has been reported by Cifuentes and Karihaloo (2013).

Korte et al (2014) compared the fracture energies of VC and SCC with the same compressive strength. Their results showed that VC can bear a higher load in TBT and the fracture process in SCC progresses easier because of the less amount of coarse aggregate and the resulting lower bridging elements, which can handover stresses along fracture front. It is similarly reported by Korte et al. that concerning the energy released through forming cracks, the lesser value detected for SCC.

In a study by Eskandari et al. (2012) it is found that the fracture energy of different SCC mixes in TBT are greater for the mixes with higher values of compressive strength.

2.10.2.5 Fracture Process Zone Length of SCC

It is known that the fracture energy calculated by way of work-of-fracture technique cannot describe the brittleness of concrete (Beygi et al 2.14). Hillerborg et al. (1976) presented an expression for describing the brittleness of materials which can be calculated from G_f and f_t . Eq (5) is named as the characteristic length (l_{ch}), which demonstrates the length of fracture process zone.

$$l_{ch} = EG_F/f_t^2 \quad (5)$$

In Eq (5), E is the young's modulus where f_t is the tensile strength. Regarding to this expression, the lower is the l_{ch} value; the more brittle is the material.

Alyhya et al. (2016) found via their studies that l_{ch} is affected by the coarse aggregate content and its value increases by decrement of strength level. Cifuentes et al. (2018) found that by decreasing the water/cement ratio, an increment in G_F occurs while the coarse aggregate portion increases l_{ch} . Likewise fracture analysis of SCC by Rosiere et al. (2007) showed that increment in the paste volume is likely to make SCC more brittle.

2.10.3 Shrinkage in Concrete, Definitions and Types

Shrinkage in concrete takes the form of a volumetric reduction which starts in a short time after casting and remains for some time afterwards. However, shrinkage is affected by variations in temperature and also carbonation reactions, this phenomenon is fundamentally according to the loss of water and the decrease in the capacity of the hydrated products in comparison with the reacting constituents.

For new generation of concretes, such as SCC and high strength concrete, increased amount of fines and binder quantities are a common explanation for the large shrinkage and cracking. Meanwhile cement paste is the foremost fraction which is responsible for volumetric changes, the greater the paste volume the greater is the shrinkage (Bissonnette et al., 1999; Roziere et al., 2005; Hammer, 2007), therefore SCC is theoretically prone to high grades of shrinkage. In this study the volume changes measured by placing pins on three different directions of the 150 mm cube specimens and length changes corresponding to x, y and z directions were recorded with the passing time and used for volumetric change calculation.

Shrinkage is known as a time-dependent reduction in concrete volume in comparison to the original volume of concrete placed. Shrinkage, after setting the concrete, is the decrement in the volume of concrete with age. The decrement is related to variations of the moisture content of concrete and physico-chemical variations and happens in lack of external stress. Shrinkage is defined as a dimensionless value named strain (in/in or m/m) in relative moisture and hotness. The actual amount of ultimate shrinkage is reliant on several factors as mentioned in ACI 209R-92 (1997).

These factors are:

- Relative humidity
- Minimum thickness
- Water cement ratio
- Slump
- Air content
- Fine material content
- Member geometry,
- Curing method
- Age of concrete.
- Shapes and types of aggregate
- Hardness of aggregate

The total shrinkage which a concrete section tolerates throughout its lifetime is created by several mechanisms. Above all, phenomena for instance evaporation, hydration or carbonation may play a role in the shrinkage value of concrete (Esping et al. 2007). Nevertheless, the influence of above phenomena on total shrinkage of concrete is absolutely time-dependent. Therefore, the total shrinkage of a concrete element can be separated to:

- Early- age shrinkage that expressed the shrinkage during the first twenty-four hours after production of concrete
- Long- term shrinkage which is related to the later shrinkage (Esping et al., 2007).

Early-age shrinkage includes plastic as well as autogenous shrinkage, while long-term shrinkage consists of autogenous and drying shrinkage. It is important to mention that early-- age shrinkage is not the purpose of this study. Instead, long-term volumetric changes are particularly investigated.

2.10.3.1 Drying Shrinkage

Drying shrinkage is initiated by loss of water from the concrete element to the atmosphere. This water loss is in general from the cement paste. However, by using some types of aggregate, the maximal water loss will be from the aggregate. Drying shrinkage is somewhat slow and the stresses it enforces are to some extent controlled by tension creep compensation. The aggregate confines the shrinkage of the paste. Therefore, with using higher volume of the aggregate and choosing the aggregate with greater E values, the lesser drying shrinkage is expected. A decrement in the maximum size of aggregate results in a greater paste volume and the drying shrinkage will be increased.

2.10.3.2 Autogenous Shrinkage

Autogenous shrinkage happens in the course of setting. This reduction produced through hydration process of concrete by internal water consuming. The volume of the products is smaller in comparison to volume of cement and water before hydration process and this decrease, affects the tensile stresses and results in autogenous shrinkage. Autogenous shrinkage take places as a result of the chemical reactions which takes place throughout cement hydration. It can be important in

concrete with a very small water-cementitious materials ratio. It is likely for such concrete to shrink in the absence of any water loss to the atmosphere. Luckily, the amount of autogenous shrinkage is not momentous in the common concrete placed where shrinkage is a concern (www.master-builders-solutions.basf.us).

2.10.3.3 Plastic Shrinkage

Plastic shrinkage is expressed as a reduction in volume by reason of water movement when the concrete is yet in its plastic state, or before its setting. This water movement may be a result of hydration and chemical reactions (Sivakumar & Santhanam 2006) or because of the environmental situations leads to evaporation of water from the surface of wet concrete. Therefore, higher amounts of bleeding in concrete will be resulted in greater plastic shrinkage. Plastic shrinkage is known to be proportional to the cement quantity and, consequently, inversely proportional to the water/cement ratio.

The value of this type of shrinking may be decreased principally by preventing the rapid water loss from concrete surface e.g. by putting a layer on the surfaces of concrete with polyethylene sheeting instantly after casting concrete; by using fog spray to preserve the surface moisture; or through casting concrete at night. Another recommended method is using few amounts of aluminum powder to compensate the influence of plastic shrinkage. Correspondingly, application of expansive cement governs the shrinkage throughout the concrete setting.

2.10.3.4 Carbonation Shrinkage

Carbon dioxide (CO₂) exists in the air reacts in the existence of water by hydrated cement. During this process, calcium hydroxide transforms to calcium carbonate and likewise some further cement combinations are disintegrated. This type of complete disintegration of calcium compound in hydrated cement is chemically probable even

at the low pressure of CO₂ in standard atmosphere. Carbonation penetrates through the exposed surface of concrete but very slowly. The rate of CO₂ infiltration is reliant on the wetness of concrete and the related humidity of the surrounding ambient. Carbonation shrinkage is likely produced through the dissolution of calcium hydroxide crystals and deposition of calcium carbonate instead. The new produced compound has lower volume compared to the product replaced product and therefore, shrinkage occurs.

2.10.3.5 Shrinkage in SCC

Studies on SCC shrinkage are restricted and very hard to compare the values reported by different researchers since each of them has used different mix proportions; however, the values and formulae known for VC are valid for SCC in many codes for instance the Eurocode. It is stated in EFNARC (2005) that the deformation affected by shrinkage can be higher in SCC mixes. Craeye et al. (2010) studies on SCC specified that SCC mixes produced by LS showed great autogenous shrinkage; Therefore, produced mixes showed greater cracking capacity. Turcry and Loukili (2003) found the plastic shrinkage of SCC minimum twice higher compared to VC. Rols et al. (1999) indicated that in SCC, drying shrinkage is 50% higher compared to that of VC which made with the equal cement content. Kim et al. (1998) obtained similar results, with drying shrinkage in SCC between 30% and 50% higher than VC. Loser and Leemann (2007) also reported higher values of shrinkage for SCC. However, other studies found minor differences among both types of concrete (Persson 2001, Vieira and Bettencourt 2003, Pons et al. 2003, Seng and Shima 2005, Collepardi 2005). Evenly in some studies, lower autogenous shrinkage found for SCC (Heirmsn et al. 2007). Piérard et al. (2005) recorded similar total shrinkage for

both types, but they specified that developed kinetics and the relationship amongst autogenous and drying shrinkage are dissimilar.

It is necessary to point out that almost above investigations compared SCC contained additions to fulfil the demand of fines and to the reference VC. The additions modify the properties of material and can consequently affect shrinkage. In fact, shrinkage could increase while silica fume or GGBS quantities are amplified (Jensen and Hansen 1996, Tazawa and Miyazawa 1999). Rao (2001) also noticed a growth in drying shrinkage of young age concrete while using silica fume, but with minor long-term effects.

2.10.4 Presence of Porosity in VC and SCC

Porosity defines as the fraction of empty space volume of the total volume and measuring the spaces between the materials. According to the above definition, porosity varies between 0 and 1. It can be also presented in the form of percentage which varies between 0 and 100%. Porosity is influenced by material type and size, pore distribution and compositions. As a well-known rule, an increase in porosity results in lower strength in solid materials.

Concrete constituents, casting, curing and hardening condition, cement reactions and freezing thawing risks, all are effective on porosity. (Tepfers 2012). The porosity of concrete induces different effects on properties of concrete.

Well-compacted VC produced with low-porosity aggregate is expected to act as a multiphase material containing of coarse aggregates particles placed in mortar matrix while the mortar matrix contains hydrated and un-hydrated cement, fine

aggregate, etc., as well as the pore system (Soroka, 1997). The pore system in cement-based materials includes four different forms of pores listed below:

- gel pores or micro-pores with the dimension of 0.5nm to 10 nm;
- capillary pores or meso-pores with average diameter alternating from 5nm to 5000 nm;
- macro-pores regarding to intentionally entrained air and
- macro-pores regarding to insufficient compaction.

Additionally, to the listed pores above, cracks may be detected at mortar-aggregate interface because of shrinkage. The gel pores, regularly with the size of 1.5–2.0 nm, have not significant effects on concrete strength because of its porosity. Capillary pores and other greater pores, alternatively, are the reasons of reduction in elasticity, strength, etc. (Neville and Brooks, 1990; Newman, 1996). Therefore, influence of the gel pores in the total porosity as well as the distribution of pore size in concrete may be overlooked, without presenting any substantial errors (Kumar and Bhattacharjee, 2003).

SCC is well-known from the perspective of “pore microstructure” mostly due to the used fillers and absence of vibration. Durability and pore distribution of SCC are interrelated and somewhat dissimilar to VC. (El Mir and Nehme 2015) Due to ultra-fine materials use in SCC, several researchers have stated that use of these materials, for example LS, enhances compactness of SCC matrix and thus the porosity of ITZ between paste and aggregate paste is expected to be decreased. Furthermore, El Mir and Nehme (2015) reported that SCC mixes had lesser total porosity values compared to VC. Moreover, overall porosity was inclined to be increased in SCC mixes with respect to water/ powder ratio.

On the other hand, Kasemchaisiri & Tangtermsirikul (2008) study stated that overall porosity of SCC was amplified by using greater amounts of bottom ash; besides, the study of Kristiawan et al. (2016) clarified the influence of incorporating high volume of fly ash (50-70% fly ash instead of total binder) on the porosity of SCC. The effect of fly ash quantity on the porosity of SCC seems to be reliant on SCC age. Earlier than 56 days age, SCC mix containing fly ash tends to have increased amounts of air voids however at 90 days age, the volume of pores tends to be decreased.

There are researches similarly which use nanomaterials with high surface area such as nano silica, graphene nanosheet, nano alumina, carbon nanotube and nano Titania as minor additions to further reduce the pore volume fraction of hydrated cementitious matrix (Konsta-Gdoutos et al., 2010; Ghafari et al., 2015).

2.10.4.1 Detection of Porosity by X-Ray CT

While porosity is one of the significant factors affecting the mechanical properties, transport properties and durability of cement-based materials, its evaluation comes to be very important. In a study, the porosity of the pervious concrete material was evaluated by measuring weights and analyzing images of X-ray CT by Ahn et al.(2014) The results of this study confirmed that the results achieved by 2D X-ray CT is close to that of weight measurements method.

In another research, Latief et al. (2017) applied digital imaging of concrete by utilization of high-resolution tomographic imaging by means of X-Ray μ CT with high, medium and standard qualities to measure the porosity and evaluate the characteristic of structural elements.. It is summarized in this study that greater resolution does not always assurance to generate images with respectable detail of specimens.

Manahiloh et al. (2012) studied the fraction of clogging in previously produced concrete specimens cored from parking lots by utilization of X-Ray CT images to evaluate the nature and ranges of clogging. In their study meaningfully lesser porosity values were found for old cores in comparison to newer cores.

KeShu and Qiong (2014) studied the local porosity distribution on cement paste by X-ray CT. Average porosities achieved by this method were comparable with the gravimetric results; however, the resultant quantities found to be greater than the results of the corresponding Mercury intrusion porosimeter. Moreover, it is concluded in this study that this method is useful since it is nondestructive and likewise it can be used for porosity studies of all types of cement-based materials such as mortars and concretes. Promentilla et al. (2008) utilized X-ray μ CT for evaluating the porosity in cementitious materials characterized the entrained air void system in all three dimensions. Similarly, in the study of Promentilla and Sugiyama (2010), the porosity and cracks in non-air-entrained as well as air-entrained Portland cement and fly ash mortars are investigated by X-ray μ CT after subjecting the specimens to freeze-thaw cycles.

Chapter 3

MATERIALS AND METHODS

3.1 Introduction

In this study, fourteen different SCC mixes including various types and proportions of powder materials incorporated with two different dosages of SP were produced. Details of the mixes and the methods of testing are available in this chapter.

3.2 Materials Used for SCC Mixes

Details and sources of used materials are as following:

- **Cement:** Type 2, 42.5 MPa slag Portland sulfate resisting cement was used which satisfies by European standard EN 197-1 (2002). Chemical compositions of used cement are tabulated in Table 7.

Table 7: Chemical and physical properties of cement and fillers used

Composition (%)	Cement	LS	SS	OW
CaO (%)	61.70	36.48	26.9	21.17
SiO ₂ (%)	18.35	0.58	45.4	31.96
Al ₂ O ₃ (%)	2.22	0	0.65	2.33
Fe ₂ O ₃ (%)	2.89	0.23	1.05	2.58
MgO (%)	2.42	15.98	3.02	4.52
SO ₃ (%)	2.6	0.18	0.08	1.81
Loss on ignition (%)	1.11	40.38	23.32	23.19
Insoluble residue (%)	0.06	-	-	-
Physical properties				
Specific gravity	3.15	2.70	2.57	2.23
Percent passed from 45 μm sieve (%)	96	-	-	-
Percent passed from 75 μm sieve (%)	-	63	76	68
Percent passed from 90 μm sieve (%)	99	-	-	-
Percent passed from 125 μm sieve (%)	-	100	100	100

- Aggregate:** Graded crushed coarse aggregate of 10 mm maximum size with specific gravity of 2.8 and water absorption of 2.1% and crushed sand with specific gravity of 2.65 and water absorption of 1.5% were used throughout this study. The grading curves of coarse and fine aggregate are shown in Figures 12 and 13 respectively.

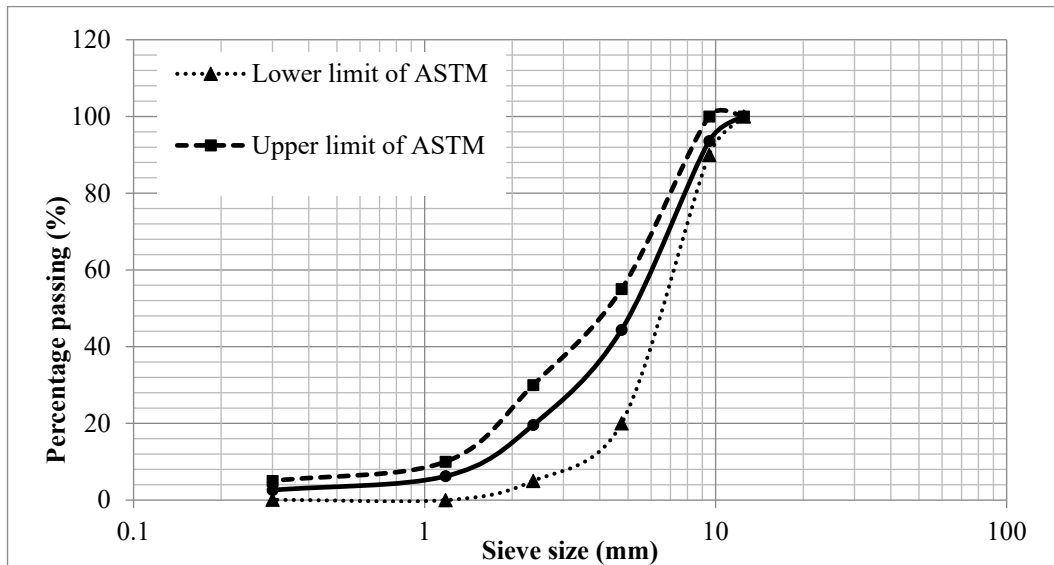


Figure 12: The gradation of the coarse aggregate and the reference curves

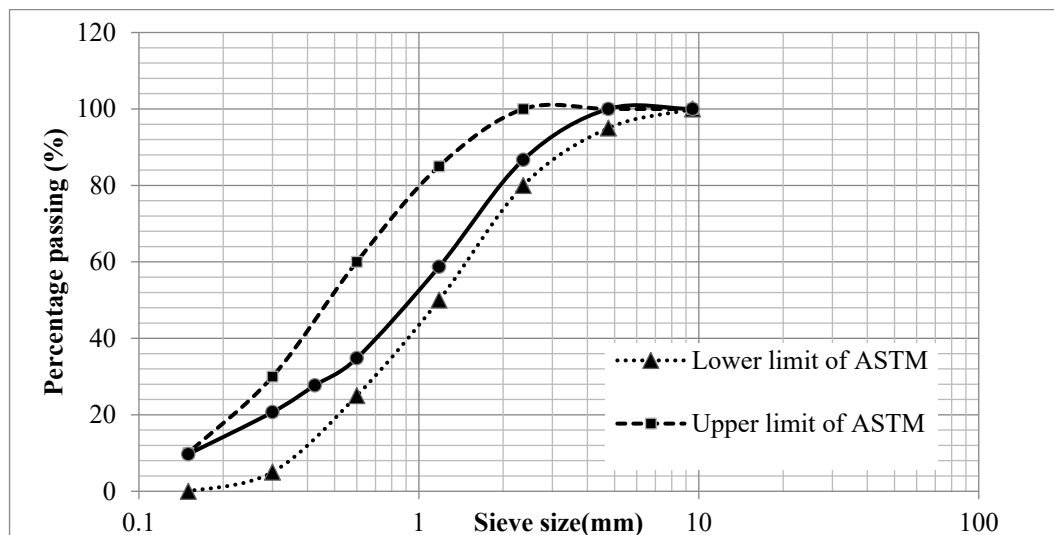


Figure 13: The gradation of the fine aggregate and the reference curves

- **Water:** Ordinary tap water was used for mixing and curing process.
- **Superplasticizer:** SP was a new generation of high range water reducing admixture with the base of polycarboxylic ether developed for using in high performance concrete and SCC which is known as Glenium 27 and consistent with EN 934-2 (2009). Chemical compositions of used SP are shown in Table 8. In this study, SP used as 1.5% and 2% of cement content in SCC mixes according to the manufacturer's suggestions.

Table 8: Manufacturer's Stated Values for Glenium 27

SG	PH	Alkali %	Chloride %	Chlorine%
1.044	7.40	less than or equal to	less than or equal to	less than or equal to
		2.0	0.10	0.10

3.2.1 Powder Materials Used for Aggregate Replacement

Details of three different powder materials used for aggregate replacement in three different proportions are given below:

3.2.1.1 Limestone Powder (LS)

LS filler was from local Mountains in Cyprus. LS used for SCC mixes passed through sieve number 120 to be smaller than 125 μm and used as 10% and 15% of total aggregate content. Chemical compositions of used LS are shown in Table 7.

3.2.1.2 Sea Sand Powder (SS)

Sea-sand gathered from different coastal areas of Mediterranean Sea in Cyprus, washed three times and ground with the grinding machine to small particles. Then similar to LS, this filler passed through sieve number 120 and used as 10% and 15%

of total aggregate content. Chemical compositions of used fillers are shown in Table 7.

Before starting the experiments, a series of tests were performed on sea sand to find the lowest rate of chloride ion content in different samples of this material. It was observed that after three times washing, the chloride ion content was the lowest and did not change by more washing. In all cases the chloride ion content found to be lower than 0.045% after 3 times washing with water.

3.2.1.3 Olive Waste Ash (OW)

In olive oil factories, after olive oil production, olive waste is self-combusted in ovens for boiling water or just pressed in shape of cylinders for energy source of chimneys (Figure 14). After collecting self-combusted olive waste from the factories; it has been ground in grinding machine in laboratory and passed through sieve number 120 to confirm the requirements for filler material and used as 5%, 10% and 15% of total aggregate content. Chemical compositions of used fillers are shown in Table 7.



Figure 14: Olive waste cylinders for energy source of chimneys

3.3 SCC Mix Materials and Proportions

The mix proportions were determined with the design based on EFNARC method (2005) as tabulated in Table 9. Total aggregate content was designed equal to 1800 kg/m³ with coarse aggregate/total aggregate ratio of 0.45. Water amount kept constant to 189 kg/m³ for all SCC mixes. SS and LS were used to replace 10 and 15% of total aggregate content where OW was used to replace 5, 10 and 15% of total aggregate by weight. At the same time, two dosages of SP as 1.5% and 2% by mass of cement were used. It is important to mention that trial mixes were made by LS before starting main mixes to achieve the self-compact ability and good quality of SCC in fresh state.

Table 9: Mix proportions and properties of SCC

Sample ID	C (kg)	C.A. (kg)	F.A. (kg)	LS (kg)	OW (kg)	SS (kg)	SP (kg)	W (kg)	W/b
LS10SP1.5	402	729	891	180	-	-	6	189	0.32
LS15S1.5	402	688	842	270	-	-	6	189	0.28
LS10SP2	402	729	891	180	-	-	8	189	0.32
LS15SP2	402	688	842	270	-	-	8	189	0.28
SS10SP1.5	402	729	891	-	-	180	6	189	0.32
SS15SP1.5	402	688	842	-	-	270	6	189	0.28
SS10SP2	402	729	891	-	-	180	8	189	0.32
SS15SP2	402	688	842	-	-	270	8	189	0.28
OW5SP1.5	402	770	940	-	90	-	6	189	0.38
OW10SP1.5	402	729	891	-	180	-	6	189	0.32
OW15SP1.5	402	688	842	-	270	-	6	189	0.28
OW5SP2	402	770	940	-	90	-	8	189	0.38
OW10SP2	402	729	891	-	180	-	8	189	0.32
OW15SP2	402	688	842	-	270	-	8	189	0.28

C: Cement, C.A: Coarse Aggregate, F.A: Fine Aggregate, W: Water, b: binder

3.4 Experimental Procedure

In this part, the methods of mixing and applying tests are describing. Moreover, for better understanding, figures and photographs are available in this chapter.

3.4.1 Mixing Procedure

The batching sequences, which are presented in Figure 15, contained of homogenizing the coarse and fine aggregates for approximately 5 seconds in the mixer, at that moment adding almost one third of the designed water to the mixer and mix for 30 seconds. Afterward, cement and filler were added. The mixing process was continued for more 30 seconds. At that point, the second third of designed water was added and let the mixer to continue mixing for 1 minute. The SP mixed with remaining water at the last step was introduced and the concrete was mixed for last 2 minutes.



Figure 15: Mixing process of SCC

3.4.2 Fresh SCC Tests

After mixing, SCC mixes were tested to evaluate fresh properties desired for self-compatibility of concrete. According to EFNARC (2005), generally it is required to specify just the consistency classification by slump-flow test. However, in this study, three different classifications (slump-flow classes, viscosity classes and passing ability classes) according to EFNARC (2005) have been specified. All fresh tests were performed during a period of 10-15 minutes after the mixing had been completed in order to decrease the influence of workability loss on the variation of test results.

3.4.2.1 Slump Flow Test

Sump flow test applied on all SCC mixes according to BS EN 12350-8 (2010). Besides, T_{500} time also recorded for all mixes during this test.

3.4.2.2 V-Funnel Test

In this study, the passing ability of all SCC mixes evaluated by V-funnel test according to BS EN 12350-8 (2010). Furthermore, beside direct results of this test, it was possible to observe any probable segregation or obstacles in passing process of SCC.

3.4.2.3 L-Box Test

The last test applied on fresh SCC was L-Box test which previously described in 2.9.3.

3.4.3 Hardened SCC Evaluation

Immediately after mixing of SCC and fresh tests, mixes were cast into 150 mm cubic molds, 150 mm x 300 mm cylinders and 100 mm x 100 mm x 500 mm prismatic molds. The test specimens were left to stand for 24 ± 2 hours in the standard curing room, after which they were demolded and immersed in water curing tank. Compressive strength, splitting tensile strength, pore analysis before loading by X-ray CT images and fracture analysis by TBT tests were carried out after different days of water curing.

3.4.3.1 Compressive Strength Measurements

Three specimens from different batches prepared for compressive strength tests for each three different ages. After 24 ± 2 hours curing in curing room, each specimen demolded and kept in water tank according to the defined tasting age (7, 28 and 91 days). After removing the specimens from water tank and removing the surface water, compressive strength test applied to SCC cubes according to ASTM C39.

3.4.3.2 Splitting Tensile Strength Test

According to ASTM C496, for correct positioning the specimens before beginning the splitting tensile test, diametral lines should be applied on each end of the specimens with a suitable device or instead, an aligning jig could be used. In this study, an aligning jig and bearing strip alignment used for SCC cylinders. The specimen positioned by use of the alignment jig in the following order (Figure 16): The splitting tensile strength calculated by Eq. 2 in section 2.10.1.



Figure 16: Placement of cylindrical specimen in aligning jig for splitting tensile strength

3.4.3.3 Porosity Analysis of SCC by X-Ray CT and ImageJ Computer Program

In this research porosity analysis was evaluated by using X-Ray CT method on 150 mm cubes. Specimens cured for 24 ± 2 hours in curing room and 7 days in a standard curing tank; kept in the laboratory area and prevented from sun light and send for X-Ray CT imaging at 91 days age in Cyprus Central Hospital in Famagusta. Later,

images exported from X-Ray CT by Radiant program, were analyzed by ImageJ computer program for sections parallel to the casting direction (1cm from each four edges and the center sections). By this inspection, for each specimen, six pore section areas were obtained. The average result of two central sections and four edge sections of each specimen is reported as an average pore area. The locations of the three defined sections in X-direction are shown in Figure 17.

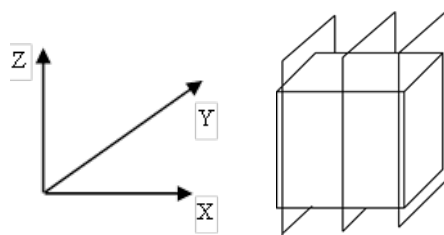


Figure 17: Schematic representation of the X-RAY CT image locations along X-direction

3.4.3.3.1 X-Ray Computed Tomography for Internal Inspection

X-Ray is extensively used for medical diagnosis because of its ability to pass through matter and provide high-resolution images. It has also used in the inspection and analysis of paintings since it can expose such details like the age of a painting and underlying brushstroke methods which help identifying or verifying the artist.

X-Ray is likewise extensively used for nondestructive analysis of industrial products for defects. It can be used to evaluate circuit boards, metal parts, concrete structure, etc. The quality of the scanned image is a quantity of the noise, the slice thickness, the low contrast resolution and the high contrast resolution. These qualities are governed by the X-ray source, X-ray detectors utilized and the scanning configuration (Onifade, 2013).

3.4.3.3.2 Concrete Assessment by X-Ray CT

At the present time, X-ray CT is being practical in the field of structural engineering. Scanning concrete specimens by X-ray CT utilization offers an insight into the inner structure without any need to destroy the specimen (Balazs et al, 2018). X-ray images can be also used for nondestructive monitoring of the beginning, extension, and arrangement of cracks in concrete (Lei et al., 2018). In Lei et al. study, they utilized CT images of the damage process of concrete under both static and dynamic loadings. They studied concrete CT images from various scanning planes to determine the relationship of concrete strength and different loadings (Lei et al., 2018).

3.4.3.3.3 Different X-Ray CT Methods for Specimen Evaluation

Both medical and industrial X-ray CTs exists for non-destructive testing. However, in spite of the noticeable accuracy and quality benefits of industrial CT systems, the cost of these systems regularly exceeds those of medical CTs. As well as purchase price, the scan-time strongly affects the price per scan to the end-user.

Usual industrial X-Ray CT times are still 30–60 minutes or more dependent to the required quality (Du Plessis and Rossouw, 2015) while complete a full scan takes just 5 seconds for medical CT scanners (and more few minutes for cooling-down for the system). This dissimilarity is momentous and permits, e.g., minimum 10 specimens to be scanned in a medical CT system, in the same time, as just one get scanned in an industrial CT system (with conservative estimates). Of course, faster industrial scanners are presented worldwide and in use nowadays dedicated for industrial CT and which are meant for in-line process applications, nevertheless these systems are more costly.

Du Plessis et al. studied the advantages and disadvantages of medical and industrial micro CT scanners on exact same four large objects (De Plessis et al., 2016). Results of this study indicated that by utilization of medical CT scans valuable data can be produced with considerably shorter times. This ability introduces medical CT scans as a certain worthy alternative for non-destructive tests, mainly where numerous numbers of specimens and only reasonable resolution is necessary. Another benefit is its aptitude in scanning larger objects compared to typical μ CT systems.

3.4.3.3.4 Rapid X-Ray CT on Concrete, Quality and Advantages

X-Ray CT has several possible uses in materials sciences particularly likewise for porosity analysis. In a research by de Plessis et al. (2014), the same specimens were studied by scanning ranges from 5 to 100 μ m resolutions, proving the multiscale aptitude of commercial CT scanners. Scans completed at typical high-quality situation (1-hour duration) compared to very rapid scans (5 minute) were also taken and it was proved that beneficial information was still achieved from faster scans with lower quality. Also, they found a decrement in average porosity quantity because of the lower quality of images, principally in line for increased noise and some pores; wherever small pores not segmented appropriately. The size distribution histogram was very comparable, and the data analysis found to be sufficiently good, particularly where larger pores are desired to determine and numerous specimens needed to be studied.

3.4.3.4 Computer programs for porosity evaluation of X-Ray CT images

Image enhancement techniques permits the increasing of the signal-to-noise ratio and accentuates image structures by adjusting the colors or intensities of an image. They similarly contain linear and nonlinear filtering, deburring and automatic contrast increment. Image processing methods have been utilized for medical

science to assist differentiating the irregular tissue growth (called tumors) from other tissues as well as further detailed information concerning head injuries, stroke, brain disease and internal structures.

Image processing programs such as Adobe Photoshop, ImageJ, Corel Photo Paint, origin software etc. are widely used for X-Ray images in order to achieve better qualities for quantitative analysis. Among all, ImageJ is well-known as a public domain Java image processing program which is appropriate for measuring distances and angles, calculating areas and pixel value statistics of selections defined by the users and preparing the density histograms.

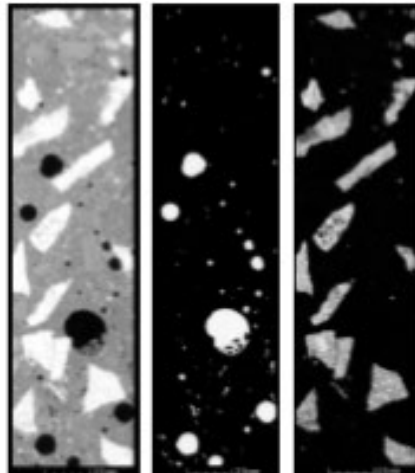


Figure 18: Tomography images of a concrete cylinder (left) and air voids (center) and the image processing of the aggregates (right)

The image processing procedures generally used to segment a tomography can be distinguished in threshold, edge detection and region based-techniques. Typically, an arrangement of techniques is used together. The threshold methods, the most common histogram-based method, are used to separate some component (foreground) from the rest of the image (background). These methods are particularly efficient when the attenuation coefficients of the components of an object are

strongly different. This can be the case for composite materials such as reinforced concrete (Lunardelli, 2017).

3.4.3.5 Fracture Energy Calculation of SCC

In this study, three 100 x 100 x 500 mm beam specimens from each fourteen mixes were cast. The specimens were de-molded after 24 ± 2 hours after casting and cured in water tank for 28 days. Afterwards, specimens kept in ambient temperature for 91 days. The beams were cut to the depth of 40 mm (notch/ depth ratio of 0.4) (Figures 19 and 20), with a thin concrete saw before starting TBT.



Figure 19: Front view of a beam with applied notch



Figure 20: Prismatic beam prepared for fracture energy test with 40 mm notch

The notch was cut in one side of the specimen regarding to its molded position hence the specimen would be turned on this side for loading, with the casting surface in vertical position.

TBT test was applied to produce stable crack growth. According to Uday (2017) it is suggested that if a closed-loop system is not available, then it is required to use a stiff testing machine.

For TBT test, both supports were hinged supports which had rollers. The supports were horizontally movable in order to prevent any restraints on the deformation till the specimen totally ruptured. With the aim of be ensured the nonappearance of horizontal restraints, according to JCI-S-001 recommendation (2003), the specimens pressed lightly with hand before applying any load to be sure that the specimen in the horizontal direction could have smooth movements.

Load was applied in the downward direction at the beam center (Figure 21) and by every load increment; deflection at center of the beam was recorded.



Figure 21: Notched beam under TBT test

3.4.3.6 Shrinkage Measurement in Concrete by Demec Gauge

The DEMEC Mechanical Strain Gauge developed as a trustworthy and perfect way of recording strain measurements at different points on an element by using a simple apparatus. Standard gauge lengths are available from 50mm to 500mm; nevertheless, larger length of maximum 2000mm may available due to requests. The DEMEC strain gauge is an appropriate instrument for measuring and monitoring shrinkage and cracks of several structures.

The desired accuracy is only achieved by precision production and care in the use of the instrument (ELE International 2003). The Demec strain gauge consists of a main beam with two conical locating points. One of these points is fixed while the other pivoting on a special knife edge. The points locate in perforated stainless-steel discs and these discs should be glued to the elements with adhesive. Movement of the pivoting point can be measured by use of the strain gauge attached to a base plate on the beam. This instrument is designed in a manner to minimize the thermal movement within Demec gauge, so this movement becomes negligible in strain calculations.

In this study, for volume change measurements, pins were placed on three different surfaces of cube specimens (Figure 23). Therefore, length changes corresponding to x, y and z directions were recorded over time. Measurements were recorded after 7 days of standard curing in water tank and continued up to 30 days. Length changes according to X, Y and Z (casting direction) directions will be ϵ_x , ϵ_y and ϵ_z (Figure 22 and 23). Consequently, the volumetric change will be calculated by Eq (6).

$$\epsilon_v = \frac{\Delta V}{V} = (\epsilon_x + \epsilon_y + \epsilon_z) \quad (6)$$

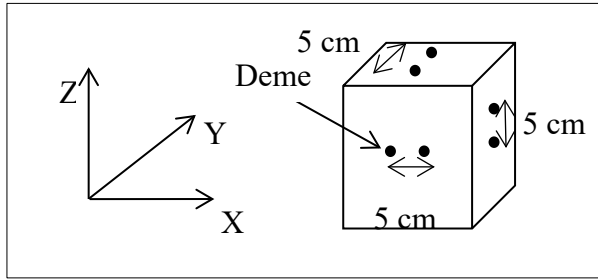


Figure 22: Demec positions on the cubes and Demec Gauge instrument



Figure 23: SS specimen with pins in three directions for volume change measurement

Chapter 4

RESULTS AND DISCUSSIONS

4.1 Effect of Filler Type and Amounts on Fresh Performance of SCC

According to BS EN 206-9 (2010), the higher the slump flow amount, the superior the SCC ability to fill formwork under its own weight and a value of 550-850 mm is required for SCC; however, it is mentioned that higher target values can be considered for particular cases; but great care must be taken about segregation. In this study, slump flow found to be in the ranges of 450-920 mm for all mixes (Table 10 and Figure 24). The consistency classifications of all SCC mixes are also tabulated in Table 10. As expected, in this study, slump flow decreased with increasing filler for both SP quantities; however maximum decrease occurred for OW mixes. In OW mix with 1.5% SP, by increasing OW amount from 10% to 15%, slump flow decreased by the highest rate equal to 25%. In general, SS specimens showed higher slump flow results compared to other mixes for both SP quantities.

Table 10: Result of SCC classification according to BS EN 206-9 (2010)

	SF	Consistency class	Viscosity class (T_{500})	VF	Viscosity class (V-Funnel)	Passing ability class (L-Box)	f_{spl}	$f'_{c,91}$
LS10SP1.5	73	SF2	VS2	9.5	VF2	PA2	4.63	76.9
LS15SP1.5	67	SF2	VS2	12.5	VF2	PA2	3.187	72.5
LS10SP2	79	SF3	VS1	10.5 3	VF2	PA2	2.78	72.6
LS15SP2	74	SF2	VS2	12	VF2	PA2	3.34	75.4
SS10SP1.5	80	SF3	VS1	9.8	VF2	PA2	4.68	74.8
SS15SP1.5	74	SF2	VS2	11.2	VF2	PA2	4.23	76.5
SS10SP2	92	*	VS1	20	VF2	PA2	4.163	65.2
SS15SP2	81	SF3	VS2	10.1	VF2	PA2	3.5	75.1
OW5SP1.5	72	SF2	VS2	11	VF2	PA2	2.6	44.5
OW10SP1.5	60	SF1	VS2	12	VF2	PA1	2.62	38.7
OW15SP1.5	45	*	VS2	∞	*	*	2.46	37.7
OW5SP2	79	SF3	VS2	9	VF2	PA2	2.8	47
OW10SP2	65	SF1	VS2	11.5	VF2	PA1	2.81	42.8
OW15SP2	55	SF1	VS2	21	VF2	*	2.68	40.5

*Not satisfied by BS EN 206-9 (2010) requirements

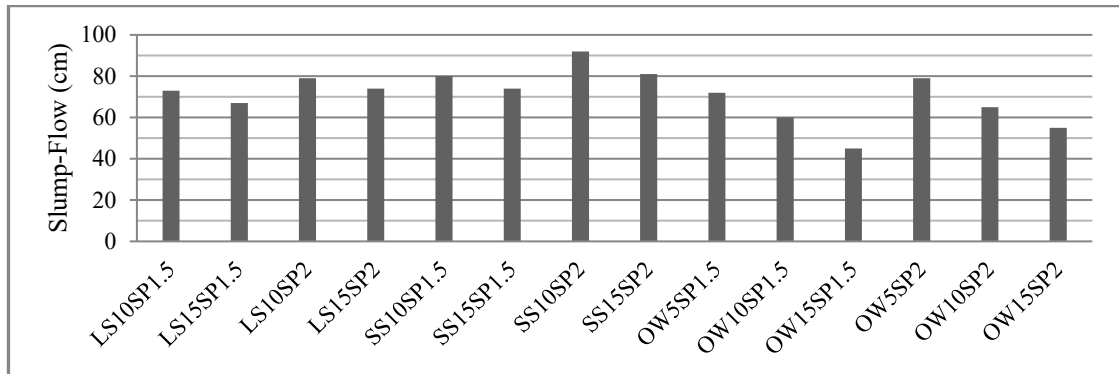


Figure 24: Effect of filler type and quantities on slump flow of SCC

In this study, all mixes were in the acceptable numerical ranges of BS EN 206-9 (2010) except SS10SP2 and OW15SP1.5. SS10SP2 found to have the highest slump flow (920mm) which is greater than 850mm (the highest limit suggested by BS EN 206-9). Furthermore, this mix showed comprehensive bleeding and segregation

(Figure 25). On the other hand, the lowest workability occurred for OW15SP1.5 mix with 450 mm slump flow result. It is worth mentioning to say that no bleeding and segregation were recorded for OW specimens while some amount of bleeding and segregation was recorded for LS10SP2 by visual inspection during slump flow test. Previously it is found that by adding LS in SCC, improved static stability and decreased bleeding can be achieved (Ghezal and Khayat 2002).

During slump-flow test, SS mixes with 10% filler (SS10SP1.5 and SS10SP2) and LS10SP2 showed less than 2 seconds results for slump flow_{T500}. All other mixes showed greater time for this test. The greatest time achieved for LS15SP1.5 with 3.2s slump flow_{T500} outcome.



Figure 25: Bleeding and segregation in slump-flow test of SS10SP2

In Figure 26 the sections of cylindrical crushed specimens under splitting test are shown. Among LS specimens, LS10SP2 found to have bleeding since the less segregation and most uniformity occurred for LS10SP1.5. It seems that 2% SP is excessive for all fillers except OW. For OW in all cases no bleeding and segregation were recorded.

Results of V-funnel tests are shown in Table 10 and Figure 27. According to EFNARC (2005), for SCC, 10 seconds flow time is stated to be appropriate while prolonged times could be the sign of the susceptibility of blocking. Moreover, mixes with less than 2 seconds results for slump flow_{T500} time should pass through the funnel in less than 8 seconds; on the other hand, if the slump flow_{T500} time is higher than 2 seconds, the time of 8-25 seconds will be acceptable for SCC mixes.



a) LS10SP1.5



b) LS10SP2



c) LS15SP1.5



d) LS15SP2



e) SS10SP1.5



f) SS10SP2



g) SS15SP1.5



h) SS15SP2



i) OW10SP1.5

j) OW10SP2

k) OW15SP1.5

l) OW15SP2

Figure 26: Effect of filler type (LS, SS, and OW) and quantities on segregation of SCC produced with 1.5% and 2% SP

In general, results showed that all mixes with lower amounts of filler had lower viscosity results and less time of passing through the V-funnel, although SS10SP2 did not follow the same trend (Figure 27). When 2% SP were used, decreasing the SS amount from 15% to 10% increased the passing time from V-funnel from 10 second to 20 seconds. It should be due to the bleeding and segregation of SS10SP2 mix which made the passing process of SCC more difficult and prolonged. Moreover OW15SP1.5 which had the lowest workability and highest viscosity among other SCC mixes got stuck in the funnel and the passing process did not complete. According to the results, viscosity classifications of the mixes are tabulated in Table 10. It can be seen that all the mixes are in VF2 class except OW15SP1.5 which has been failed in V-funnel test.

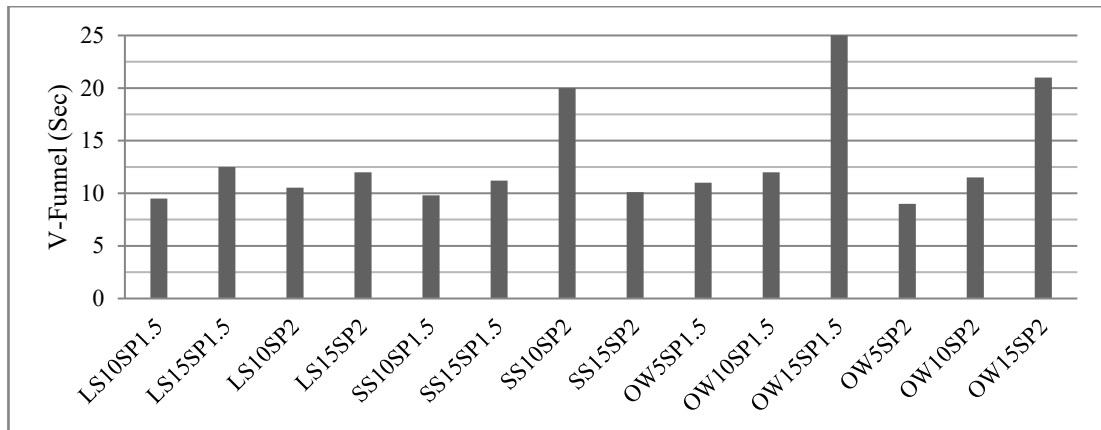


Figure 27: Effect of filler type and quantities on V-Funnel test of SCC

L-Box test results are shown in Figure 28. It can be observed from this figure that SS mixes had better results for L-Box (0.96-1.0) compared to other mixes and passed easily through rebars. Moreover, variations of filler amount and SP dosages did not make significant effects on passing ability of L-Box for SS mixes.

It is specified in EFNARC (2005) Annex-A, section A7 that, the conformity of the passing ability of SCC can be confirmed if the L-Box value is greater than 0.75 for both PA1 and PA2 classes. Therefore, OW mixes with 15% filler did not satisfy the passing ability requirements for SCC. Moreover, OW10SO1.5 and OW10SP2 classified as PA1.

It can be concluded from fresh tests that with OW filler more viscosity occurred in SCC mixes (OW15SP1.5 and OW15SP2 did not satisfy the BS EN 206-9 (2010) requirements), while SS filler introduced greater workability to the mixes.

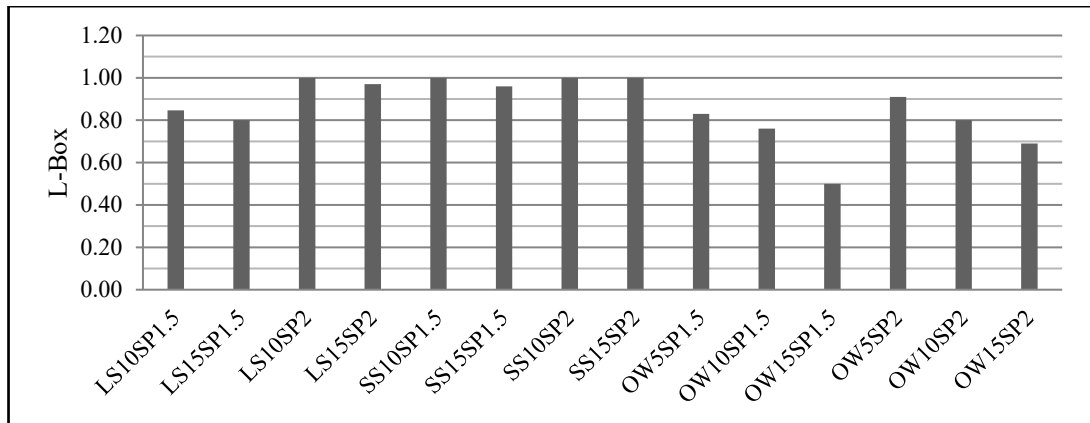


Figure 28: Effect of filler type and quantities on L-Box test of SCC

4.2 Behavior of SCC with Different Filler Types and Amounts under Compressive Strength

Results of the compressive strength on SCC mixes are shown in table 11 and Figure 29. As a general conclusion, it is noticeable that while w/c ratios are constant and equal to 0.47 for all mixes, but compressive strengths of OW mixes are much lower than the other SCC mixes (approximately half of the others). It might be mainly because of decreasing in workability and increasing in viscosity with OW filler which can be resulted in more porous concrete. The outcome of compressive strength test has good correlation with Ghezal & Khayat (2002) findings which specifies that, concrete compressive strength can be improved by enhanced workability.

To obtain a better conclusion of the very lower f_c results found for OW mixes, a VC mix named as Control; produced with the similar w/c ratio ($w/c= 0.47$) and similar materials and proportions without using any filler and SP. f_c results of this mix are tabulated in Table 11. According to Table 11, it could be observed that 91 days strength values of OW mixes, especially for the mixes with higher workability values (OW5SP1.5 and OW5SP2), do not have significant differences compared to the Control mix value. Moreover, the rate of increment in f_c values after 28 days found

to be higher for OW mixes (higher than 19%) while this value is 16% for Control mix.

Table 11: Compressive strength results of Control and SCC mixes after 7, 28 and 91 days of casting

Mix ID	f_c 7days	f_c 28days	f_c 91days
Control	31.00	41.10	47.60
LS10SP1.5	58.10	73.05	76.90
LS15SP1.5	58.20	65.40	72.50
LS10SP2	50.00	61.85	72.60
LS15SP2	54.40	67.30	75.40
SS10SP1.5	54.10	63.60	74.80
SS15SP1.5	55.20	66.10	76.50
SS10SP2	45.40	56.80	65.20
SS15SP2	54.35	65.00	75.10
OW5SP1.5	27.70	36.50	44.50
OW10SP1.5	25.80	32.40	38.70
OW15SP1.5	24.85	30.55	37.70
OW5SP2	28.50	39.50	47.00
OW10SP2	28.00	36.05	42.80
OW15SP2	26.80	33.80	40.50

Results showed that, the 28 days strength of SS mixes were lower than LS; however, in 91 days age, they were approximately in the same ranges. Also, when 15% SS amount used, 91 days compressive strength values increased with the rate of 15% compared to the related values of 28 days and SS15SP2 became very close to the compressive strengths of LS10SP1.5 and LS15SP2 mixes which had the highest compressive strength among all others. These occurrences could be the reason of higher SiO₂ content of SS specimens which reacts in cement paste in long term.

Moreover, compressive strength value of SS10SP2 was relatively lower compared to other LS and other SS mixes. It has good correlation with the fresh results in which it had lower homogeneity and more segregation and bleeding among all other mixes.

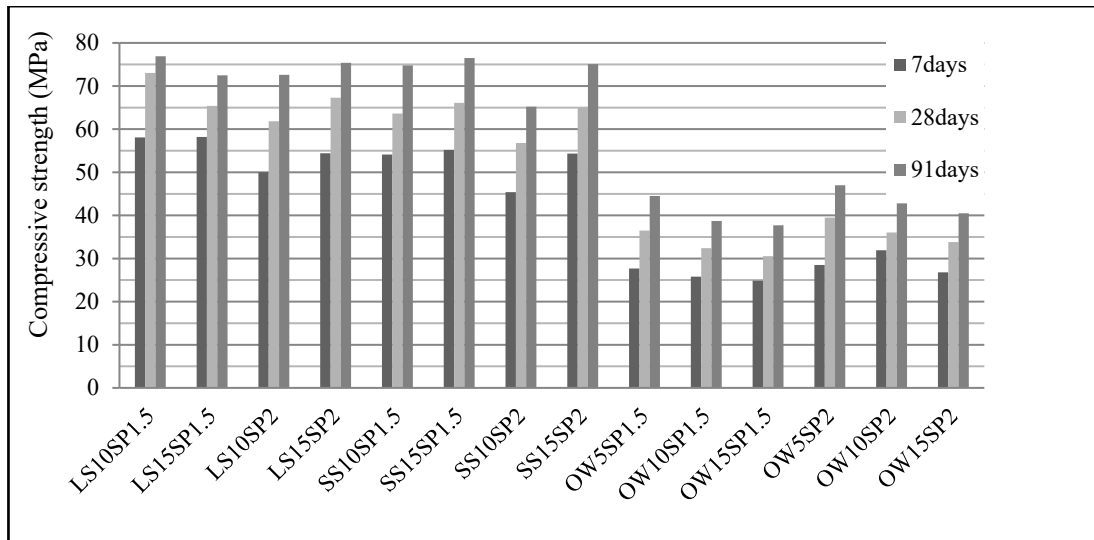


Figure 29: Effect of filler type and quantities on 7, 28 and 91 days fc

4.3 Effect of OW, SS and LS Replacement to Aggregate on Splitting Tensile Strength of SCC

For splitting tensile strengths (f_{spl}), the SS containing specimens showed higher f_{spl} compared to the other mixes (Table 11 and Figure 30). The highest f_{spl} belonged to SS10SP1.5 where the lowest achieved for OW15SP1.5. In LS specimens, when 10% LS was used increment in SP values from 1.5% to 2% reduced 40% the tensile strength. It should be because of the existence of bleeding and segregation in LS10SP2. On the other hand, when 15% LS was used SP increment from 1.5% to 2% was not excessively effective on f_{spl} . In SS specimens; for both 10% and 15% of SS used, increment in SP value from 1.5% to 2% reduced the tensile strength 11% and 17%, respectively. In OW case; filler amount did not make considerable effects on tensile strength but increment in SP amount from 1.5 to 2% increased the tensile strength approximately 8% for the related mixes.

The results showed that while the highest compressive strength achieved for LS containing SCC mixes, the highest splitting tensile strength were recorded with SS containing SCC specimens.

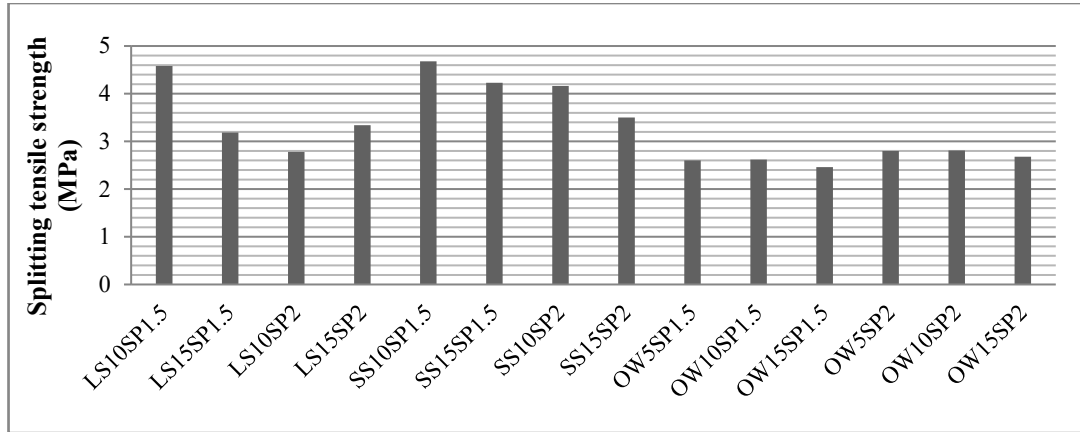


Figure 30: Effect of filler type and quantities on 28 days split tensile strength

4.4 Porosity Analysis of SCC with Different Filler Types and Amounts by X-Ray CT

The pores in each image taken by X-Ray CT were calculated by ImageJ program and the average pore areas determined. Porosity distribution of the images taken from the center sections along Y-direction of SS specimens are shown in Figure 31.

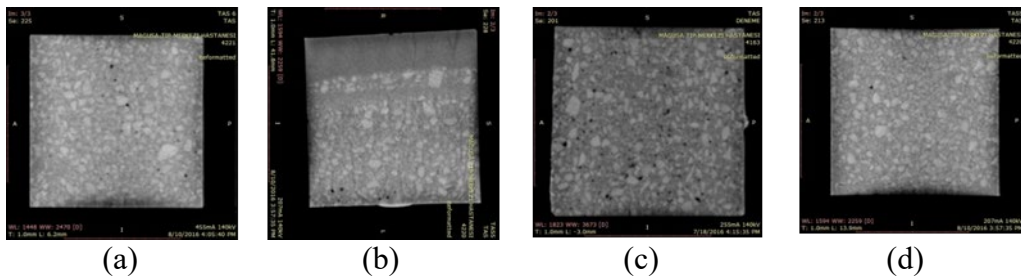


Figure 31: X-Ray CT images of a) SS10SP1.5, b) SS10SP2, c) SS15SP1.5 and d) SS15SP2 from center sections

For all specimens, six different images were taken by X-Ray CT method. Figure 32 shows X-Ray CT images taken for OW5SP2. In this figure, XZ2 and YZ2 are the

center sections of 150mm cube specimen in XZ and YZ planes, while XZ1, XZ3, YZ1 and YZ3 are the sections one centimeter far from surface sections.

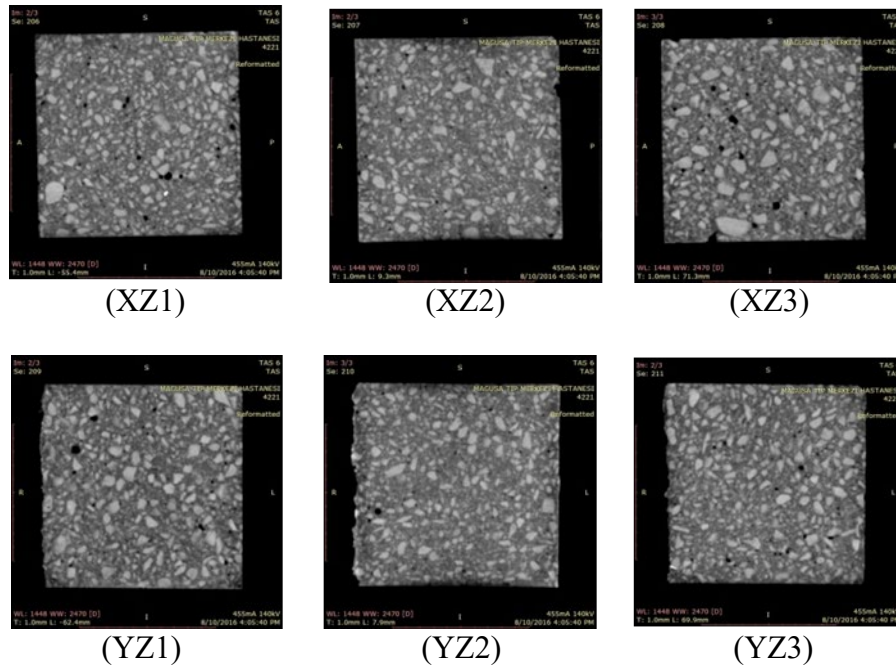


Figure 32: X-Ray CT images of OW5SP2 in six different directions of specimen

Average pore areas versus specimen names found in this study are plotted in Figure 33 and found to be between 0.42 cm^2 and 6.03 cm^2 . As it can be seen in this figure, in general, OW specimens had higher porosities while SS specimens found to have lower porosity amounts compared to LS mixes. It has good correlation with the fresh test and compressive strength results. The highest porosities have been observed in OW15SP1.5 and OW10SP1.5 specimens with porosity values more than two times higher than the related values of mixes produced with other fillers. It could mainly be happened in case of the lowest workability of these mixes. It is obvious that while vibration is not applying to SCC, less workability will result in more porous concrete. On the other hand, the lowest porosity occurred in SS15SP2 and SS10SP1.5 which had the highest workability and passing ability results in Slump-Flow and L-Box tests. SS15SP1.5 specimens found to be the most porous SCC with

a clear difference with other SS specimens. It similarly had the lowest result for Slump-Flow (74cm) and L-Box test (0.96) among other SS mixes.

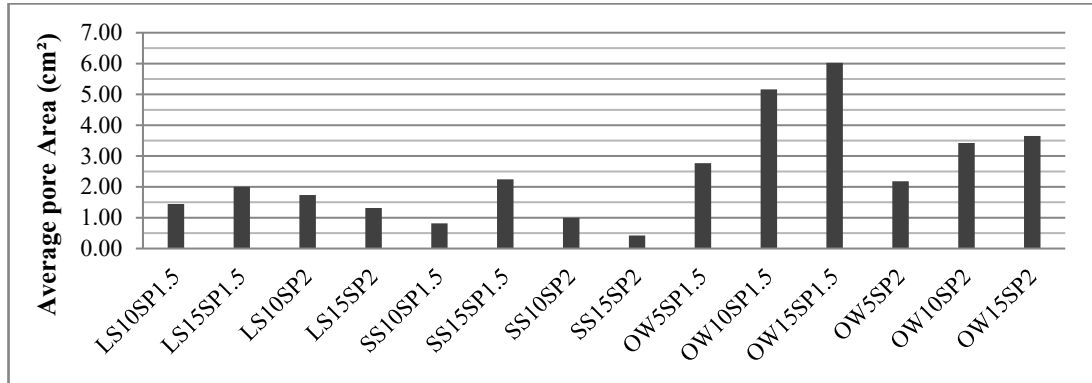


Figure 33: Effect of filler types and quantities on porosity of SCC

According to the Figure 34, in this study, the relationship between total pore area and slump-flow results found to be exponential with the coefficient of 0.80.

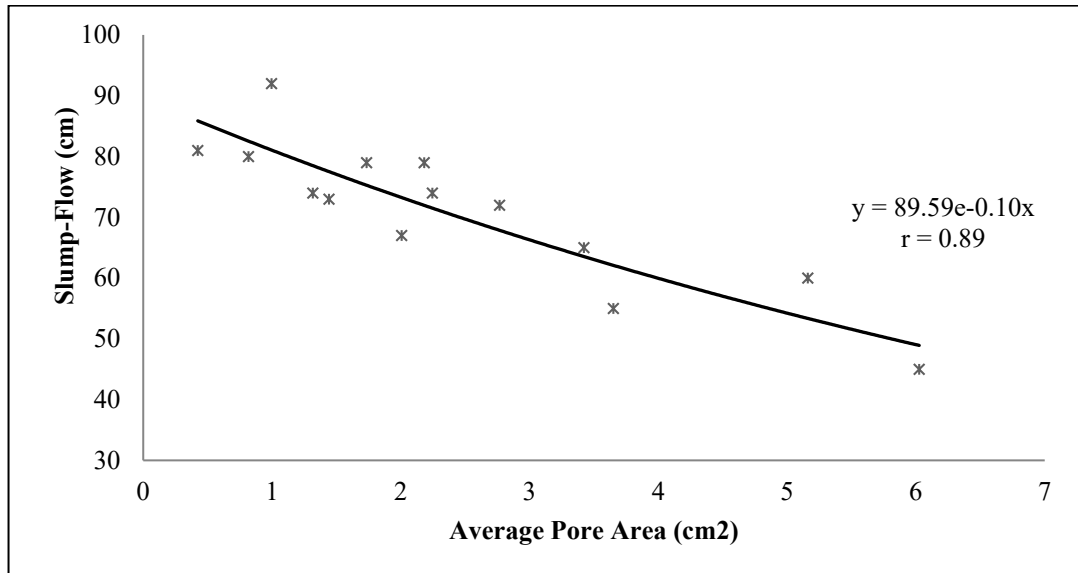


Figure 34: Total pore areas versus slump flow of SCC

Fig 35 represents the relationship between average pore area and maximum pore area of all SCC mixes. In this study, maximum pore area is defined as the greatest individual area found among all six images in each specimen. From Figure 35, it is

found that with higher porosity, greater maximum pore area might occur in the specimens; although there are some clear exceptions in case of OW mixes with 15% replacement of filler.

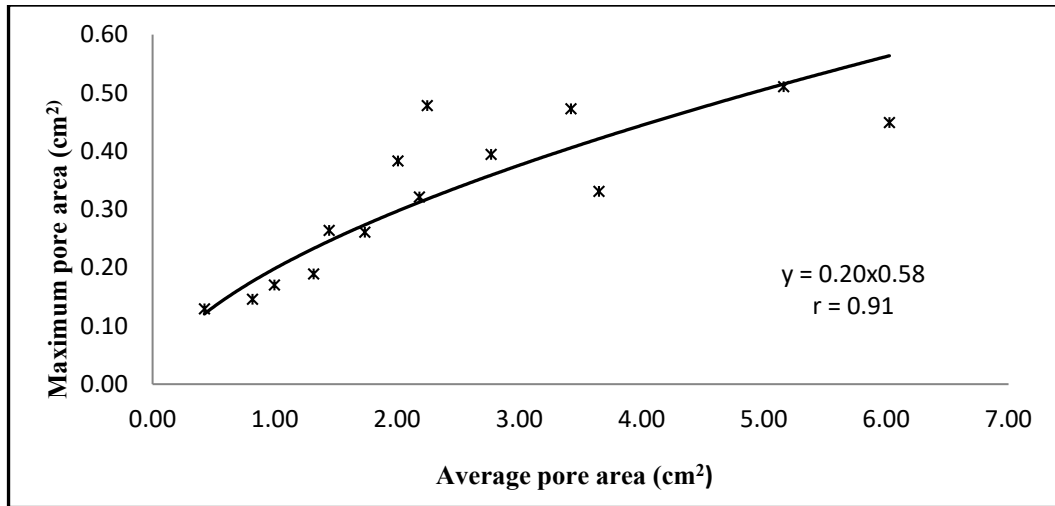


Figure 35: Average pore areas versus maximum pore areas of SCC

Figure 36 presents correlation of 91 days f_c and total pore area of OW mixes. It is obvious that when the total pore area is higher, the f_c will be lower. The rate of decrement in 91 days f_c increased considerably for the specimens having total pore area greater than 1.5%.

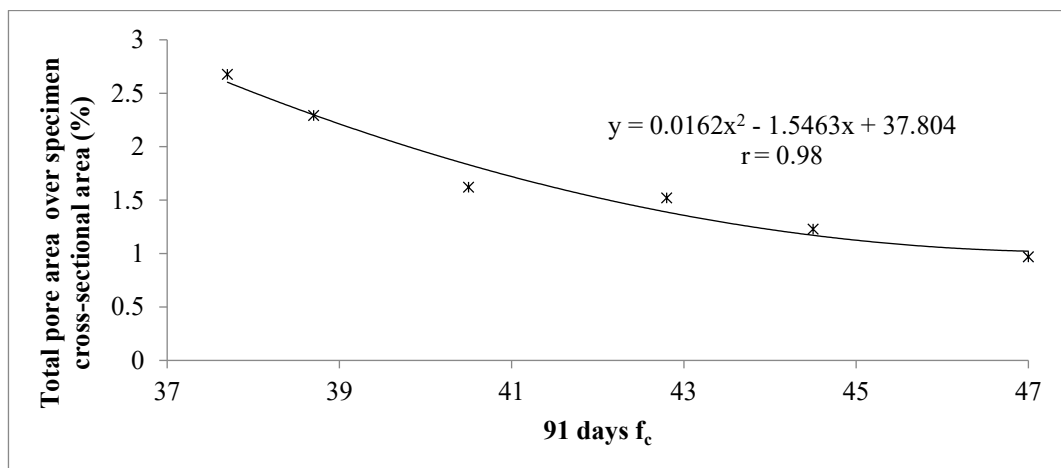


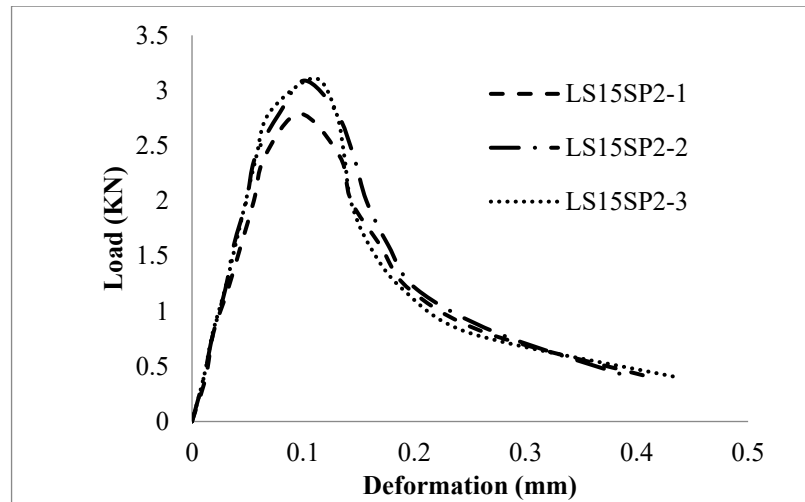
Figure 36: Correlation between pore areas along casting direction and 91 days f_c for OW specimens

4.5 Experimental Results on Fracture Energy of SCC with Different Filler Types and Quantities

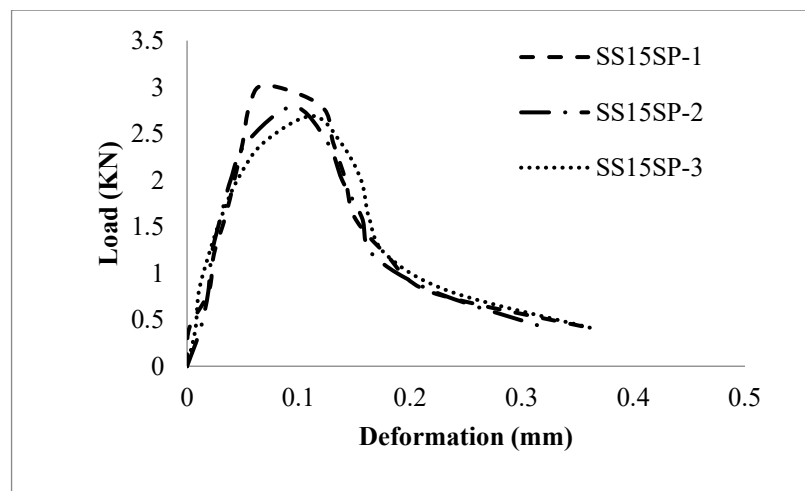
In this study, during TBT, failure of all beams was through pre-notch which was expected. Load- deformation diagrams of LS, SS and OW mixes with 15% filler and 2% SP are shown in Figure 37 (a), (b) and (c) respectively. The area under the load- deformation curve is calculated by excel program by means of calculating trapezoidal areas between each two outputs of load- deformation values recorded by TBT machine; consequently, G_f calculated according to Eq. 4 .

Figure 38 presents G_f results obtained from TBT on notched beams. Generally, LS and SS mixes showed higher and almost similar outcomes for G_f where the LS mixes had slightly higher results. The ranges of G_f found to be 85-110 N/m for LS mixes, 79-105 N/m for SS mixes and 73-93 N/m for OW mixes.

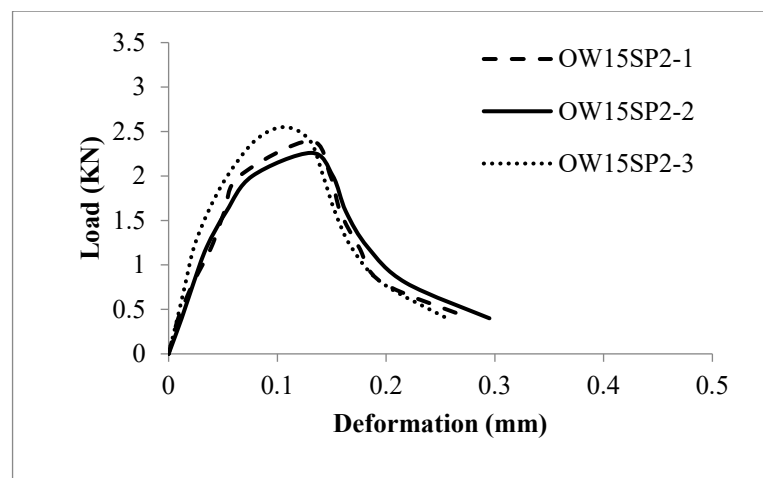
From Figure 38 it could be observed that, higher dosages of LS, SS and OW replacement to total aggregate results in lower G_f , mainly due to reduced aggregate content; however, SS10SP2 and LS10SP2 did not follow the same trend. It was expected due to the existence of bleeding and segregation in these two mixes followed by lower f_c . Moreover, In SS mixes, it seems that the higher SiO_2 content of SS, compensated the negative effect of lower amounts of coarse aggregate in mixes with 15% SS. Therefore, both SS15SP1.5 and SS15SP2 had lower decrement in G_f compared to the same LS mixes (see Appendix A and B for all LS and SS diagrams).



(a)



(b)



(c)

Figure 37: Load-deformation curves of a) LS15SP2, b) SS15SP2 and c) OW15SP2 notched beams

In OW mixes, as a general conclusion, SP increment from 1.5% to 2% resulted in higher fracture energy. OW5SP2 reached the peak amount of G_f among all other OW mixes but less than two other types of mixes. In this study, the higher is the OW and lower is the SP, the lower are the G_f values (see Appendix C for all OW diagrams).

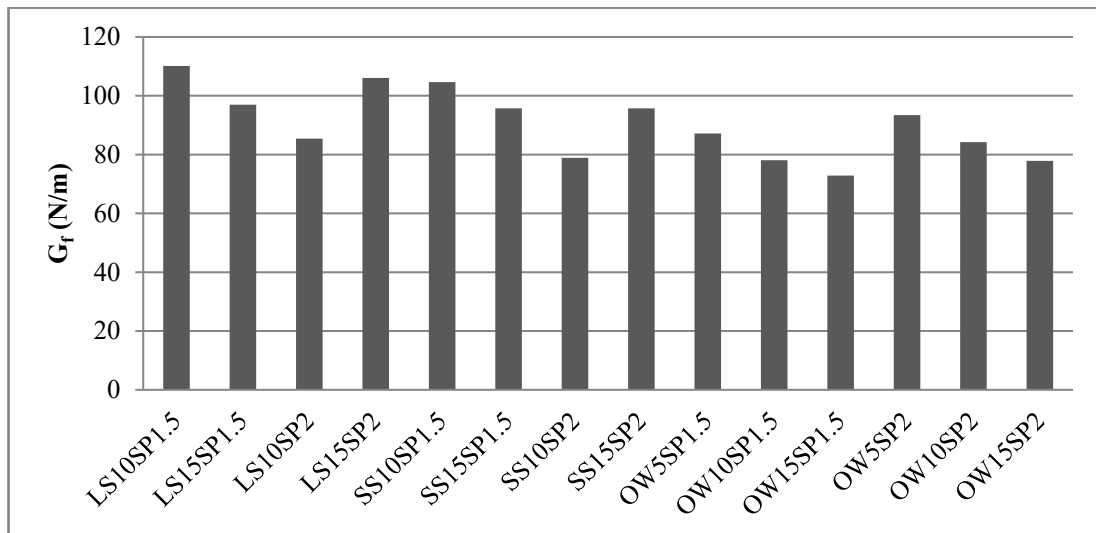
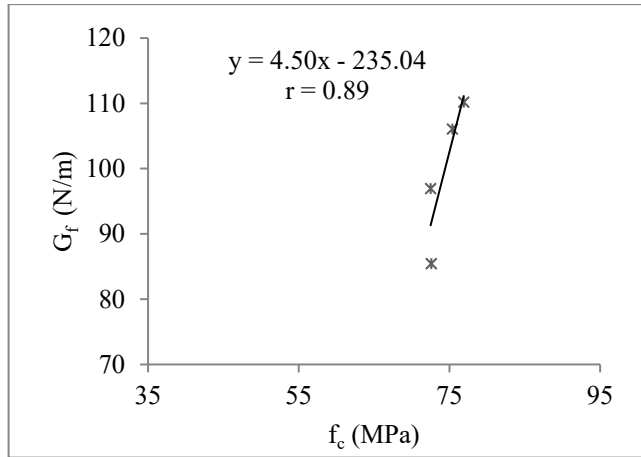


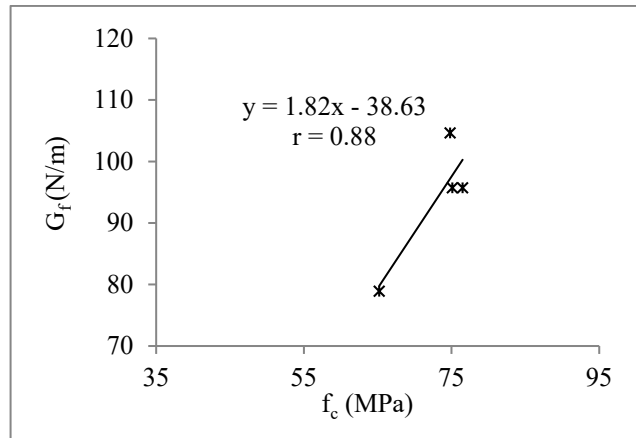
Figure 38: Effect of filler type and quantities on fracture energy of SCC

Figures 39 (a), (b) and (c), show the correlation of 91 days f_c and fracture energy of SCC mixes. It is visible from these figures that, the best linear correlation found for OW with the coefficient of 0.97. It is previously concluded for VC that; fracture energy increases when compressive strength increases (Alyhya et al. 2016). Same outcome found in this study in case of SCC with different filler types and quantities.

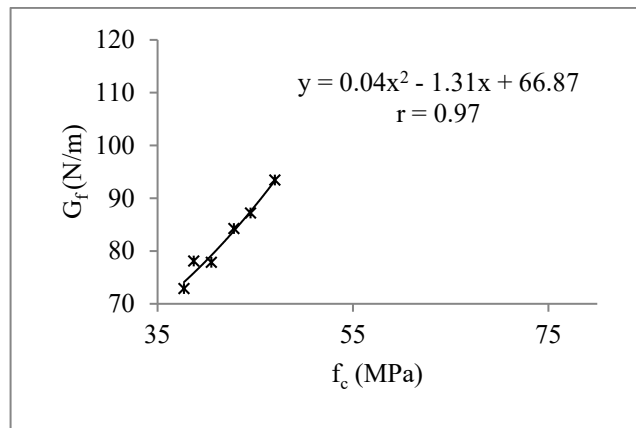
Figure 40 presents tensile strengths (f_t) obtained from TBT on notched beams. From general view, it could be seen that the higher f_t values found for LS specimens however there were not significant differences between the f_t results of LS and SS mixes and OW5SP1.5 and OW5SP2.



(a)



(b)



(c)

Figure 39: Correlation of 91 days f_c and G_f for (a) LS, (b) SS and (c) OW mixes

In this study, by 10% replacement of LS or SS in SCC, f_t decreased by increasing SP value. Oppositely, by replacing 15% LS or SS instead of total aggregate, increment in SP increased the f_t value.

It is found that adding 2% SP in OW mixes resulted in higher f_t . This might be because of superior workability and recovering homogeneity which also resulted in higher f_c of OW mixes with higher amount of SP. On the other hand, adding more OW reduced f_t with a maximum reduction for OW15SP1.5.

Similar to f_c and f_{spl} , OW replacement reduced f_t values as well, while increased SP from 1.5% to 2% compensate this negative effect and result in f_t increment. Therefore, as it can be seen in Figure 39, f_t value of OW5SP2 is the highest among OW specimens. The higher is the OW replacement and the lower is the SP content, the lower is the f_t value.

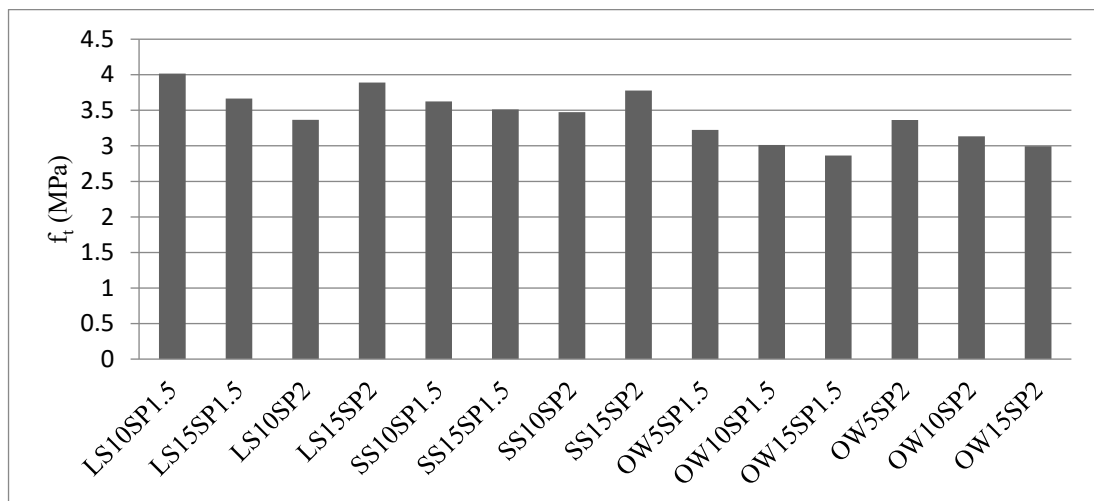


Figure 40: Effect of filler type and quantities on f_t

Figure 41 shows the characteristic length results of notched beams found via TBT by Eq. 4. In the present study, l_{ch} changes from 257 to 270 mm for LS, 217-294 mm for

SS and 236-261mm or OW mixes. SS10SP1.5 and SS15SP1.5 found to have the higher l_{ch} among all other mixes where SS10SP2 with the highest slump flow and extreme segregation and bleeding found to have the lower l_{ch} . From these results, it could be concluded that mixes with SS are very sensitive to SP dosages and increment of SP from 1.5% to 2% decreased the ductility of SCC with maximum reduction of 26% for 10% SS replacement.

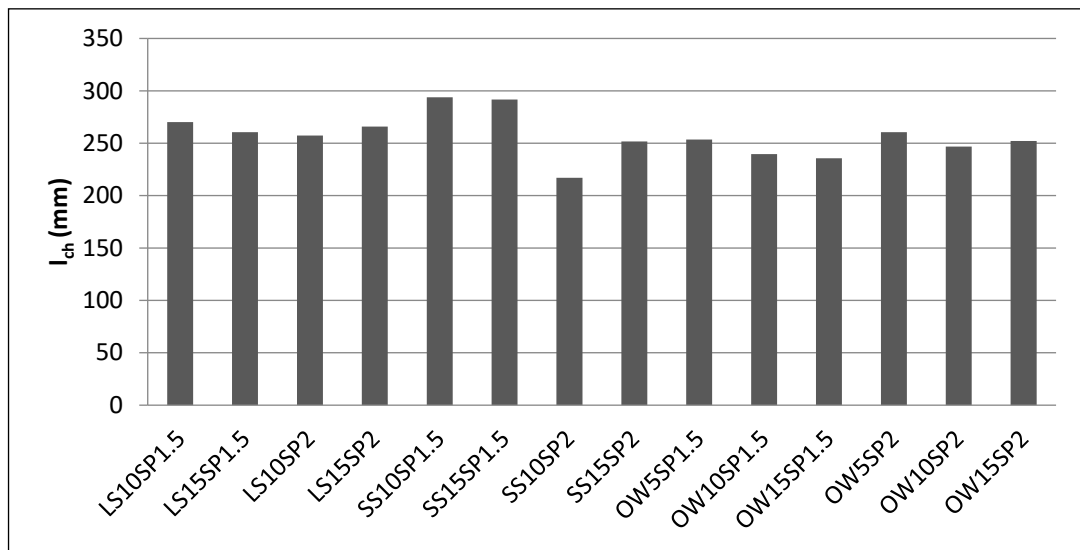
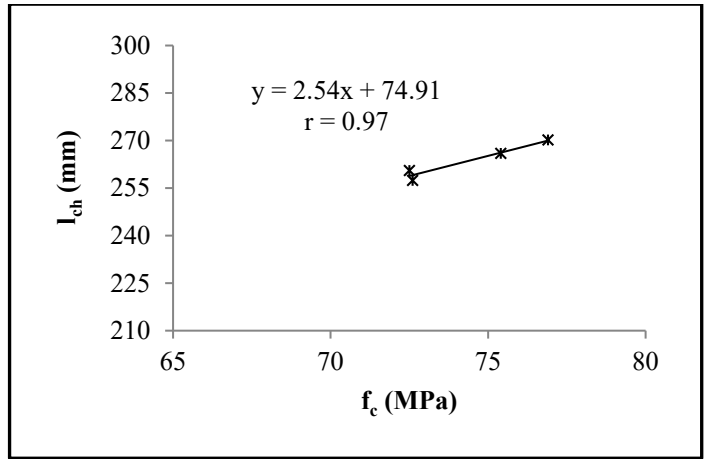
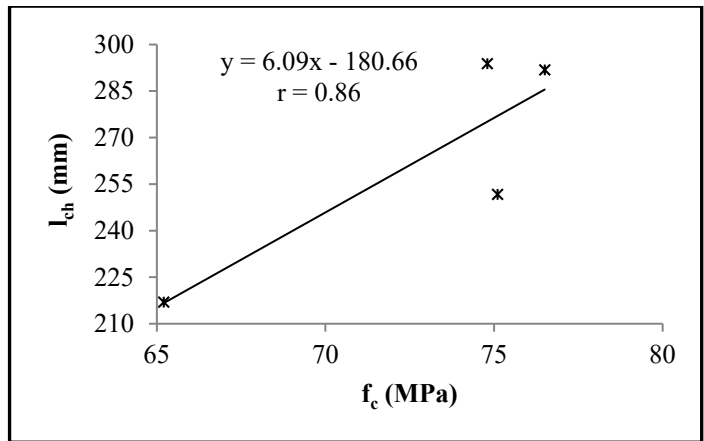


Figure 41: Characteristic length of SCC mixes in TBT

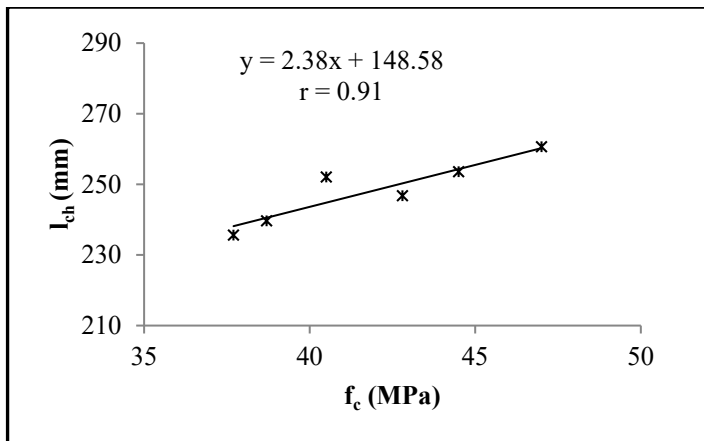
Figures 42(a), (b) and (c) present the correlation of l_{ch} and 91 days f_c for all three fillers. As it can be seen in these figures, the best correlation found for LS mixes with the coefficient of 0.97 and the least one achieved for SS mixes. It is important to mention that in SS mixes, SS10SP1.5 and SS15SP2 had almost similar f_c after 91 days (74.8 and 75.1 MPa respectively) but showed different values for l_{ch} (294 and 252 mm respectively). It is again concluded that reduction of coarse aggregate beside sensitivity of SS containing SCC mixes to SP could be the reasons of this outcome.



(a)



(b)



(c)

Figure 42: Correlation of f_c and G_f for a) LS mixes, b) SS mixes and c) OW mixes

4.6 Effect of Filler Types and Quantities on Volumetric Shrinkage of SCC

In this section, effects of filler types and quantities on volumetric changes of SCC mixes are determined. Changes in volumetric shrinkage ($\Delta V/V_0$) with respect to the passing time for the specimens produced with 1.5% SP are plotted in Figure 43. The rate of increment in $\Delta V/V_0$ for OW15SP1.5 is the highest and in that of LS15SP1.5 was the lowest. All others were among these two. Same graphs for the specimens containing 2% SP are plotted in Figure 44. It is worth noting that, in this case the rate of increment in $\Delta V/V_0$ was more uniform for all specimens relative to 2% SP.

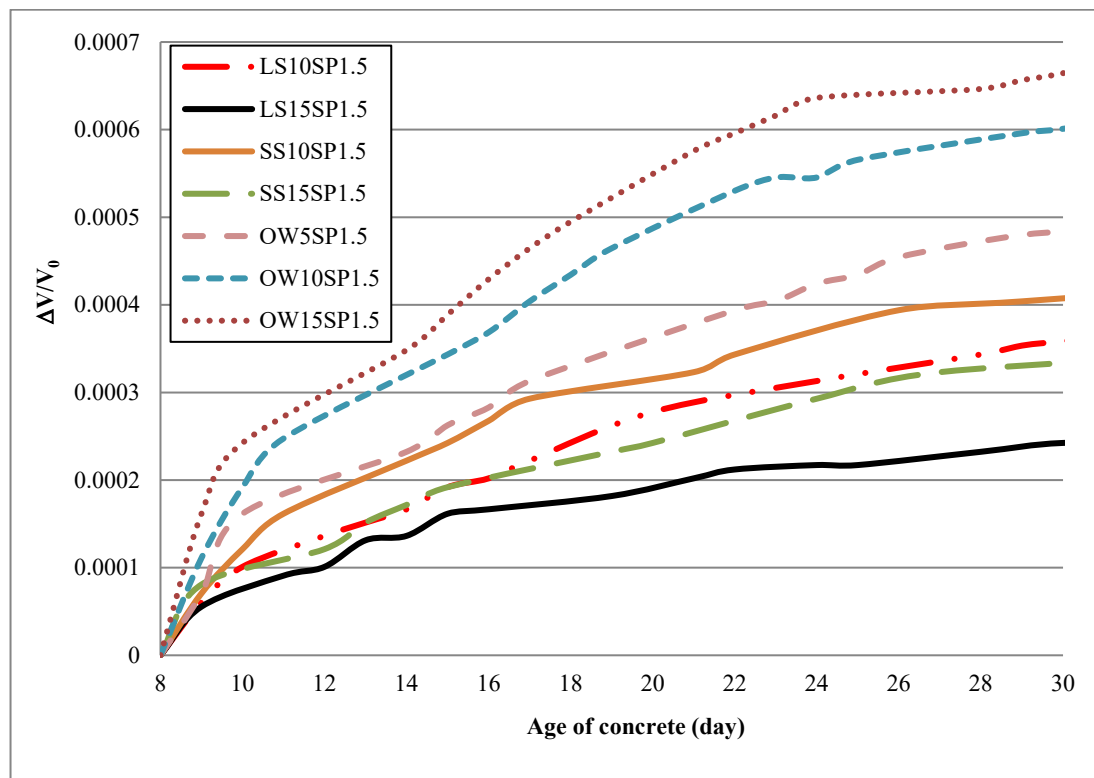


Figure 43: Effect of filler type and quantities on volumetric shrinkage of SCC produced with 1.5% SP

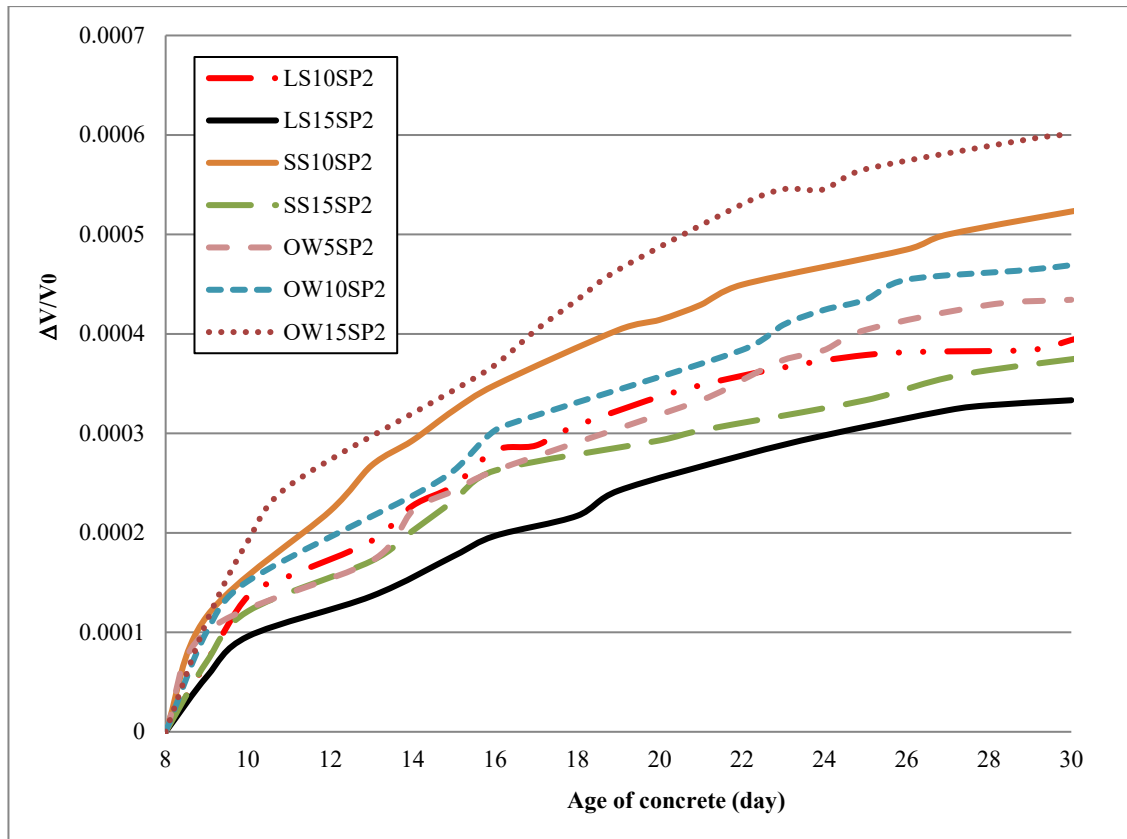


Figure 44: Effect of filler type and quantities on volumetric shrinkage of SCC produced with 2% SP

In general, positive effect (decreased $\Delta V/V_0$) of increased mineral filler replacement from 10% to 15% has been observed in all the mixes produced with either 1.5% or 2% SP; except the mixes produced with OW filler. In LS specimens, with 1.5% SP, increment in fillers decreased $\Delta V/V_0$ while increment in SP dosage increased $\Delta V/V_0$ for all the SS specimens. On the other hand, increasing OW content resulted in increasing $\Delta V/V_0$ for the related specimens while increment in SP amount had positive effect on the volumetric shrinkage. Table 12 and Figure 45 presents the 30days volumetric shrinkage of SCC mixes. As it can be seen from Figure 45, the highest $\Delta V/V_0$ occurred for OW specimens with the maximum amount for 15% filler and 1.5% SP content while the lowest achieved for LS15SP1.5. SS10SP2 which had

the excessive bleeding and segregation also presented higher volumetric shrinkage among other LS and SS mixes.

Table 12: 30 days volumetric shrinkage of SCC specimens produced with LS, SS and OW

Specimen ID	30 days volumetric shrinkage
LS10SP1.5	0.00036
LS15SP1.5	0.00024
LS10SP2	0.00039
LS15SP2	0.00033
SS10SP1.5	0.00041
SS15SP1.5	0.00033
SS10SP2	0.00053
SS15SP2	0.00037
OW5SP1.5	0.00048
OW10SP1.5	0.00057
OW15SP1.5	0.00066
OW5SP2	0.00043
OW10SP2	0.00046
OW15SP2	0.00060

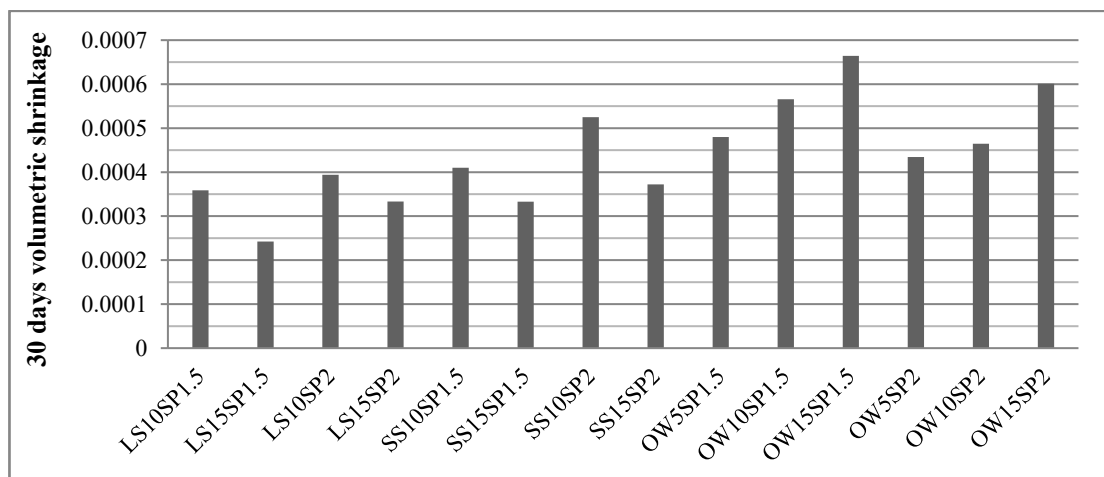


Figure 45: Effect of filler type and quantities on 30 days volumetric shrinkage of SCC specimens

4.6.1 Correlation of 28 days Compressive Strength and 30 Days Volumetric Shrinkage of SCC

The relation between compressive strength and 30 days volumetric shrinkage is presented in Figure 46. From this figure with higher $\Delta V/V_0$, lower compressive strength is expected.

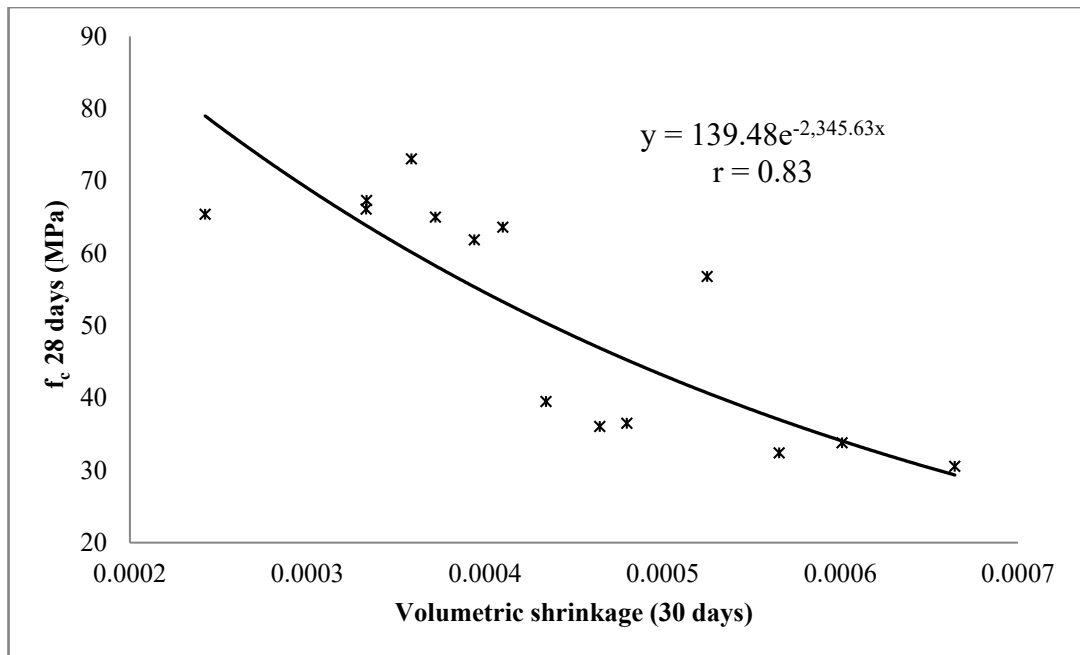


Figure 46: 30 days volumetric shrinkage of SCC versus 28 days f_c

Chapter 5

CONCLUSION AND RECOMMENDATIONS FOR FURTHER RESEARCH

5.1 Conclusion

Considering the results of this study, the following conclusions may be derived:

- SS found to be the best filler among all three (SS, LS and OW) in terms of giving higher workability and passing ability with lower viscosity. Moreover, mixes produced with this filler found to be more sensitive to increment in SP dosages compared to LS and OW mixes with similar filler and SP content.
- SS10SP, which showed comprehensive bleeding and segregation during slump flow test, did not satisfy the requirements for self-compactability.
- SS effects on 7 and 28 days compressive strength development was lower than LS; however, mixes with both LS and SS fillers showed nearly the same 91 days compressive strength values.
- SS mixes showed higher values of volumetric shrinkage compared to LS mixes. Moreover, with higher value of SS, lower results of volumetric shrinkage achieved.
- SS filler presented positive effect in case of porosity and the related mixes had lower porosities compared to LS specimens.

- Fracture energy calculations of SS mixes showed slightly lower G_f and f_t than LS mixes. However, characteristic lengths of SS mixes with 1.5% SP were higher than the related values of LS and OW mixes.
- Adding OW as filler in SCC extremely decreased workability compared to LS and SS mixes, but improved viscosity. No segregation and bleeding found for OW mixes through this study. Moreover OW15SP1.5 did not satisfy BS EN 206-9 (2010) requirements and failed in all three fresh tests. Similarly, in L-box test, OW15SP2 did not satisfy the self-compactability requirements according to the mentioned standard.
- Results of all tested mixes indicated that with OW filler, compressive strength decreased drastically compared to the other two fillers according to lower workability results and higher porosity values.
- OW mixes showed highest values of volumetric shrinkage compared to LS and SS mixes especially for the mixes with higher values of OW content which showed lower workability and passing ability results.
- SCC mixes containing OW showed higher porosities compared to the mixes made by LS.
- It is found that more than 5% replacement of OW instead of total aggregate decreased G_f , f_t and l_{ch} .

As an overall conclusion, SS filler seems to be a good replacement for LS filler however controls should be applied for bleeding and segregation. On the other hand, in SCC wherever high strength is not intended, desired viscosity could be achieved easily with small amounts of OW filler, but shrinkage and porosity should be controlled.

According to the test results of this study, it seems that OW can act easily as a viscosity modifying agent in SCC. According to EFNARC (2005), the dosage of viscosity modifying agent for using in SCC usually varies from 0.1% to 1.5% by weight of cement. In this study it is found that SCC with lower OW (even lower than 5%) content had better characteristics in terms of fresh and hardened concrete properties. Since the powder type SCC is characterized by the large amounts of powder dosages and with this low amount of OW, produced SCC cannot be categorized as a powder type SCC, therefore, considering OW as a viscosity modifying agent could be more meaningful.

5.2 Recommendations for Future Studies

The aim of this study was to investigate the feasibility in utilization of two new materials in SCC instead of traditional fillers. After finishing the experiments and collecting the results, it is found that both SS and OW could be utilized in SCC from mechanical point of view, but it is necessary to find the best proportion and dosages of these materials in SCC to have desired concrete with optimized properties. Moreover, it is necessary to study the durability of SCC made by these materials especially for SS filler.

REFERENCES

- Abdalla, H. M., & Karihaloo, B. L. (2003). Determination of size-independent specific fracture energy of concrete from three point-bend and wedge splitting tests. *Magazine of concrete research*, 55(2), 133-141.
- ACI Committee 222, Corrosion of Metals in Concrete. (2001). Protection of metals in concrete against corrosion. American Concrete Institute.
- ACI 209R, Prediction of creep, shrinkage, and temperature effects in concrete structures, ACI Report 209R-92, 1997, Detroit, 47 p.
- Ahmadi, M. A., Alidoust, O., Sadrinejad, I., & Nayeri, M. (2007). Development of mechanical properties of self compacting concrete contain rice husk ash. *International Journal of Computer, Information, and Systems Science, and Engineering*, 1(4), 259-262.
- Ahn, J., Jung, J., Kim, S., & Han, S. I. (2014). X-ray image analysis of porosity of pervious concretes. *International Journal of GEOMATE*, 6(1 SERL 11), 796-800.
- Akçaoğlu, T., Tokyay, M., & Çelik, T. (2004). Effect of coarse aggregate size and matrix quality on ITZ and failure behavior of concrete under uniaxial compression. *Cement and concrete composites*, 26(6), 633-638.

- Al-Akhras, N. M., & Abdulwahid, M. Y. (2010). Utilisation of olive waste ash in mortar mixes. *Structural Concrete*, 11(4), 221-228.
- Al-Akhras, N. M., Al-Akhras, K. M., & Attom, M. F. (2009). Performance of olive waste ash concrete exposed to elevated temperatures. *Fire safety journal*, 44(3), 370-375.
- Alyhya, W. S., Dhaheer, M. A., Al-Rubaye, M. M., & Karihaloo, B. L. (2016). Influence of mix composition and strength on the fracture properties of self-compacting concrete. *Construction and Building Materials*, 110, 312-322.
- American Concrete Pavement Association. (2013). "What are admixtures." <http://www.pavement.com/Concrete_Pavement/Technical/FATQ/Materials/Admixtures.asp> (Sept. 7, 2013).
- Avram, C., Facaoaru, I., Filimon, I., Mirsu, O. & Terteza, I. (1981). Concrete strength and strain. *Elsevier Scientific Publishing Company*, Amsterdam -Oxford - New York.
- Badry, F. (2015). *Experimental and numerical studies in self-compacting concrete* (Doctoral dissertation, Cardiff University).
- Balázs, G. L., Lublós, É., & Földes, T. (2018). Evaluation of concrete elements with X-ray computed tomography. *Journal of Materials in Civil Engineering*, 30(9), 06018010.

- Bazant, Z. P. (2004). Scaling theory for quasibrittle structural failure. *Proceedings of the National Academy of Sciences*, 101(37), 13400-13407.
- Bazant, Z. P., & Oh, B. H. (1983). Crack band theory for fracture of concrete. *Matériaux et construction*, 16(3), 155-177.
- Bazant, Z. P., & Kazemi, M. T. (1991). Size effect on diagonal shear failure of beams without stirrups. *ACI Structural journal*, 88(3), 268-276.
- Bazant, Z. P., & Planas, J. (1997). *Fracture and size effect in concrete and other quasibrittle materials* (Vol. 16). CRC press.
- Beygi, M. H., Kazemi, M. T., Nikbin, I. M., & Amiri, J. V. (2013). The effect of water to cement ratio on fracture parameters and brittleness of self-compacting concrete. *Materials & Design*, 50, 267-276.
- Beygi, M. H., Kazemi, M. T., Amiri, J. V., Nikbin, I. M., Rabbanifar, S., & Rahmani, E. (2014). Evaluation of the effect of maximum aggregate size on fracture behavior of self compacting concrete. *Construction and Building Materials*, 55, 202-211.
- Bissonnette, B., Pierre, P., & Pigeon, M. (1999). Influence of key parameters on drying shrinkage of cementitious materials. *Cement and Concrete Research*, 29(10), 1655-1662.

- Bradu, A., Cazacu, N., Florea, N., & Mihai, P. (2016). Compressive Strength of Self Compacting Concrete. *Buletinul Institutului Politehnic din Iasi. Sectia Constructii, Arhitectura*, 62(2), 59.
- Carpinteri, A., & Chiaia, B. (1996). Size effects on concrete fracture energy: dimensional transition from order to disorder. *Materials and Structures*, 29(5), 259.
- Chindapasirt, P., Jaturapitakkul, C., & Rattanasak, U. (2009). Influence of fineness of rice husk ash and additives on the properties of lightweight aggregate. *Fuel*, 88(1), 158-162.
- Cifuentes-Bulté, H., Ríos, J. D., & Gómez Álvarez, E. J. (2018). Effect of mix design on the size-independent fracture energy of normal-and high-strength self-compacting concrete. *Materiales de Construcción*, 68(329), 1-11.
- Collepari, M., Borsoi, A., Collepari, S., & Troli, R. (2005). Strength, shrinkage and creep of SCC and flowing concrete. In *Second North American Conference on the Design and Use of Self-Consolidating Concrete and the Fourth International RILEM Symposium on Self-Compacting Concrete* (pp. 911-920).
- Concrete Technology in Focus: Shrinkage of Concrete, Master builders solutions, www.master-builders-solutions.basf.us

- Craeye, B., De Schutter, G., Desmet, B., Vantomme, J., Heirman, G., Vandewalle, L., ... & Kadri, E. H. (2010). Effect of mineral filler type on autogenous shrinkage of self-compacting concrete. *Cement and Concrete Research*, 40(6), 908-913.
- Cuenca, J., Rodríguez, J., Martín-Morales, M., Sánchez-Roldán, Z., & Zamorano, M. (2013). Effects of olive residue biomass fly ash as filler in self-compacting concrete. *Construction and Building Materials*, 40, 702-709.
- De Weerd, K., Justnes, H., Kjellsen, K. O., & Sellevold, E. (2010). Fly ash-limestone ternary composite cements: synergetic effect at 28 days. *Nordic Concrete Research*, 42(2), 51-70.
- Deeb, R. (2013). *Flow of self-compacting concrete* (Doctoral dissertation, Cardiff University).
- Dehn, F., Holschemacher, K., & Weiße, D. (2000). Self-compacting concrete (SCC) time development of the material properties and the bond behaviour. *Selbstverdichtendem Beton*, 115-124.
- Desnerck, P., Boel, V., Craeye, B., & Van Itterbeeck, P. (2014). Mechanical properties. In *Mechanical Properties of Self-Compacting Concrete* (pp. 15-71). Springer, Cham.

- De Schutter, G. (2011). Effect of limestone filler as mineral addition in self-compacting concrete. In *36th Conference on Our World in Concrete & Structures: 'Recent Advances in the Technology of Fresh Concrete' (OWIC'S 2011)* (pp. 49-54). Ghent University, Department of Structural engineering.
- Domone, P. L. (2007). A review of the hardened mechanical properties of self-compacting concrete. *Cement and concrete composites*, 29(1), 1-12.
- Du Plessis, A., Olawuyi, B. J., Boshoff, W. P., & Le Roux, S. G. (2016). Simple and fast porosity analysis of concrete using X-ray computed tomography. *Materials and structures*, 49(1-2), 553-562.
- Du Plessis, A., & Rossouw, P. (2015). X-ray computed tomography of a titanium aerospace investment casting. *Case Studies in Nondestructive Testing and Evaluation*, 3, 21-26.
- Du Plessis, A., le Roux, S. G., & Guelpa, A. (2016). Comparison of medical and industrial X-ray computed tomography for non-destructive testing. *Case Studies in Nondestructive Testing and Evaluation*, 6, 17-25.
- El Mir, A., & Nehme, S. G. (2015). Porosity of self-compacting concrete. *Procedia Engineering*, 123, 145-152.
- Elyamany, H. E., Elmoaty, A. E. M. A., & Mohamed, B. (2014). Effect of filler types on physical, mechanical and microstructure of self compacting concrete and Flow-able concrete. *Alexandria Engineering Journal*, 53(2), 295-307.

- EN, B. (2010). 206-9, Concrete—Part 9: Additional Rules for Self-Compacting Concrete (SCC). *British Standards publication*.
- Eskandari, H., Muralidhara, S., Prasad, B. R., & Reddy, B. V. (2012). Fracture properties of self compacting concrete for notched and un-notched beams. *Global Journal of Research In Engineering*, 12(1-E).
- Esping, O., & Löfgren, I. (2005). Investigation of early age deformation in self-compacting concrete. In *the Knud Højgaard conference on Advanced Cement-Based Materials-Research and Teaching*.
- Figueiras, H., Nunes, S., Sousa-Coutinho, J., & Figueiras, J. (2011). Durability performance of SCC mortars including different types of metakaolin. In *Proceedings 12th international conference on durability of building materials and components. Porto, Portugal: FEUP edições* (pp. 1387-94).
- Figueiras, H., Nunes, S., Coutinho, J. S., & Andrade, C. (2014). Linking fresh and durability properties of paste to SCC mortar. *cement and concrete composites*, 45, 209-226.
- Fuchs, W., Hofmann, J., & Tepfers, R. (2012). *Befestigungstechnik, Bewehrungstechnik und... II*. ibidem-Verlag.
- Gibbs, J. C., & Zhu, W. (1999, September). Strength of hardened self-compacting concrete. In *Proceedings of First international RILEM Symposium on Self-Compacting Concrete (PRO 7)*, Stockholm, Suede (pp. 199-209).

- Ghafari, E., Costa, H., & Júlio, E. (2015). Critical review on eco-efficient ultra high performance concrete enhanced with nano-materials. *Construction and Building Materials*, 101, 201-208.
- Goodier, C. I. (2003). Development of self-compacting concrete.
- Granata, M. F. (2015). Pumice powder as filler of self-compacting concrete. *Construction and Building Materials*, 96, 581-590.
- Grauers, M. (1997). Rational production and improved working environment through using selfcompacting concrete. *EC Brite-EuRam Contract No. BRPR-CT96, 366*, 1997-2000.
- Guinea, G. V., Planas, J., & Elices, M. (1992). Measurement of the fracture energy using three-point bend tests: Part 1—Influence of experimental procedures. *Materials and Structures*, 25(4), 212-218.
- Hammer, T. A. (2007). 84. The Influence of some mix design parameters on drying shrinkage of SCC. In *5th International RILEM Symposium on Self-Compacting Concrete* (pp. 559-564). RILEM Publications SARL.
- Heirman, G., Vandewalle, L., & Van Gemert, D. (2007, September). Influence of mineral additions and chemical admixtures on setting and volumetric autogenous shrinkage of SCC-equivalent mortars. In *Proceedings of the 5th International RILEM Symposium on Self-Compacting Concrete (SCC2007), Ghent, Belgium* (pp. 3-5).

- Hillerborg, A., Modéer, M., & Petersson, P. E. (1976). Analysis of crack formation and crack growth in concrete by means of fracture mechanics and finite elements. *Cement and concrete research*, 6(6), 773-781.
- Hillerborg, A. R. N. E. (1983). Concrete fracture energy tests performed by 9 laboratories according to a draft RILEM recommendation. *Report to RILEM TC50-FMC, Report TVBM-3015, Lund, Sweden.*
- Hillerborg, A. (1984). Additional concrete fracture energy tests performed by 6 laboratories according to a draft RILEM recommendation. *Report TVBM, 3017.*
- Hillerborg, A. (1985). Influence of beam size on concrete fracture energy determined according to a draft RILEM recommendation. *Report to RILEM TC50-FMC, Report TVBM-3021, Division of Building Materials, Lund Institute of Technology, Lund, Sweden.*
- Hu, X. Z., & Wittmann, F. H. (1992). Fracture energy and fracture process zone. *Materials and Structures*, 25(6), 319-326.
- Hu, X. Z., & Wittmann, F. H. (1992). Fracture energy and fracture process zone. *Materials and Structures*, 25(6), 319-326.
- Hu, X., & Wittmann, F. (2000). Size effect on toughness induced by crack close to free surface. *Engineering fracture mechanics*, 65(2-3), 209-221.

- Ismail, Z. Z., & Al-Hashmi, E. A. (2008). Use of waste plastic in concrete mixture as aggregate replacement. *Waste management*, 28(11), 2041-2047.
- Jalal, M., Fathi, M., & Farzad, M. (2013). Effects of fly ash and TiO₂ nanoparticles on rheological, mechanical, microstructural and thermal properties of high strength self compacting concrete. *Mechanics of Materials*, 61, 11-27.
- JCI : " Colloquium for Fracture Mechanics of Concrete Structures", Japan Concrete Institute, 1990
- JCI: " Method of test for fracture energy of concrete by use of notched beam Japan Concrete Institute JCI-S-001-2003
- Jensen, M., & Hansen, P. F. (1996). Autogenous deformation and change of the relative humidity in silica fume-modified cement paste. *Materials Journal*, 93(6), 539-543.
- Jueshi, Q., & Hui, L. (1997). Size effect on fracture energy of concrete determined by three-point bending. *Cement and Concrete Research*, 27(7), 1031-1036.
- Karihaloo, B. L., Abdalla, H. M., & Xiao, Q. Z. (2003). Size effect in concrete beams. *Engineering fracture mechanics*, 70(7-8), 979-993.
- Karihaloo, B. L., Abdalla, H. M., & Imjai, T. (2003). A simple method for determining the true specific fracture energy of concrete. *Magazine of concrete research*, 55(5), 471-481.

- Kasemchaisiri, R., & Tangtermsirikul, S. (2008). Properties of self-compacting concrete in incorporating bottom ash as a partial replacement of fine aggregate. *Science Asia*, 34, 87-95.
- Khayat, K. H. (1998). Use of viscosity-modifying admixture to reduce top-bar effect of anchored bars cast with fluid concrete. *Materials Journal*, 95(2), 158-167.
- Khayat, K. H. (1999). Workability, testing, and performance of self-consolidating concrete. *Materials Journal*, 96(3), 346-353.
- Kim, J. K., Han, S. H., Park, Y. D., & Noh, J. H. (1998). Material properties of self-flowing concrete. *Journal of Materials in Civil Engineering*, 10(4), 244-249.
- Klug, Y., & Holschemacher, K. (2003, August). Comparison of the hardened properties of self-compacting and normal vibrated concrete. In *3rd RILEM symposium on self compacting concrete, Reykjavik* (pp. 596-605). RILEM Bagneux, France.
- Konsta-Gdoutos, M. S., Metaxa, Z. S., & Shah, S. P. (2010). Highly dispersed carbon nanotube reinforced cement based materials. *Cement and Concrete Research*, 40(7), 1052-1059.
- Korte, S., Boel, V., De Corte, W., & De Schutter, G. (2014). Fracture toughness and cracking behaviour of SCC compared to VC. In *Key Engineering Materials* (Vol. 577, pp. 205-208). Trans Tech Publications.

- Kristiawan, S. A., & Murti, G. Y. (2017, February). Porosity of Self-Compacting Concrete (SCC) incorporating high volume fly ash. In *IOP Conference Series: Materials Science and Engineering* (Vol. 176, No. 1, p. 012043). IOP Publishing.
- Kumar, R., & Bhattacharjee, B. (2003). Porosity, pore size distribution and in situ strength of concrete. *Cement and concrete research*, 33(1), 155-164.
- Kubba, S. (2010). *Green construction project management and cost oversight*. Butterworth-Heinemann.
- Kurihara, N., Ando, T., Kunieda, M., Uchida, Y., & Rokugo, K. (1996). Determination of tension softening diagram of concrete by poly-linear approximation analysis and flexural failure behavior of fiber reinforced concrete. *Doboku Gakkai Ronbunshu*, 1996(532), 119-129.
- Latief, F. D. E., Mohammad, I. H., & Rarasati, A. D. (2017, November). Digital 3D Microstructure Analysis of Concrete using X-Ray Micro Computed Tomography SkyScan 1173: A Preliminary Study. In *IOP Conference Series: Materials Science and Engineering* (Vol. 267, No. 1, p. 012020). IOP Publishing.
- Leemann, A., & Hoffmann, C. (2005). Properties of self-compacting and conventional concrete—differences and similarities. *Magazine of Concrete Research*, 57(6), 315-319.

- Lei, G., Han, J., & Dang, F. (2018). Using X-Ray CT Scanning to Study the Failure Mechanism of Concrete under Static and Dynamic Loadings. *Advances in Materials Science and Engineering*, 2018.
- Ling, T. C., & Poon, C. S. (2011). Properties of architectural mortar prepared with recycled glass with different particle sizes. *Materials & Design*, 32(5), 2675-2684.
- Loser, R., & Leemann, A. (2007). 81. Effects of curing time and drying behaviour of SCC in case of restrained shrinkage deformations. In *5th International RILEM Symposium on Self-Compacting Concrete* (pp. 539-544). RILEM Publications SARL.
- Lunardelli, M., Varady, P., Köhnke, D., Lehmborg, S., & Budelmann, H. (2017, October). X-ray computed tomography: Image processing and applications. In *von Scheven, M.; Keip, M.-A.; Karajan, N.(Ed.): Proceedings of the 7th GACM Colloquium on Computational Mechanics for Young Scientists from Academia and Industry* (pp. 39-43).
- Manahiloh, K. N., Muhunthan, B., Kayhanian, M., & Gebremariam, S. Y. (2012). X-ray computed tomography and nondestructive evaluation of clogging in porous concrete field samples. *Journal of Materials in Civil Engineering*, 24(8), 1103-1109.

- Meeravali, K., Balaji, K. V. G. D., & Kumar, T. S. (2014). Partial replacement of cement in concrete with sugarcane bagasse ash behaviour in HCl solution. *International Journal of Advance Research in Science and Engineering*, 3(7), 368-373.
- Mehta, P. K. (1987). Supplementary cementing materials for concrete. *CANMET Special Publication*, 86, 1-33.
- Ministry of Construction of the PR China (2006). Standard for technical requirements and test method of sand and crushed stone (or gravel) for ordinary concrete, JGJ 52, Beijing.
- Mohamed, H. A. (2011). Effect of fly ash and silica fume on compressive strength of self-compacting concrete under different curing conditions. *Ain Shams Engineering Journal*, 2(2), 79-86.
- Moretti, J. P., Nunes, S., & Sales, A. (2018). Self-compacting concrete incorporating sugarcane bagasse ash. *Construction and Building Materials*, 172, 635-649.
- Naik, T. R., Chun, Y. M., Kumar, R. & Bruce, W. R., (2004). Development of high strength self-consolidation concrete, Center of by- products utilization, Report No. CBU-2003-14, Department of Civil Engineering and Mechanics College of Engineering and Applied Science The university of Wisconsin – Milwaukee, 1-27.

- Nalbantoglu, Z., & Tawfiq, S. (2006). Evaluation of the effectiveness of olive cake residue as an expansive soil stabilizer. *Environmental Geology*, 50(6), 803-807.
- Nehdi, M., Mindess, S., & Aïtcin, P. C. (1998). Rheology of high-performance concrete: effect of ultrafine particles. *Cement and Concrete Research*, 28(5), 687-697.
- Neville, A. M. (1971). Hardened concrete: physical and mechanical aspects.
- Neville, A. M., & Brooks, J. J. (1990). Concrete Technology. Revised Reprint.
- Neville, A. M. (1995). Properties of concrete 4th edn.
- Newman, K. (1966). Concrete systems. *Composite materials*, 336-452.
- Noguchi, T., Oh, S. G., & Tomosawa, F. (1999, September). Rheological approach to passing ability between reinforcing bars of self-compacting concrete. In *Self-Compacting Concrete: Proceedings of the First International RILEM Symposium* (pp. 59-70).
- Okamura, H., & Ouchi, M. (2003). Self-compacting concrete. *Journal of advanced concrete technology*, 1(1), 5-15.
- Onifade, I. (2013). Internal structure characterization of asphalt concrete using x-ray computed tomography.

- Operatin instructions ‘Demec’ Mechanical Strain Gauges. (2003). 35-2838, 35-2846, 35-2854, ELE International.
- Pamnani, N. J. (2014). Effect of curing techniques on mechanical properties of self compacting concrete.
- Parra, C., Valcuende, M., & Gómez, F. (2011). Splitting tensile strength and modulus of elasticity of self-compacting concrete. *Construction and Building materials*, 25(1), 201-207.
- Persson, B. (2001). A comparison between mechanical properties of self-compacting concrete and the corresponding properties of normal concrete. *Cement and concrete Research*, 31(2), 193-198.
- Petersson, P. E. (1981). Crack growth and development of fracture zones in plain concrete and similar materials.
- Piérard, J.; Dieryck, V.; Desmyter, J. (2005), Autogenous shrinkage of self-compacting concrete. 4th International RILEM symposium on SCC, Shah, S. (Ed.), Chicago, USA.
- Planas, J., Elices, M., & Guinea, G. V. (1992). Measurement of the fracture energy using three-point bend tests: Part 2—Influence of bulk energy dissipation. *Materials and Structures*, 25(5), 305-312.

- Pons, G., Proust, E., & Assié, S. (2003, August). Creep and shrinkage of self-compacting concrete: a different behaviour compared with vibrated concrete. In *Proceedings of the 3rd International RILEM Symposium on Self-Compacting Concrete* (Vol. 17, pp. 17-20).
- Promentilla, M. A. B., & Sugiyama, T. (2010). X-ray microtomography of mortars exposed to freezing-thawing action. *Journal of Advanced Concrete Technology*, 8(2), 97-111.
- Promentilla, M. A. B., Sugiyama, T., & Shimura, K. (2008, November). Three dimensional characterization of air void system in cement-based materials. In *3rd ACF International Conference ACF/VCA* (pp. 940-947).
- Ranjbar, M. M., Madandoust, R., Mousavi, S. Y., & Yosefi, S. (2013). Effects of natural zeolite on the fresh and hardened properties of self-compacted concrete. *Construction and Building Materials*, 47, 806-813.
- Rajamma, R., Ball, R. J., Tarelho, L. A., Allen, G. C., Labrincha, J. A., & Ferreira, V. M. (2009). Characterisation and use of biomass fly ash in cement-based materials. *Journal of hazardous materials*, 172(2-3), 1049-1060.
- Rao, G. A. (2001). Long-term drying shrinkage of mortar—influence of silica fume and size of fine aggregate. *Cement and concrete research*, 31(2), 171-175.
- Report 237R-07 (2007). Self-consolidating concrete. American Concrete Institute.

- Rozière, E., Granger, S., Turcry, P., & Loukili, A. (2007). Influence of paste volume on shrinkage cracking and fracture properties of self-compacting concrete. *Cement and concrete composites*, 29(8), 626-636.
- Rols, S., Ambroise, J., & Pera, J. (1999). Effects of different viscosity agents on the properties of self-leveling concrete. *Cement and Concrete Research*, 29(2), 261-266.
- Roussel, N., Nguyen, T. L. H., Yazoghli, O., & Coussot, P. (2009). Passing ability of fresh concrete: a probabilistic approach. *Cement and Concrete Research*, 39(3), 227-232.
- Rozière, E., Turcry, P., Loukili, A., & Cussigh, F. (2005). Influence of paste volume, addition content and addition type on shrinkage cracking of self-compacting concrete. In *Second North American Conference and Fourth RILEM International Conference on Self Compacting Concrete SCC 2005*.
- Sahmaran, M., & Yaman, I. O. (2007). Hybrid fiber reinforced self-compacting concrete with a high-volume coarse fly ash. *Construction and Building Materials*, 21(1), 150-156.
- Samad, A. A. A., Hadipramana, J., Mohamad, N., Ali, A. Z. M., Ali, N., Inn, G. W., & Tee, K. F. (2018). Development of Green Concrete from Agricultural and Construction Waste. In *Transition Towards 100% Renewable Energy* (pp. 399-410). Springer, Cham.

- Sandhya, B., & Reshma, E. K. (2013). A study on mechanical properties of cement concrete by partial replacement of fine aggregates with bottom ash. *International Journal of students research in Technology & Management*, 1(04), 416-430.
- Satish, K., Kumar, S., & Rai, B. (2017). Self Compacting Concrete Using Fly Ash and Silica Fumes as Pozzolanic Material. *Journal of Engineering Technology (ISSN: 0747-9964)*, 6(2), 394-407.
- Self-Compacting Concrete European Project Group. (2005). *The European guidelines for self-compacting concrete: Specification, production and use*. International Bureau for Precast Concrete (BIBM).
- Seng, V., & Shima, H. (2005). Creep and shrinkage of self-compacting concrete with different limestone powder contents. In *Second North American Conference on the Design and Use of Self-Consolidating Concrete and the Fourth International RILEM Symposium on Self-Compacting Concrete* (pp. 981-987).
- Sivakumar, A., & Santhanam, M. (2006). Experimental methodology to study plastic shrinkage cracks in high strength concrete. In *Measuring, Monitoring and Modeling Concrete Properties* (pp. 291-296). Springer, Dordrecht.
- Soroka, I. (1979). Portland cement paste and concrete.
- Specification, J. A. S. (1993). 5 (JASS 5). *English Version, 10th Edition*, Architectural Institute of Japan, 25-29.

- Tazawa, E., & Miyazawa, S. (1999). Autogenous shrinkage and drying shrinkage of high strength concrete. 5th international Symposium on Utilization of High Strength, High Performance Concrete. *Sandefjord, Norway*, 1254-1263.
- Tragardh, J. (1999, September). Microstructural features and related properties of self-compacting concrete. In *Self-Compacting Concrete: Proceedings of the First International RILEM Symposium held in Stockholm* (pp. 175-186).
- Turcry, P., & Loukili, A. (2003). A study of plastic shrinkage of self-compacting concrete. In *Proceedings of the 3rd International RILEM Symposium Reykjavik. Reykjavik. RILEM Publications* (pp. 576-585).
- Uday, N. P. (2017). Experimental Determination of Fracture Energy by RILEM Method. *The International Journal of Engineering and science (IJES)*, 6(3), 106-115.
- Uysal, M., & Yilmaz, K. (2011). Effect of mineral admixtures on properties of self-compacting concrete. *Cement and Concrete Composites*, 33(7), 771-776.
- Vieira, M., & Bettencourt, A. (2003, August). Deformability of hardened SCC. In *International RILEM Symposium on Self-Compacting Concrete* (pp. 637-644). RILEM Publications SARL.
- Wahyuni, A. S., Supriani, F., & Gunawan, A. (2014). The performance of concrete with rice husk ash, sea shell ash and bamboo fibre addition. *Procedia Engineering*, 95, 473-478.

- Wan, K., & Xu, Q. (2014). Local porosity distribution of cement paste characterized by X-ray micro-tomography. *Science China Technological Sciences*, 57(5), 953-961.
- Yahia, A., Tanimura, M., & Shimoyama, Y. (2005). Rheological properties of highly flowable mortar containing limestone filler-effect of powder content and W/C ratio. *Cement and concrete Research*, 35(3), 532-539.
- Yang, C., Chong, W., Tao, Y., Wang, Y., Wang, Z., Jianxiong, Y., & Lin, Y. (2009). Analysis on ITZ structure of self-compacting concrete. In *2nd Int. Symposium on Design, Performance and Use of Self Consolidating Concrete* (pp. 426-434). RILEM Publications sarl.
- Zhu, W., & Bartos, P. J. (2003). Permeation properties of self-compacting concrete. *Cement and Concrete Research*, 33(6), 921-926.

APPENDICES

Appendix A: Three Point Bending Load-Deformation Curves of Limestone Powder (LS) mixes (Figure A.1 to A. 4)

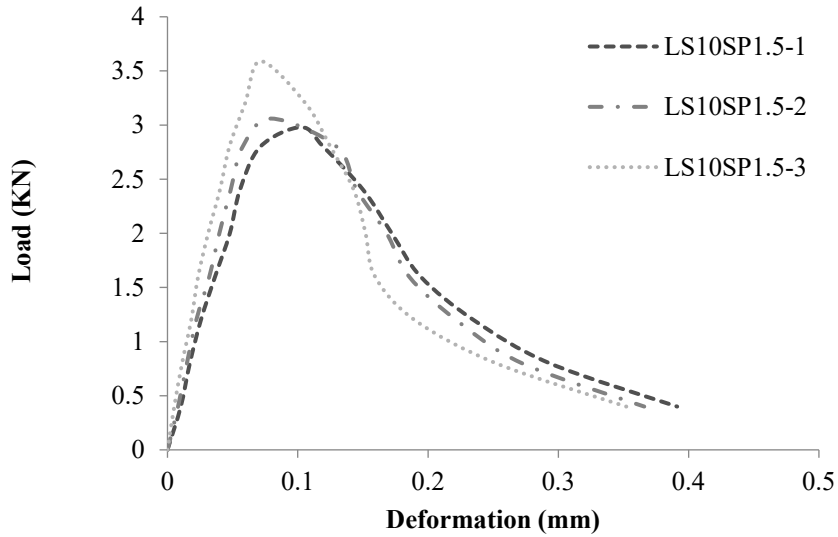


Figure A.1: LS10SP1.5 Load-deformation curve

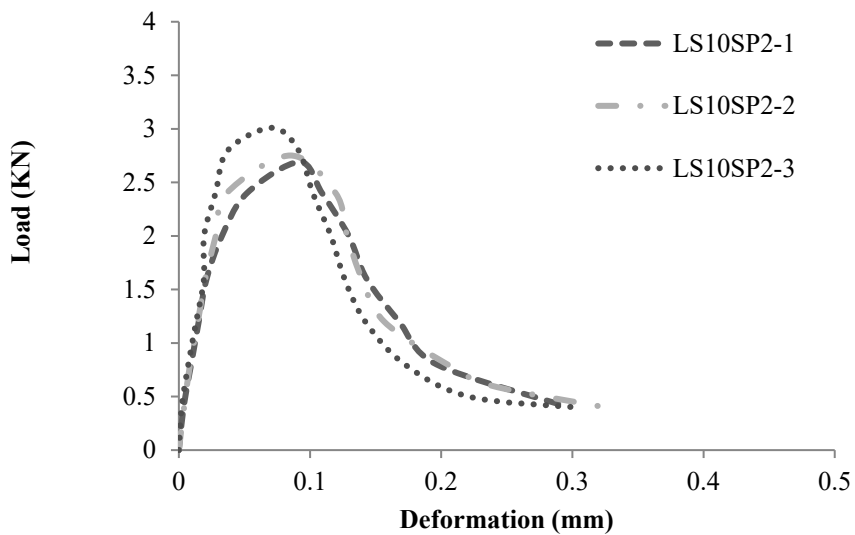


Figure A.2: LS10SP2 Load-deformation curve

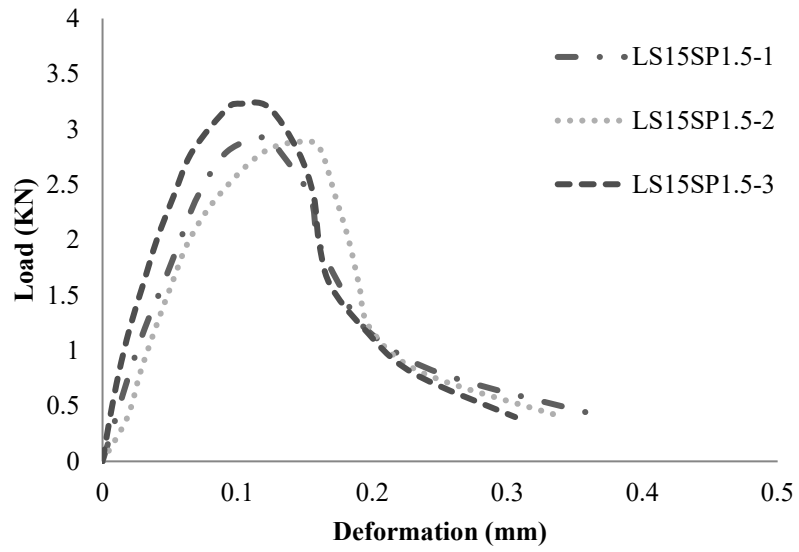


Figure A.3: LS15SP1.5 Load-deformation curve

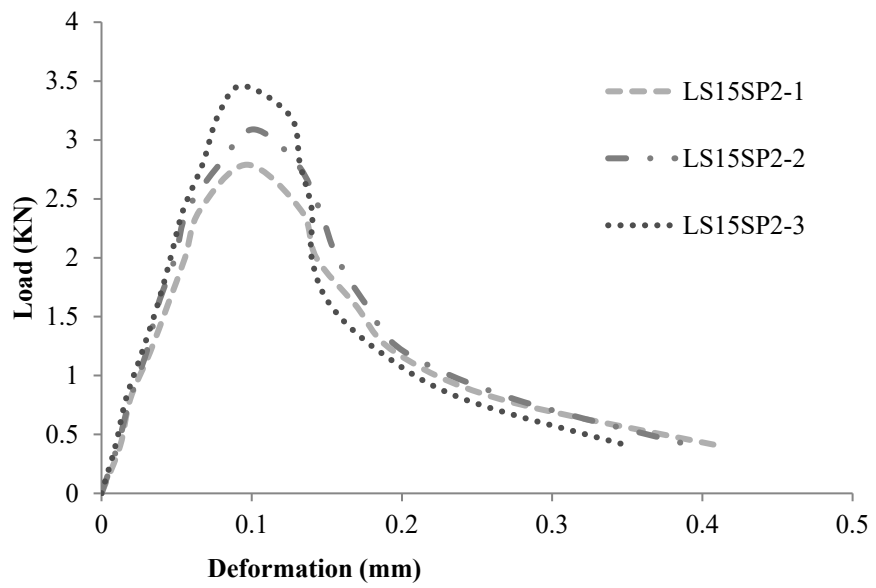


Figure A.4: LS15SP2 Load-deformation curve

Appendix B: Three Point Bending Load-Deformation Curves of Sea Sand Powder (SS) mixes (Figure B. 1 to B. 4)

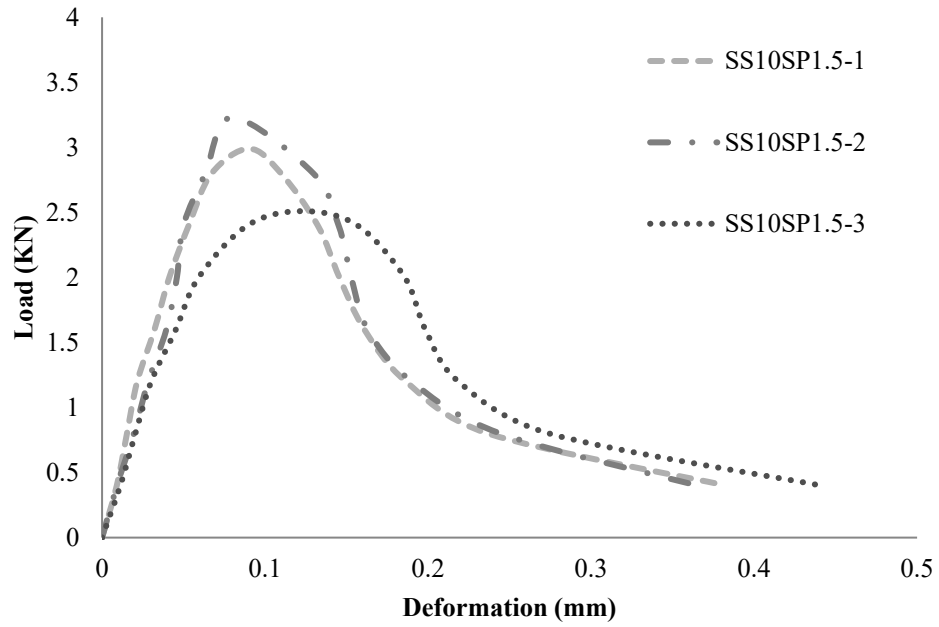


Figure B. 1: SS10SP1.5 Load-deformation curve

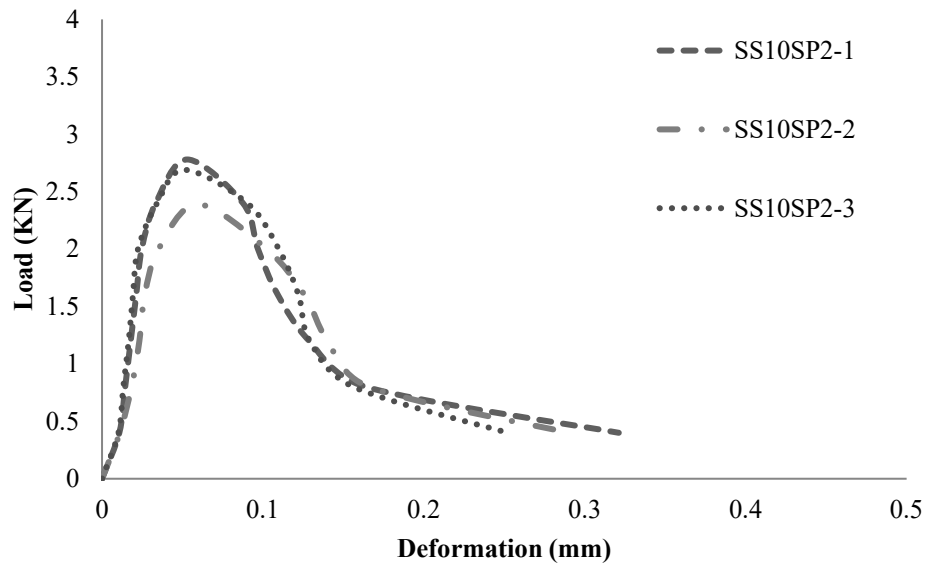


Figure B. 2: SS10SP2 Load-deformation curve

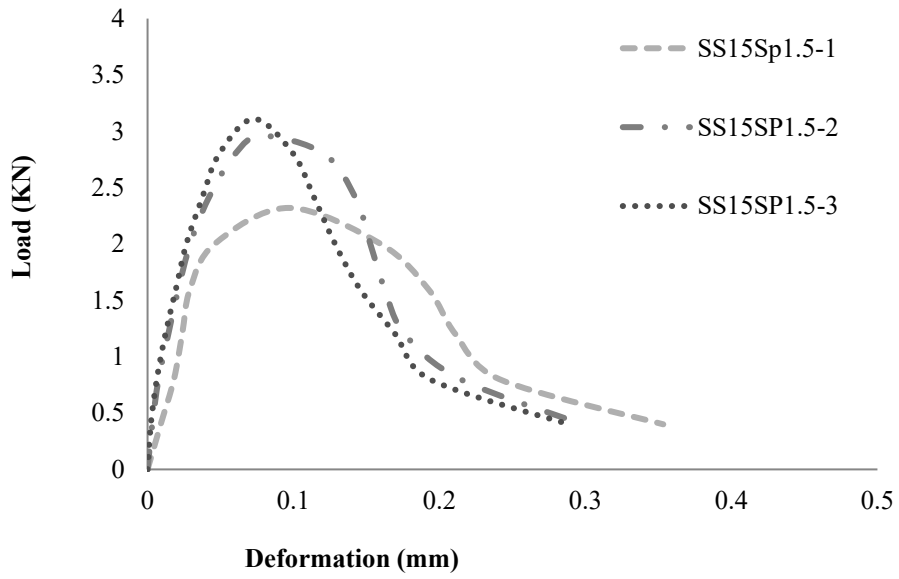


Figure B. 3: SS15SP1.5 Load-deformation curve

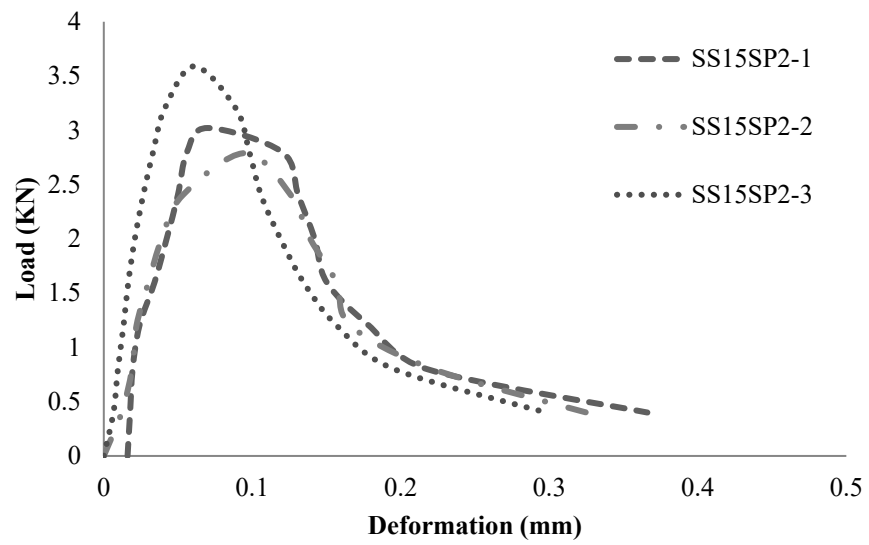


Figure B. 4: SS15SP2 Load-deformation curve

Appendix C: Three Point Bending Load-Deformation Curves of Olive Waste Ash (OW) mixes (Figure C. 1 to C. 6)

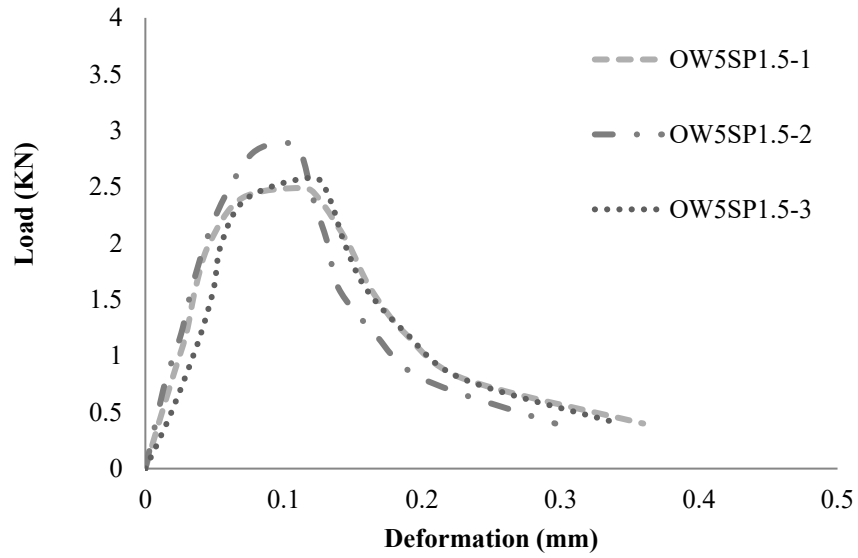


Figure C. 1: OW5SP1.5 Load-deformation curve

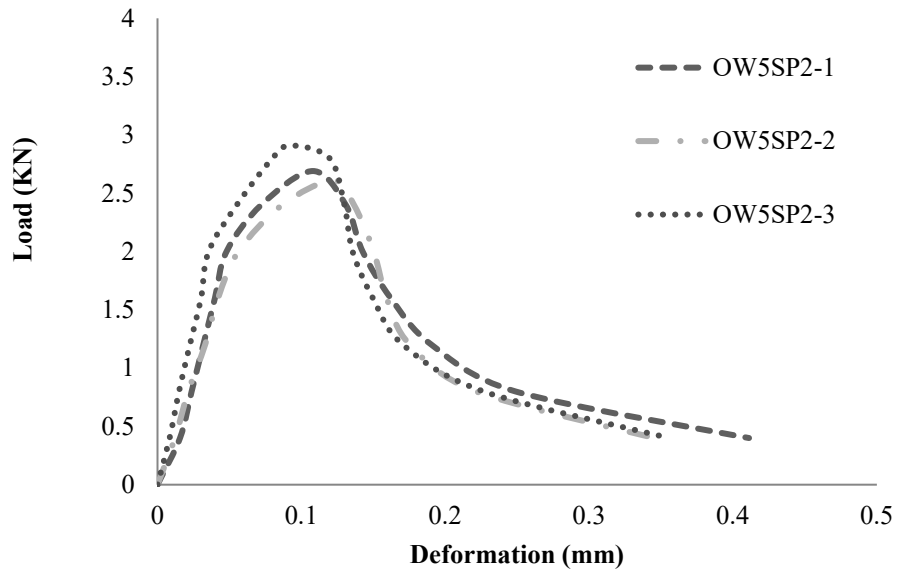


Figure C. 2: OW5SP2 Load-deformation curve

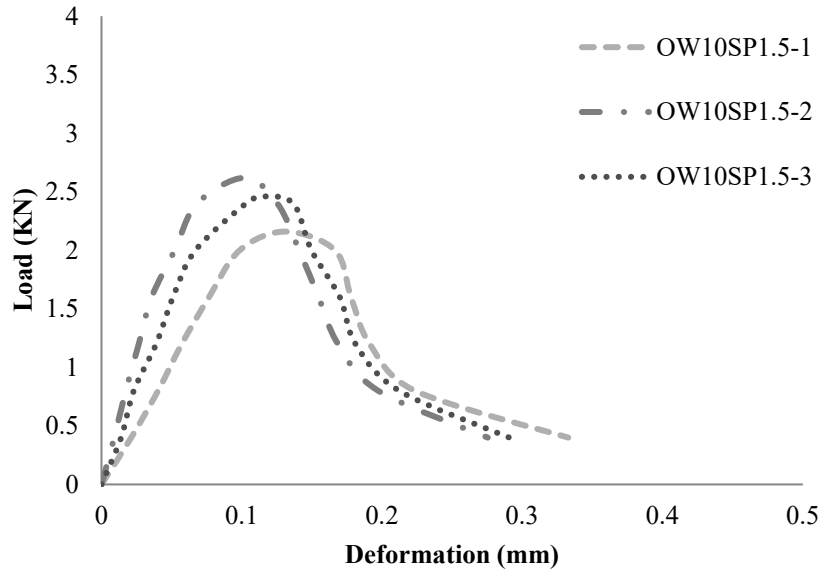


Figure C. 3: OW10SP1.5 Load-deformation curve

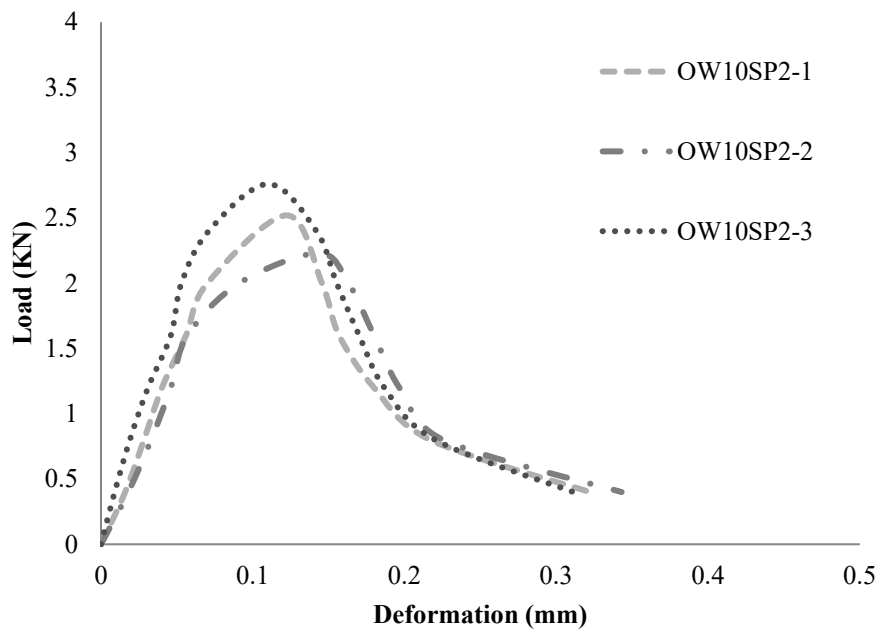


Figure C. 4: OW10SP2 Load-deformation curve

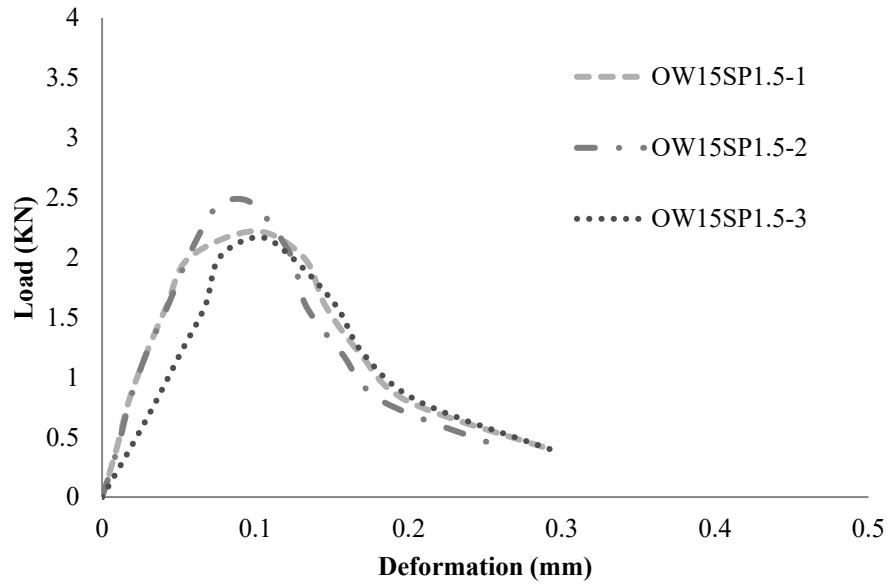


Figure C. 5: OW15SP1.5 Load-deformation curve

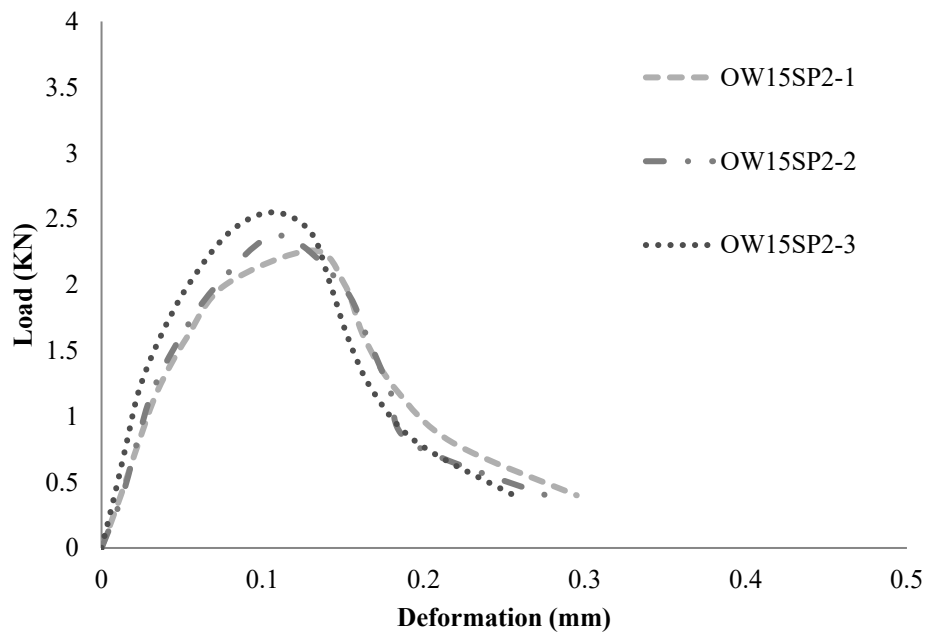


Figure C. 6: OW15SP2 Load-deformation curve